



ADVANCED MASTERS IN STRUCTURAL ANALYSIS
OF MONUMENTS AND HISTORICAL CONSTRUCTIONS



Master's Thesis

Seyed Ali Nayeri

Seismic Assessment of the Roman Temple in Évora, Portugal

This Masters Course has been funded with support from the European Commission. This publication reflects the views only of the author, and the Commission cannot be held responsible for any use which may be made of the information contained therein.

This page is left blank on purpose

DECLARATION

Name: Seyed Ali Nayeri

Email: sanayeri@gmail.com

Title of the Msc Dissertation: Seismic Assessment of the Roman Temple in Évora, Portugal

Supervisor(s): Daniel V. Oliveira and José Vieira de Lemos

Year: 2012

I hereby declare that all information in this document has been obtained and presented in accordance with academic rules and ethical conduct. I also declare that, as required by these rules and conduct, I have fully cited and referenced all material and results that are not original to this work.

I hereby declare that the MSc Consortium responsible for the Advanced Masters in Structural Analysis of Monuments and Historical Constructions is allowed to store and make available electronically the present MSc Dissertation.

University: Universidade do Minho

Date: July 19, 2012

Signature: _____

This page is left blank on purpose

*To my beloved grandmother for her love of life and learning
and to my aunt Soraya for her unconditional love and unwavering support*

This page is left blank on purpose

ACKNOWLEDGMENTS

This present work was developed within the framework of SAHC Erasmus Mundus Masters Course (www.msc-sahc.org) as a collaborative research between University of Minho and the Regional Directorate of Culture of Alentejo (DRCA). The research was carried out under the joint supervision of Prof. Daniel Oliveira at the University of Minho and Dr. J. V. Lemos at the Laboratório Nacional de Engenharia Civil (LNEC).

I would like to thank Prof. Oliveira for giving me a chance to work on this incredible project and for his trust and belief in my abilities. This research strongly relied on his expertise, and I have thoroughly enjoyed tackling many challenging problems under his mentorship. His enthusiasm and interest in my work, as well as his vision made this project possible.

I am forever indebted to Dr. J. V. Lemos for sharing his wealth of knowledge and expertise and for introducing me to the wonderful possibilities of the discrete element method. A major part of the present work would not have been possible without his patience and unwavering support. It has been a privilege and an honour to have had a chance to conduct this research with him. I would also like to extend my appreciation to the researchers and staff at LNEC for their hospitality, warmth and generosity.

I would like to acknowledge the support and guidance of archaeologists Dr. Rafael Alfenim (DRCA) and Dr. Panagiotis Sarantopoulous (city council of Évora) as well as Dr. Ludovina Grilo (city council of Évora) whose written material about the Roman temple and the city proved most valuable. I would like to thank Dr. Alfenim in particular for patiently sharing with me his wealth of knowledge about the history of Évora and the Temple and giving me a chance to appreciate the cultural heritage which is being preserved in the region. I am forever grateful for his support and diligent review of my work.

I would like to thank Prof. Agustín Orduña Bustamante at Universidad de Colima in Mexico for his invaluable advice as well as review of my work on limit analysis.

This project is in many ways an extension of the excellent work completed previously by my colleagues at the University of Minho as part of their integrated project. Therefore, I would like to thank Giulia Grecchi, Alex McCall, Jungtae Noh, Evan Speer, and Mohammed Tohidi without whose support, generosity and cooperation the current work would not be possible. I also thank Nuno Mendes for his tireless effort in analysing the results of the dynamic identification tests and sharing his insights about the behaviour of the structure. I would like to express my gratitude to Dr. Francisco Fernandes from the University of Minho who was responsible for the GPR tests completed in Évora.

I would like to thank the European Union for providing me with the opportunity to be a part of the Advanced Masters in Structural Analysis of Monuments and Historical Construction (SAHC) program and for their generous financial support through the Erasmus Mundus Scholarship.

My participation in this program was made possible through the hard work and dedication of the MSc Secretariat, in particular Ms. Ana Fonseca and Ms. Dora Coelho. I am very appreciative of their

Erasmus Mundus Programme

patience and support throughout my enrollment in the program. Their work behind the scenes has made this work possible.

I would like to express my gratitude to Prof. Petr Kabele, Mrs. Kurfurstova and other professors and staff at the České vysoké učení technické v Praze for their tireless effort to make our stay in Prague productive and memorable. Special thanks to Prof. Miloš Drdáký and Prof. Eva Burgetová for making our stay so unforgettable and showing us the beauty of Czech Republic.

I am grateful to my friends and colleagues from Prague for their friendship, help and encouragement. I feel very lucky to have been able to participate in this program and to have met a wonderful group that I can now call my friends. I would like to especially thank my friends in Guimarães for their constant support and encouragement. A special thanks to Juan Mora for telling me to never use a broken pencil.

I cannot overstate the debt of gratitude I owe to my family for their continued support through many difficult times and for their belief in my abilities and my dreams. Their sacrifice, love and unwavering resolve have made this work a reality.

Last, but certainly not least, I would like to thank my dear friend Lola who has been a constant source of strength and love. I hope we can travel the world together someday.

ABSTRACT

Strong earthquakes are a common cause of destruction of classical monuments, especially structures which have been damaged in the past and are now incomplete. Therefore understanding the dynamic behaviour of these types of structures is an essential part of insuring their preservations for future generations. The dynamic response of these structures is characterised by a complex set of rocking and sliding motions and is highly non-linear. The current study investigates the application of three well-known analysis techniques, namely limit analysis, static non-linear (pushover) analysis and non-linear time history analysis for the seismic assessment of multi-drum classical monuments.

The Roman Temple located in the historic centre of Évora, Portugal is used as a case study and its seismic behaviour presented. First, the stability of structure is evaluated using limit analysis and pushover approach. The results significantly underestimate the capacity of the structure due to their inability to account for dynamic stability of blocks during an earthquake. However, the results accurately evaluate the failure mechanism of the structure.

A discrete element model of the structure is also analysed in the time domain. The discrete element model utilizes rigid elements with frictional joints and accommodates both geometrical as well as material nonlinearity at the joints. The model is calibrated using the results of the experimental dynamic identification. The dynamic analysis is performed as a series of parametric studies based on the concept of incremental dynamic analysis. Both far field and near field earthquakes are considered. The structural response is evaluated over a range of earthquake intensities. The results indicate that large deformations can sometimes be accommodated by the structure while still maintaining stability. The results provide a more complete picture of the structure's behaviour and safety.

A comparison of the numerical methods is presented along with a discussion of limitations of the application of the static methods. Finally, a set of three damage indicators are proposed and their results discussed and compared.

This page is left blank on purpose

RESUMO

Os sismos são uma causa comum de destruição de monumentos clássicos, especialmente para estruturas danificadas no passado e agora incompletas. Assim, torna-se essencial compreender o comportamento dinâmico deste tipo de estruturas para assegurar a sua preservação para as gerações futuras. A resposta dinâmica destas estruturas é caracterizada por um sistema complexo de rotações de deslizamentos altamente não linear. O presente estudo investiga a implementação de três conhecidas técnicas de análise, nomeadamente análise limite, análise não linear estática (pushover) e análise temporal não-linear, para a avaliação do comportamento sísmico de monumentos clássicos compostos por blocos.

O Templo Romano localizado no centro histórico de Évora, Portugal é usado como caso de estudo de avaliação do comportamento sísmico deste tipo de estruturas. Inicialmente faz-se a avaliação da estabilidade da estrutura utilizando a análise limite e pushover. Observa-se que estes resultados subestimam significativamente a capacidade da estrutura devido à sua incapacidade para reproduzir fenómenos de estabilidade dinâmica que ocorrem durante o sismo. No entanto, é possível estimar os modos de colapso com precisão.

A análise não-linear temporal é realizada com base num modelo de elementos discretos. O modelo numérico utiliza blocos rígidos e juntas friccionais e incorpora tanto não linearidades geométricas como materiais das juntas. A calibração do modelo é feita com base em resultados disponíveis de identificação dinâmica experimental. A análise dinâmica é realizada como uma sequência de estudos paramétricos baseados no conceito de análise dinâmica incremental. Consideraram-se ambos os cenários sismogénicos de sismo próximo e afastado. A resposta estrutural é avaliada para uma gama de intensidades sísmicas crescentes. Os resultados indicam que as grandes deformações podem, por vezes, ser acomodadas pela estrutura, mantendo esta a estabilidade.

A comparação dos três métodos numéricos é apresentada juntamente com a discussão das limitações associadas aos métodos estáticos. Finalmente, propõe-se um conjunto de três Indicadores de dano sendo os resultados discutidos e comparados entre si.

This page is left blank on purpose

RESUME

Les puissants tremblements de terre sont une raison fréquente de la destruction des monuments traditionnels, notamment des structures qui ont été endommagés dans le passé et qui maintenant demeurent incomplètes. Comprendre le comportement sismique de ce type de structures a par conséquent un rôle important afin d'assurer leur conservation pour les générations futures. La réponse dynamique de ces structures est caractérisée par un mélange complexe de mouvement de rotation et de glissement qui est loin d'être linéaire. Cette étude se penche sur l'application de trois techniques d'analyse très connues, à savoir l'analyse limite, l'analyse statique non-linéaire (« pushover »), et l'analyse historique temporelle non-linéaire pour l'évaluation sismique des monuments traditionnels à colonnes à blocs superposés.

Le temple romain situé dans le centre historique d'Évora au Portugal sert de cas d'étude et son comportement vis-à-vis des tremblements de terre est présenté. En premier lieu, la stabilité de la structure est évaluée en utilisant l'analyse limite et l'approche « pushover ». Les résultats sous-estiment grandement la capacité de la structure du fait de leur incapacité de prendre en considération la stabilité dynamique des blocs pendant le tremblement de terre. Cependant, les résultats estiment précisément le mécanisme de rupture de la structure.

Un modèle élément discret de la structure est aussi analysé dans le temps. Le modèle élément discret utilise des éléments rigides avec des interfaces de friction et reproduit la non-linéarité des joints sur le plan géométrique et matériel. Le modèle est calibré aux regards des résultats des tests dynamiques. L'analyse dynamique est effectuée comme une série d'études paramétriques basées sur le concept de l'analyse dynamique incrémentale. Les deux types de tremblements de terre à champ proches et lointains sont étudiés. La réponse structurelle est évaluée sur une plage d'intensité de tremblements de terre. Les résultats montrent que de grandes déformations peuvent parfois être admises par la structure tout en restant stable. Les résultats fournissent une description plus complète du comportement de la structure et de sa sécurité.

Une comparaison des méthodes numériques est présentée de même qu'une discussion sur les limitations de l'application des méthodes statiques. Enfin, un ensemble de trois indicateurs de dégâts est proposé et leurs résultats sont examinés et comparés.

This page is left blank on purpose

TABLE OF CONTENTS

Chapter 1 Introduction	1
1.1 Global context for seismic assessment of masonry	1
1.2 Research motivations and objectives.....	3
1.3 Outline of the thesis.....	5
Chapter 2 Literature Review	7
2.1 Methods of analysis for masonry structures.....	8
2.1.1 <i>Quasi-static analysis methods</i>	8
2.1.2 <i>Dynamic analysis methods</i>	11
2.2 Modelling strategies for masonry structures	14
2.2.1 <i>Finite element representation</i>	14
2.2.2 <i>Macroelement representation</i>	15
2.2.3 <i>Discrete element representation</i>	16
Chapter 3 The Roman Temple of Evora	19
3.1 Historical Overview.....	19
3.2 Description of the Temple	27
3.3 Previous Studies.....	31
3.4 Remaining Issues.....	31
Chapter 4 Quasi-Static Analysis Using Limit and Pushover Analysis	33
4.1 Overview.....	33
4.2 Limit analysis	33
4.2.1 <i>Overview of methodology</i>	33
4.2.2 <i>Description of Numerical Models</i>	34
4.2.3 <i>Results and Discussion</i>	36
4.3 Non-linear static (pushover) analysis	38
4.3.1 <i>Overview of methodology</i>	38
4.3.2 <i>Description of numerical model</i>	38
4.3.3 <i>Results and discussion</i>	39

Chapter 5 Incremental Dynamic Analysis Using Discrete Element Model	43
5.1 Incremental dynamic analysis approach	43
5.2 Description of the numerical model	45
5.2.1 <i>Geometric definition</i>	45
5.2.2 <i>Block and contact representation</i>	48
5.2.3 <i>Material properties and joint parameters</i>	49
5.2.4 <i>Representation of reinforcements</i>	50
5.2.5 <i>Damping</i>	50
5.3 Dynamic identification and calibration of numerical model.....	50
5.3.1 <i>Overview</i>	50
5.3.2 <i>Numerical modal analysis</i>	51
5.3.3 <i>Experimental dynamic identification</i>	52
5.3.4 <i>Calibration of numerical model</i>	53
5.4 Seismic input	57
5.5 Discussion of results.....	59
5.5.1 <i>Response of a free-standing column</i>	60
5.5.2 <i>Response of the overall structure</i>	64
Chapter 6 Performance Assessment	69
6.1 Comparison of numerical methods	69
6.2 Definition and application of damage indicators	70
6.2.1 <i>Maximum permanent displacement</i>	71
6.2.2 <i>Failed blocks</i>	72
6.2.3 <i>Contact area loss</i>	74
6.2.4 <i>Summary of results</i>	76
Chapter 7 Conclusions	77
7.1 Main conclusions	77
7.2 Opportunities for further research.....	78
References	81
Appendix A: Final State of Models for Dynamic Analysis	87
Appendix B: Typical Failure Patterns of Dynamic Analysis	93

LIST OF FIGURES

Figure 1-1: (a) Minaret of Samarra, Iraq (Iraqi State Antiquities Authority), (b) Basilica di Santa Maria del Fiore, Florence (UNESCO), and (c) archaeological site of Olympia, Greece (UNESCO).	1
Figure 1-2: (a) Sliding of column drums of the Propylaea of the Acropolis of Athens (Guillaume Piolle) and (b) over-turned columns at the archaeological site of Olympia, Greece (UNESCO).	2
Figure 1-3: Northwest façade of the Roman Temple of Évora, Portugal.	4
Figure 2-1: Application of 3D limit analysis to the seismic evaluation of historic masonry structures (after (a) Orduña et. al [9] and (b) Orduña [7])	10
Figure 2-2: Example of macro-element representation of masonry (after (a) Orduña et.al [9] and (b) Modena [8])	16
Figure 2-3: Examples of discrete element representation of masonry block structures applied to (a) a section of Parthenon Pronaos and (b) to a pointed masonry arch (after Lemos [3]).	18
Figure 3-1: Map of Portugal and Spain, inset with plan of Medieval and Roman centre of Évora.	20
Figure 3-2: Evolution of the city of Évora from (a) the first century AD until (d) the medieval era (after Gustavo Silva Val-Flores, 2006).....	22
Figure 3-3: Woodcuts showing (a) the state of the structure in 1795, as drawn by Murphy and (b) the structure in 1865 with the base exposed and prior to the removal of the medieval walls and tower (after Pereira [39]).	24
Figure 3-4: Evolution of the temple structure: (a) reconstruction of the “original” structure from first century AD; (b) remains of the medieval structure from mid eighteenth century (after Pereira [39]); (c) current condition.	26
Figure 3-5: View of the south façade and the entrance to the temple showing the exposed interior stone fill structure of the podium.	27
Figure 3-6: Alternative proposals regarding the entrance on the south façade.	28
Figure 3-7: East elevation of the temple (after Direção Regional de Cultura do Alentejo [44]).	28
Figure 3-8: Plan view of the temple structure and the structural grid (after DRC do Alentejo [44]).	29
Figure 3-9: Typical damages recorded during preliminary visit.	30
Figure 3-10: Location and detail of architrave steel tie reinforcement.	31
Figure 4-1: Limit analysis model types (a) m01 using single blocks and (b) m02 using discretized blocks.	35
Figure 4-2: Macro-block representation of (a) actual column drums (b) with a single block and (c) with discretized block sections.....	35

Figure 4-3: Failure mechanisms for (a) east façade ($\alpha=0.097$) and (b) column D6 ($\alpha=0.130$) due to negative horizontal forces.....	37
Figure 4-4: Pushover capacity curves for selected models.....	40
Figure 4-5: Failure mechanisms for (a) east façade ($\alpha=0.107$) and (b) column D6 ($\alpha=0.146$) due to negative horizontal forces.....	40
Figure 5-1: Maximum permanent displacement of a free-standing column, with or without imperfections, subject to earthquake records: (a) Kalamata (PGA = 0.27 g), (b) Aigion (PGA = 0.50 g) and (c) Bucharest (PGA = 0.20 g) (after Psycharis et al. [27]).....	44
Figure 5-2: Discrete element model (a) plan and (b) perspective view.....	45
Figure 5-3: Perspective view of (a) the refined 3D scan mesh and (b) the simplified block model for discrete element analysis with 3DEC.	46
Figure 5-4: Illustrative example of the application of the general algorithm for generating the simplified block model based on real geometry data using Rhinoceros 3D and Grasshopper.....	47
Figure 5-5: Fourier amplitude spectrum of the experimental results for Column E6 (setup 5) using four accelerometers.	53
Figure 5-6: Numerical and experimental mode shapes and frequencies for column D6.	54
Figure 5-7: Numerical and experimental mode shapes and frequencies for column E6.	55
Figure 5-8: Numerical and experimental mode shapes and frequencies for the global model.....	56
Figure 5-9: Seismic hazard map for continental Portugal (after Norma Portuguesa [58]).	58
Figure 5-10: Examples of artificially generated accelerograms for Eurocode type 1 and 2 earthquakes.	58
Figure 5-11: Comparison of the acceleration and displacement response spectrum of artificial records and the Eurocode specified spectra for type 1 and 2 earthquakes.	59
Figure 5-12: Location of the nine control points monitored during the time history analysis.	60
Figure 5-13: Displacement time history response of control point 2 (top of column D6) in the transverse (x) and longitudinal (y) directions, due to type 2 earthquake in the y-direction (PGA 0.66g).	60
Figure 5-14: Horizontal time history response of control point 2 (top of column D6) as viewed from the top, due to type 2 earthquake in the longitudinal (y) direction with scale factor of 6.0 (PGA 0.66g).....	61
Figure 5-15: Horizontal displacement time history response of control point 2 (top of column D6), showing the magnitude of the total displacements, due to type 2 earthquake in the longitudinal (y) direction with scale factor of 6.0 (PGA 0.66g).	62

Figure 5-16: Vertical displacement time history response of control point 2 (top of column D6) due to type 2 earthquake in the longitudinal (y) direction with scale factor of 6.0 (PGA 0.66g).	62
Figure 5-17: Time history response of column D6 (in the y-plane) due to type 2 earthquake in the longitudinal (y) direction with scale factor of 6.0 (PGA 0.66g). Note that the response has been magnified by a factor of five in order to emphasize the behaviour.....	63
Figure 5-18: Joint opening time history response at the joint between the second and third block in column D6, due to type 2 earthquake in the longitudinal (y) direction with scale factor of 6.0 (PGA 0.66g).	63
Figure 5-19: Joint normal stress time history at the joint between the second and third block in column D6, due to type 2 earthquake in the longitudinal (y) direction with scale factor of 6.0 (PGA 0.66g).....	64
Figure 5-20: Joint sliding time history at the joint between the second and third block in column D6, due to type 2 earthquake in the longitudinal (y) direction with scale factor of 6.0 (PGA 0.66g).	64
Figure 5-21: Time history response of the of the entire structure due to type 1 earthquake in the transverse (x) direction with a scale factor of 6.0 (PGA 0.6g). Note that the response has not been magnified.	65
Figure 5-22: Examples of structure response due to type 1 and type 2 earthquake applied in the transverse (x) direction at various PGA scale factors.	66
Figure 5-23: Type 1 and type 2 elastic response spectrum for Évora according to the Eurocode.	66
Figure 6-1: Maximum permanent displacement at various PGA intensities for earthquake runs in both x and y directions.	71
Figure 6-2: Failed blocks are identified when the block centroid moves outside (b and c) of the initial position bounding box (a).	72
Figure 6-3: Percentage of failed blocks at various PGA intensities for earthquake runs in both x and y directions.	73
Figure 6-4: Percentage of contact area loss at various PGA intensities for earthquake runs in both x and y directions.	74
Figure 6-5: Distribution of block contact area loss for type 1 earthquake in the x-direction.	75
Figure 6-6: Distribution of block contact area loss for type 2 earthquake in the x-direction.	75
Figure 6-7: Comparison of damage indicators at various PGA intensities for earthquake runs in both x and y directions.	76

This page is left blank on purpose

LIST OF TABLES

Table 4-1: Material parameters used for limit analysis.	36
Table 4-2: Comparison of the results of limit analysis for model types m01 and m02.....	36
Table 4-3: Summary of pushover response of models, including the horizontal acceleration and components of the horizontal displacements.	39
Table 5-1: Mechanical properties of joints for discrete element model.....	49
Table 5-2: Features of four discrete element models used for modal analysis.	51
Table 5-3: Modal frequencies for the first ten modes of numerical models.	52
Table 5-4: Comparison of modal frequencies of the calibrated model and the experimental results...	54
Table 5-5: Seismic parameters for the Roman Temple of Évora (return period 475 years).	57
Table 6-1: Comparison of the seismic coefficient calculated using limit and pushover analysis	69

This page is left blank on purpose

Chapter 1

INTRODUCTION

1.1 Global context for seismic assessment of masonry

Masonry construction constitutes a substantial and diverse portion of building stock in the world, especially monumental and historically significant structures. Figure 1-1 presents three examples of such structures. Yet, almost all historic masonry heritage structures in the world have been designed without consideration of seismic actions and dynamic behaviour of the structure and are thus more vulnerable to damage and collapse due to earthquakes [1].

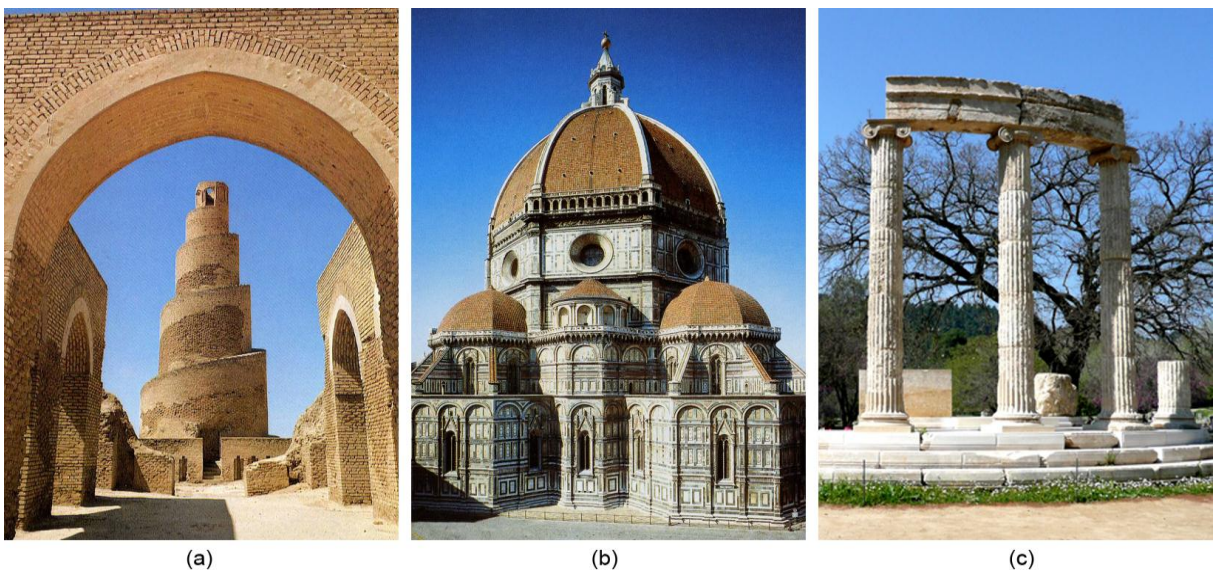


Figure 1-1: (a) Minaret of Samarra, Iraq (Iraqi State Antiquities Authority), (b) Basilica di Santa Maria del Fiore, Florence (UNESCO), and (c) archaeological site of Olympia, Greece (UNESCO).

Despite the fact that masonry is one of the oldest construction materials and has been widely used for millennia by many cultures and civilizations, a thorough understanding of the seismic behaviour of such structures has proved challenging. At a material level, the heterogeneous nature of masonry construction as well as the distinct separation between the components that make up the fabric of masonry structures creates difficulties which are not present when dealing with other materials.

The primary feature of unreinforced masonry construction is its composite nature, composed of discrete units separated by dry or mortared joints. The discontinuous nature of the construction makes the application of the more conventional methods of continuum mechanics more difficult. More complex constitutive models are required to take into account the complex interaction between the masonry units and their bond matrix. Investigations of collapsed structures and deformations in existing buildings demonstrate that for some masonry structures the modes of failure are often governed solely by the behaviour of the blocks at their interfaces (Figure 1-2). Thus, the most significant components of deformations are a result of relative movement of blocks against each other rather than through deformation of the blocks themselves. The study of this behaviour is made even more challenging due to the non-linearity of the response both at a material level, due to masonry's low tensile strength and complex stress-strain relation for both the blocks and their joints, as well as geometrically due to the significant contribution of rocking and sliding experienced under dynamic conditions.

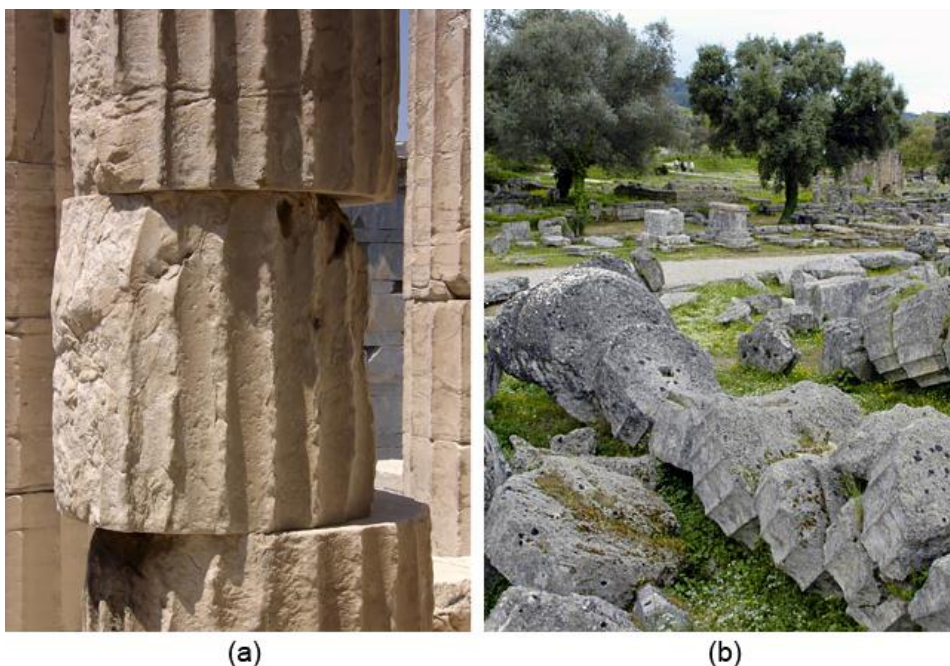


Figure 1-2: (a) Sliding of column drums of the Propylaea of the Acropolis of Athens (Guillaume Piolle) and (b) over-turned columns at the archaeological site of Olympia, Greece (UNESCO).

The great variety of structural topologies, building technologies and the geometric complexity of these monuments, as well as lack of information about the construction techniques and history of modifications and changes to the structure, makes development and application of generalized

methods much more challenging and complex. Moreover, given that most monuments are several centuries old and have suffered damage and degradation due to ageing, natural hazards and man-made forces, an accurate characterisation of their mechanical behaviour requires more complicated physical models that take into account the unique history and state of each monument.

One of the most significant classes of masonry heritage structures are the remains of monuments of classical antiquity which can be found in abundance around the Mediterranean region, as well as outposts of the Roman Empire in Western Europe. These remains were once a part of massive structures of religious and civic importance. However, over the millennia most of these structures have deteriorated and collapsed, leaving behind only free-standing columns and colonnades.

Since many of these works of classical antiquity are located in regions of moderate to high seismicity, the assessment of their structural safety and the evaluation of alternative rehabilitation proposals require robust analysis tools which are capable of accurately representing the response of such structures under seismic loads [2]. These structures are considered to be especially vulnerable given that most are incomplete and thus cannot use the overall integrity of the original structure to withstand the applied seismic loads [3].

Along with historical investigation, in-situ inspections and laboratory testing, analysis of mechanical behaviour remains one of the most important tools available to conservators as they try to determine the most appropriate techniques for preserving historical monuments. Thus in order to preserve these monuments for future generations, a pragmatic approach is required through which new techniques are applied together with existing tools in order to understand the overall behaviour of these structures and insure their safety.

1.2 Research motivations and objectives

The current study aims to use the Roman Temple of Évora as a case study in assessment of multi-drum classical colonnade using three different numerical methods. The study will also present the challenges and issues which analysts are faced with in evaluating and quantifying seismic risks for such monuments.

The Roman Temple of Évora (Templo Romano de Évora), is an ancient temple in the historic Portuguese city of Évora, located 100 kilometers east of the Portuguese capital, Lisbon. Dating back to the first century AD, the temple is part of the historical centre of the city which is collectively classified as a UNESCO World Heritage Site. As one of the most significant evidences of the Roman settlement in the Iberian Peninsula, the temple has a special place within the architectural heritage of the region and Portugal as a whole. Figure 1-3 presents a view of the remains of the temple as it stands today.

Over its long history, the temple has endured numerous changes and alterations and presently only fourteen columns remain, twelve of which include the Corinthian capitals and support the partial

remains of the north architrave. In its current condition, the structure is incomplete and thus more vulnerable to loss of integrity due to seismic loads.

Given its history, cultural significance, structural topology and current state, the Roman Temple of Évora can be taken to represent a prototype of ancient multi-drum structures, thus allowing the results of the present study to be applied and extended to other such structures.

The principal goals of the present study are as follows:

- To analyse and understand the seismic behaviour of the monument and to quantify its resistance to seismic effects through the use of three well known numerical methods, namely limit analysis, pushover analysis and incremental dynamic time history analysis;
- To compare and evaluate the applicability and limitation of the numerical methods to accurately demonstrate the behaviour of the structure;
- To characterise the effect of existing damage and explore the influence of uncertainties on the structural response. The study will also explore the non-linear behaviour of the structure and provide guidelines on appropriate approaches for the analysis of multi-drum structures;
- To propose and evaluate damage indicators appropriate for the assessment and quantification of damage as a function of ground motion parameters.



Figure 1-3: Northwest façade of the Roman Temple of Évora, Portugal.

1.3 Outline of the thesis

The current study is presented in seven chapters, of which this introductory section constitutes the first chapter.

Chapter two provides an overview of the state of the art in the seismic analysis of masonry structures, with a special focus on multi-drum classical columns and colonnades. The chapter presents the evolution of the research in the area of dynamics of blocky structures as well as the main numerical techniques currently available for modelling and analysis of masonry structural behaviour.

A brief historical overview of the origin and evolution of the city of Évora and the Roman Temple is presented in chapter three. A discussion of the main architectural and stylistic elements of the temple structure is followed by a survey of the current state of the monument and the extent of damages observed in a visit to the temple site. The chapter ends with an overview of previous archeological and structural studies of the temple and the outstanding issues which will be addressed in the following chapters.

The application of two static methods, namely limit analysis and pushover analysis, are presented in chapter four. Along with an overview of the salient features of each method, the chapter contains a complete description of the structural models considered for each analysis and presents a discussion of the results of each analysis.

The incremental dynamic analysis of the structure is presented in chapter five. The chapter begins with reviewing the objectives of incremental dynamic analysis and its application to time history analysis. Following the preliminary discussions, a description of the numerical model used for the dynamic analysis of the temple structure is presented. The description includes the methods used for generating the geometric model from 3D scan data as well as the representation of blocks and contacts used in the analysis. Chapter five also presents the results of the experimental dynamic identification test performed at the site and explores the challenges faced in calibration of numerical models to the experimental data. The chapter ends with a discussion of the results.

Chapter six presents a summary of the results of the three numerical models and provides a comparison of their results. The overall behaviour of the structure will be explored and contribution of each type of analysis to the understanding of this behaviour is presented.

The main conclusions of the case study as well as recommendations are presented in the final chapter. The chapter also includes a short survey of opportunities for further research.

This page is left blank on purpose

Chapter 2

LITERATURE REVIEW

While the past few decades have witnessed new developments in the science and design of masonry construction as well as computational tools available to simulate and understand its behaviour, the seismic behaviour of masonry remains a subject of intense research. Widely used for millennia, masonry construction encompasses a broad spectrum of structures, from ordinary houses to monumental palaces and bridges. Even though the techniques of assembling the blocks have remained essentially unchanged for thousands of years, availability of materials, tools and know-how as well as local customs, culture and aesthetics have given rise to a wide array of material and construction techniques. It is therefore not surprising that faced with such diversity of materials and applications, many computational and numerical approaches for the modelling of masonry structures have been developed.

Given the scope of the present study, it is unrealistic to aim to provide a comprehensive enumeration of the many techniques and advances in this area. Instead, this chapter will provide a brief overview of the two main classes of analysis techniques (i.e. quasi-static and dynamic methods), with the aim of putting into context the choice of numerical techniques employed in the present case study and highlighting the features which make each class of techniques unique and the situations where they may be applied successfully. The chapter will also present the general modelling approaches which may be applied for masonry structures using one or both of the analysis techniques explored earlier.

2.1 Methods of analysis for masonry structures

2.1.1 Quasi-static analysis methods

Quasi-static analysis methods are simple, yet surprisingly powerful tools for analysis of dynamic behaviour. By neglecting dynamic effects entirely, or by approximating them in a quasi-static fashion, they allow for a preliminary (or first-order) assessment of the behaviour of the structure under seismic conditions. Having relatively smaller requirements in terms of computational time and power, these methods have gained widespread acceptance as primary tools for assessment of masonry structures today (see [3] and [4] for further details).

2.1.1.1 *Limit equilibrium methods*

Limit equilibrium or limit analysis methods are based on fairly old ideas and some of the most amazing architectural works built in the eighteenth and nineteenth century, such as the Paris Pantheon and Saint Paul's Cathedral, were built based on the concepts of limit equilibrium. The scientific foundation of the concept of the inverted catenary was laid down by Hooke in 1675 and formalized by Gregory in 1697 [5]. The results of this discovery were later combined with graphic statics methods, developed by Culmann in 1866, thus allowing designers to evaluate the stability of vaults, buttresses and arches through drawing of thrust lines [5]. While the graphic statics method has been largely replaced by numerical tools, there has been a resurgence of interest in the application of this method through modern computer graphics [6].

Perhaps the most famous application of the static equilibrium method in architecture was the hanging models created by Catalan architect Antonio Gaudi. This design methodology takes advantage of the fact that masonry structures act predominantly in compression. Once Gaudi had established the most efficient form in tension, he inverted that form to construct a pure compression structure.

Couplet in 1730 and Coulomb in 1773 further developed Hooke's initial model to formulate a general approach that could describe the conditions of stability of masonry arches based on three assumptions: (1) masonry has no tensile strength, (2) masonry has infinite compressive strength, and (3) sliding failure between arch voussoirs does not occur [5]. Coulomb postulated that collapse will be caused by the rotation between parts due to the appearance of a sufficient number of hinges. The location of the hinges is a priori unknown but can be determined by the method of maxima and minima calculated iteratively.

In 1966 Heyman further generalised Coulomb's method for the study of block assemblies of any configuration through the application of bounding theorems of plasticity. Initially developed for calculation of collapse loads in plastic analysis of steel structures, Heyman demonstrated that these concepts can be successfully applied to the calculation of collapse loads in masonry structures. Using rigid-perfectly plastic block elements to represent an assembly of elements, it is possible to evaluate the load capacity and failure mechanisms of structures. This assumption means that the

deformations in the elastic field are considered to be negligible with respect to those produced in the plastic field.

However, the solution of the upper-bound theorem is not trivial and can become difficult for complex masonry structures [3]. Numerous numerical techniques have been proposed in order to extend the use of this technique for the study of more general block assemblies. Using a combination of vector analysis and linear programming algorithms, computer codes are now available which can establish whether it is kinematically possible for any block in a block assembly to move and become detached from the system. The main contributors to these efforts include Liveley in 1978, who pioneered the use of linear programming procedures, as well as Gilbert and Melbourne, whose rigid block model developed in 1994 applied compatibility conditions on the block system [3].

The modern methods of limit analysis can be used for both micro-modelling, where the interface elements explicitly model the weak mortar joints and mortar-unit interfaces, while the blocks model the masonry pieces, as well as for macro-modelling, where the joints model location of potential cracks and the blocks model undamaged, homogenous materials [7].

The principal advantage of the limit analysis approach continues to be its simplicity and ease of use. In comparison to more complicated techniques, limit analysis can provide a quick, often first order, understanding of the structural behaviour. This method also allows for rapid evaluation of the effect of interventions on the structural behaviour. Contrary to other analysis methods which are based on computation of stresses, limit analysis can provide forces which can then be used directly in the design process [8]. However, the application of this method to masonry structures requires experience and a thorough understanding of structural behaviour in order to construct representative block assemblies which properly capture the behaviour of the entire system.

The work of Orduña at the University of Minho has resulted in creation of tools which allow for modelling of block assemblies in both 2D and 3D ([7] and [4]). This work allows for the seismic evaluation of historic structures through the calculation of horizontal forces which are required to create a mechanism in the structure. This method simplifies dynamic loads into a series of varying horizontal loads, applied at the centroid of each block, which are proportional to a seismic coefficient, α . The seismic coefficient is a direct measure of the level of ground acceleration required to destabilize the structure [7]. Examples of the application of this method to historic masonry structures are presented in Figure 2-1.

It is important to note that limit analysis has very limited applications for seismic analysis of slender multi-drum structures such as the Temple in Évora. This is due to the fact that the limit analysis approach does not examine subsequent behaviour of the system of blocks or redistribution of loads, nor does it include consideration of dynamic stability caused by equilibrium of self-weight and inertial forces. These ideas will be further developed in section 4.2 of the study where the application of limit analysis to the present case study is presented.

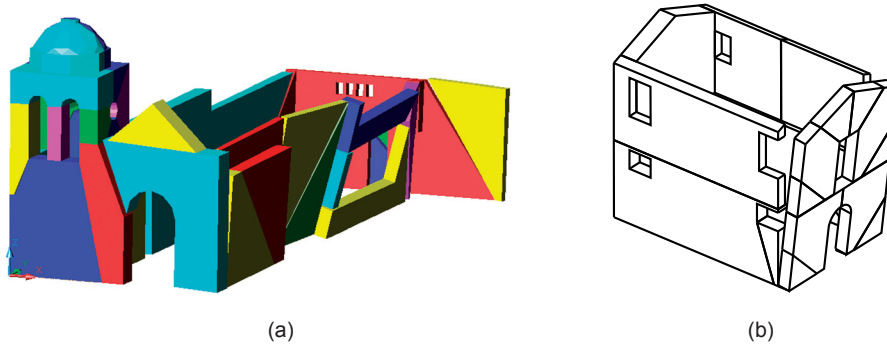


Figure 2-1: Application of 3D limit analysis to the seismic evaluation of historic masonry structures (after (a) Orduña et. al [9] and (b) Orduña [7])

2.1.1.2 Non-linear (pushover) analysis

Pushover analysis is a non-linear static analysis carried out under conditions of constant gravity loads and monotonically increasing horizontal loads [10]. Initially developed for the analysis of frame-type concrete and steel structures, this technique has also been applied in recent years to seismic analysis of masonry structures.

The inelastic static pushover analysis is a method of predicting seismic force and deformation demands while accounting for the redistribution of the internal forces that develop when the structure is subjected to inertia forces that can no longer be resisted within the elastic range of structural behavior [11]. This behaviour along with the appropriate material constitutive model can be used to determine the onset of cracking in the structural model. However, an accurate prediction of the ultimate or collapse loads remains very difficult due to instability of the solutions at higher displacements.

The quasi-static non-linear analysis method requires a simplification of dynamic earthquake loads. This is often accomplished in one of two ways: 1) to apply a constant horizontal acceleration to the structure, which is the equivalent of applying a constant horizontal ground motion and 2) to apply horizontal forces distributed along the height of the structure, which are meant to more closely approximate the effects of an earthquake. In fact, section 4.3.3.4.2.2 of Eurocode 8 [10] specifies that “at least two distributions of the lateral loads should be applied:”

- a “uniform” pattern, based on lateral forces that are proportional to mass regardless of elevation (uniform response acceleration);
- a “modal” pattern, proportional to lateral forces consistent with the lateral force distribution in the direction under consideration determined in elastic analysis (in accordance with lateral force method or modal response spectrum analysis).

In addition to these load distributions, several other load patterns have been developed in recent years. These include the inverted triangular pattern, which can be used to approximate the structure’s

first mode of response, as well as multi-modal and adaptive patterns [12]. These methods have been developed in order to address the shortcoming of pushover analysis when dealing with irregular structures where accumulation of damage alters the initial modal properties of the structure. Thus, these methods allow the numerical model to be progressively updated to take into account evolution of the structural response in terms of stiffness degradation as well as variation of modal properties [12].

The most important consideration in the application of pushover analysis to masonry structures is the proper formulation of the material constitutive models or damage models. This is especially important when the pushover method is applied through continuum modelling techniques such as finite element method. Several approaches have been developed over the years which can be used in order to characterise these relations. The two major models are the micro-mechanical and macro-scale damage models. These issues will be dealt with in greater detail in section 2.2.1.

Just as with limit analysis, the applicability of pushover analysis to slender multi-drum structures is limited. Although pushover analysis offers advantages in terms of required computational power in comparison to full dynamic time history analysis, it cannot be applied reliably to multi-drum structures since it does not account for dynamic stability caused by equilibrium of self-weight and inertial forces during a seismic event. Furthermore, since the failure mode for this type of slender structures is almost due to sliding or rotation of the blocks against each other rather than the failure of the blocks themselves, pushover analysis offers limited advantages in comparison to limit analysis. These ideas will be further developed in section 4.3 of the study where the application of pushover analysis to the present case study is presented.

2.1.2 Dynamic analysis methods

In contrast to static methods explored in the previous section, dynamic analysis methods take into account inertial effects caused due the oscillating nature of strong ground motion. These methods generally provide a better approximation of the structural response under dynamic loads.

2.1.2.1 Analytical approaches

The dynamic behaviour of blocky structures, subject to dynamic loads is an extremely complex phenomenon, characterized by highly non-linear behaviour consisting of a complicated sequence of rocking and sliding motion. The response is made even more complicated when a system of blocks is under investigation, since each block can undergo displacements due to rocking or sliding either individually or in groups. This behaviour often leads to unpredictable and highly-sensitive switching between different natural modes of vibration for the structure.

The investigation of the dynamics of rigid blocks dates back to the beginning of the twentieth century with the ground breaking work of Japanese seismologist Fusakichi Omori at the Imperial University of Tokyo. In a series of experiments published at the turn of the century ([13] and [14]), Omori investigated the complex nature of the motion of the blocks when subjected to simple initial

displacements. These experiments lead him to conclude that the response of such a system is highly complex and dependant on the input excitations.

It would take a half century until a fundamental analytical study of the response of single rigid blocks was provided by Housner in 1963 [15]. In his analytical calculations, Housner considered the rocking motion of rigid blocks having sufficiently large coefficients of friction so as to restrict sliding. He then provided analytical solutions to the calculation of the period of oscillation of a block, first assuming no loss of energy at impact, followed by a complete formulation consisting of reductions due to loss of kinetic energy at impact. Housner's analytical solutions for both cases remain benchmarks for testing of new numerical techniques dealing with motion of distinct rigid block elements. Housner also provided an estimate of the minimum horizontal acceleration at the base that is required to overturn an infinitely rigid body.

Yim et al. applied a probabilistic approach to the problem of rigid body rocking [16]. Having discovered that the response of the block varied greatly, between minimal movement and complete overturning, when subjected to the same magnitude of randomly generated horizontal ground motion, Yim et al. concluded that overturning of a block by a ground motion of particular intensity does not imply that the block will necessarily overturn under the action of more intense ground motion.

A recent and comprehensive investigation into the dynamic behaviour of rigid blocks was conducted by Prieto in 2007 [17]. In his dissertation, Prieto proposes a novel formulation for the rocking motion of rigid-blocks which can be extended to analysis of multi-block systems.

2.1.2.2 Response-spectrum modal analysis

Modal analysis is probably the most widely used dynamic method in practice for the design of modern structures. This approach utilises the principal of linear superposition of modal response in order to provide the dynamic response of the structure based on a linear-elastic response spectrum. Thus the method is especially useful for implementation as a part of modern building codes.

The procedure for application of response spectrum analysis begins with the decomposition of the multi-degree of freedom structural system into a series of linear single degree of freedom systems. Next the response of each system based on the required response spectrum is computed and combined algebraically to achieve the total response of the entire system. This procedure is continued mode by mode until the contribution of the additional modes become negligible and the cumulative modal mass participation reaches levels above 90%.

Even though the modal analysis technique provides a quick method for dynamic analysis of structures, its failure to account for material and geometrical non-linearities make this method unsuitable for application in the seismic evaluation of masonry structures [7]. However, modal analysis may prove a useful tool in understanding the overall behaviour of the structure, including the principal modes of vibration and the likely locations where cracks would form.

2.1.2.3 *Non-linear time history analysis*

Although analytical solutions provide insight into the nature of the dynamic behaviour of masonry structures, their complexity, even at the level of two stacked blocks, demonstrates the need for computational tools which can correctly address the problem of rigid block dynamics. Non-linear dynamic analysis provides the most complete method of analysis of structures subject to seismic action. This method takes into account material and geometrical non-linearity of the structure as well as capturing the full dynamic effects through the time integration of the differential equations of motion in response to the input ground accelerations. As with the non-linear static (pushover) method, an important consideration in the application of the non-linear dynamic analysis is the constitutive models used to represent the material non-linearities [18].

The application of non-linear time-history analysis requires an input of ground accelerations with respect to time. These acceleration records are generally created artificially based on the design elastic response spectrum presented in building codes. Section 4.3.3.4.3 of Eurocode 8, Part 1 deals specifically with non-linear time history analysis and sets out guidelines on the requirements for its application in design situations [10]. Eurocode 8 requires at least three independent time-history analysis to be performed, from which the most unfavourable response shall be used for design purposes.

Although time-history analysis provides an accurate way to measure the structural response to seismic loads, for highly non-linear systems its results can be misleading. As it was explained before, the dynamic response of rigid blocks is characterised by highly complex and highly non-linear behaviour. When subjected to an initial displacement of random base accelerations of the same intensity, rigid blocks could have widely different responses which are not always dependant on intensity level. Thus for such systems, a more comprehensive, parametric approach is needed where the response of the system over a range of ground motions intensity is studied.

Incremental Dynamic Analysis (IDA) is a parametric analysis method which was developed at Stanford University and formalised by Cornell in 1990s to more thoroughly evaluate structural performance under seismic loads [19]. It involves subjecting a structural model to one (or more) ground motion record(s), each scaled to multiple levels of intensity, thus producing one (or more) curve(s) of response parameterized using a desired measure versus intensity level. While this method was impractical in the past and was reserved mainly for academic pursuits, the growth of computational power now allows for a complete analysis of response across a range of intensities in order to obtain a better understanding of the overall trend and to characterise the extent of non-linearity/sensitivity of the structural model to input parameters.

The present study includes a multi-record incremental dynamic analysis of the temple's response completed using a discrete element model. Three accelerograms for each type of seismic action are used at various intensity levels in order to demonstrate the behaviour of the structure's dynamic response and evaluate its performance with respect to the current design codes.

2.2 Modelling strategies for masonry structures

In addition to the available methods of analysis explored in the previous section, there exists a whole array of modelling techniques which allow for the numerical representation of the structure and its constituent elements so that the required analysis method could be applied. While some of the modelling techniques are applicable over a range of analysis types, some are limited to a particular case, often becoming synonymous with the analysis technique.

2.2.1 Finite element representation

The finite element method is the most widely used numerical modelling technique in engineering. Developed in the 1950s, this method has been a subject of intense research over the past sixty years, leading to many advances and a wide variety of implementations and features. However, the basic principles remain unchanged. In finite element computations, the structure is divided, or discretized, into smaller elements, each with their own material properties for which relations between the nodal forces and displacements are known. These elements are assembled together with the boundary conditions, resulting in a system of equations whose solution can be used to compute nodal displacements as well as strains and stresses at integration points [20].

Finite element representation has been used for the modelling of masonry for many years. However, given the heterogeneous and non-linear nature of the material, especially the effect of mortar joints on the overall characteristics of the material, accurate representation of material behaviour has been very challenging [21]. The need to consider the influence of joints has led to the development of two broad modelling approaches for modelling of masonry using the finite element formulations: the continuum and discontinuum representations [18].

2.2.1.1 Continuum finite element models

In this approach, masonry is simulated as a homogeneous continuum taking into account the mechanical effects of the joints through an appropriate constitutive material model. While modern computing power allows for construction of detailed finite element meshes composed of millions of degrees of freedom, the most challenging aspect of continuum analysis of masonry remains the choice of the applicable material model. Elastic material models have been used with great efficiency to provide a first approximation of the stress distribution as well as the overall behaviour of historic structures [18] (see also [1]). The elastic analysis is quite reliable when general compression states are prevailing. However, this approach is only applicable until the first masonry joint begins to open, thus limiting its ability to predict the collapse loads and failure mechanism [22].

Continuum methods are widely used to assess the dynamic response of masonry structures and are mostly used to determine the steady-state dynamic response through modal analysis. The modal response of the structure is often used to determine where stresses are highest and where cracking might occur [22]. Thus, continuum methods can be effective in predicting locations of damage, but fall

short when trying to predict collapse or the actual transient dynamic response of interacting distinct bodies.

A more realistic modelling of the behaviour of masonry components can be achieved through application of homogenisation theories for periodic media. These techniques allow the global behaviour of masonry to be derived from the behaviour of its constituent parts, namely the masonry units and the joints [18].

2.2.1.2 Discontinuum finite element models

In masonry structures, joints are the largest contributors to the non-linear behaviour of structures observed in the field and in experiments. This fact has led many researchers to consider modelling techniques through which the joints are explicitly represented in the numerical models [18], [21]. Discontinuum idealizations using joint or interface elements allows for representation of masonry as a continuous medium cut by joints. This approach originated from the field of rock mechanics in order to allow the discontinuity of individual faults to be modelled using finite elements [18]. This development draws the finite element formulation closer to the discrete element approach presented in section 2.2.3, which was also developed to address slope stability in rock mechanics [3].

This approach, usually termed micro-modelling, uses continuum finite elements to represent blocks and specifically formulated joint elements to represent the interfaces between the blocks, where relative displacements and local failures are accommodated through an appropriate constitutive model [21]. Thus the combined action of the masonry block, joint material and the interface between the blocks and the joint material can be explicitly modeled, studied and compared with experimental results.

Although finite element methods can be used for the analysis of problems with some discontinuities, these methods are not suitable for the analysis of systems that are characterized by continuous changes of their geometry and the contact conditions among individual bodies [23]. This is especially true for multi-drum structures where rocking motion of the drums are the primary means of energy dissipation, thus requiring a robust contact detection scheme capable of accommodating large displacements and rotations. Furthermore, most modern general discrete element formulations are now capable of representing deformable blocks through internal finite element discretization [3]. Thus the present study will not consider a finite element model of the Temple structure.

2.2.2 Macroelement representation

The macroelement modelling method has been devised as a rapid approach to model the collapse behaviour of masonry structures. Having some prior knowledge about the likely location of cracks and discontinuities, achieved either through other dynamic approaches (e.g. modal analysis or non-linear dynamic analysis) or by reference to abacuses of possible collapse mechanisms based on typical damage patterns for the constructive type under consideration (e.g. row houses, churches, etc.), the

macroelement models can be used to apply the static approaches discussed in section 2.1.1 without the need for complicated numerical models.

In order to apply the method, the structure is divided into smaller components along the lines of potential cracks. Each macroelement is considered to be a homogenous entity with specific constructive characteristics and structural behaviour. When applied with limit analysis, all possible rigid body collapse mechanisms are enumerated and the seismic mass multiplier, α , required to destabilize the block assembly is evaluated. Figure 2-2 includes two examples of macro-element representation used for seismic limit analysis of historic masonry structures.

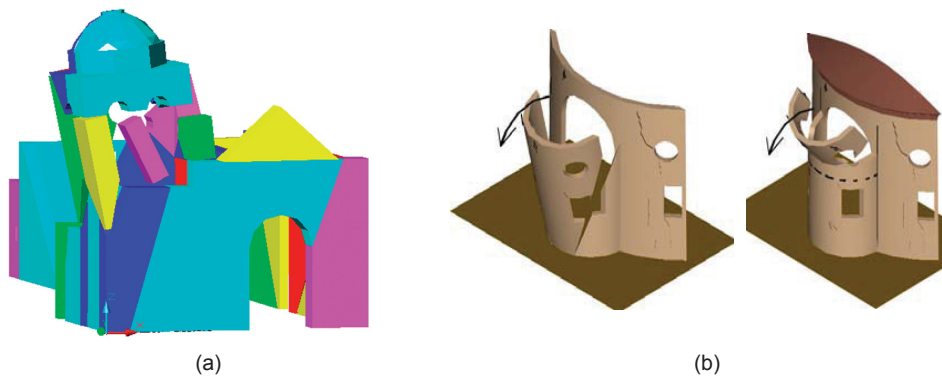


Figure 2-2: Example of macro-element representation of masonry (after (a) Orduña et.al [9] and (b) Modena [8])

3MURI developed by S.T.A. DATA and University of Genova is an example of commercial macro-element modelling software with the capability to run quasi-static analysis procedures. *Block*, developed by Orduña at the University of Minho is an example of a macro-element modeling tool which, together with a solver engine written on the *GAMS* modelling system, performs 2D and 3D limit analysis on block assemblage models [24]. The present study will use *Block* in order to create and run the numerical models of the temple structure using limit analysis approach.

For the purposes of seismic analysis of multi-drum structures, the macroelements are often taken to be equivalent to individual column drums and architrave elements, with the boundaries representing contacts between the blocks. Thus in many ways, the results of the discretization of the structure is the same as that which is used in the discrete element representation. However, unlike discrete element codes, the macro-element or macro-block modelling codes do not generally incorporate automatic contact detection and generation logic and are thus unsuitable for analysis techniques which allow for large displacements and rotations.

2.2.3 Discrete element representation

The discrete, or distinct, element method was proposed by Cundall in 1971 for the study of jointed rock and fractured rock masses, modeled as an assemblage of rigid blocks [3]. Later, this approach was extended to other fields of engineering, where the detailed study of the mechanical behaviour of multiple bodies, blocks or particles is required, ranging from geotechnical engineering to pharmaceutical process design [25].

There have been many applications of the discrete or distinct element approach to the problems of representing masonry behaviour. Most approaches, however, share a common goal which is to represent the masonry fabric as a discontinuous assemblage where the mechanical behaviour of the constituent blocks are treated separately from the interaction between them, thus “regarding joints as surfaces of contact between distinct bodies” [3].

In recent years, the boundary between discrete element method and finite element method have been blurred by the latter’s introduction of contact or interface elements to allow for modelling of discontinuous mediums. However, most finite element codes still lack automatic contact detection and the formulation of the interface elements based on contact mechanics remains somewhat problematic, especially for complex models [3].

One of the most powerful features of the discrete element method is the ability to model the response of structures up to stages of collapse without the loss of stability in the explicit solution. Thus large displacements in a system accompanied by a high level of geometrical non-linearity are accommodated and represented with a high level of accuracy. Coupled with the ability to model material non-linearities for both blocks and contacts, the discrete element technique has become indispensable in the analysis of deformations and stability of blocky structures under seismic loads. Lemos [3] provides an excellent and comprehensive overview of recent efforts in the application of discrete element analysis for analysis of masonry structures, including a variety of methods available as a sub-set of discrete element method, for example dealing with damage.

The past ten years have witnessed considerable amount of research in the use of discrete element methods for static and dynamic modelling of problems in masonry. In particular, there is a growing body of work related to the use of discrete element models for the study of the dynamic response of multi-drum structures. These include the comparison of discrete element analysis and experimental data obtained through shaking table test of drum columns by Papantonopoulos et al. in 1998 [26] as well 3D seismic analysis of the proposed interventions for the Parthenon Pronaos conducted by Lemos et al. in 2003 [27]. This increase in research interest is in due in large part to the increased computational power and availability of general purpose modelling software such as UDEC and 3DEC created by Cundall and Itasca Consulting.

The most recent concerted effort in the application of discrete element method to multi-drum structures has been initiated by Papaloizou and Komodromos [28], [29]. Their investigations focus on development of discrete element tools which are specifically designed for the analysis of classical multi-drum columns and colonnades. However, at present, their efforts are limited to planar analysis of drum assemblies. As it will be shown in later chapters, even in cases where the ground acceleration is applied in-plane, considerable out-of-plane motion can occur, thus rendering the planar assumption invalid. Figure 2-3 provides two examples of application of discrete element modeling to the dynamic evaluation of masonry structures.

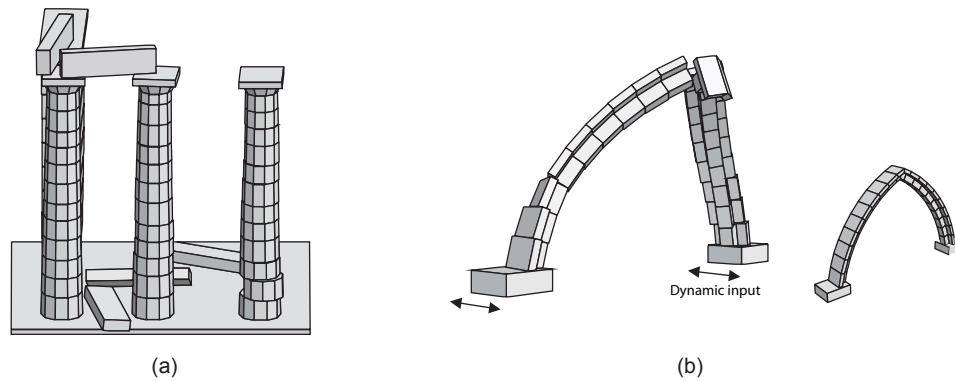


Figure 2-3: Examples of discrete element representation of masonry block structures applied to (a) a section of Parthenon Pronaos and (b) to a pointed masonry arch (after Lemos [3]).

As with the continuum finite element models, discrete element models can be used in analysis of structural failure using either quasi-static or fully dynamic analysis methods discussed earlier [3]. Many analysis tools are now available for discrete element modelling of structures. However, UDEC and 3DEC, developed by Itasca consulting are arguably the most widely applied discrete element tools. Both software applications are based on the research of Cundall, Hart, Strack and Lemos between 1970 and 1980 [3]. Explicit integration is used with sufficiently small time steps to ensure computational stability. Blocks can be either rigid or deformable, and joint properties and Rayleigh damping properties must be defined. The current study will consider a 3D discrete element model of the temple structure, developed for the discrete element code 3DEC, for both non-linear static (pushover) analysis as well as non-linear incremental dynamic analysis. Further details about the application of this method are provided in Chapter 5.

Chapter 3

THE ROMAN TEMPLE OF EVORA

This chapter provides a brief historical overview of the city of Évora as well as the Roman Temple from the Roman settlement of the area until the end of nineteenth century. In addition, a complete description of the Temple, including its architectural style, material and current state is provided. Finally, a brief survey of previous archeological and structural studies of the structure is presented.

3.1 Historical Overview

Évora is a Portuguese city in the municipality of Évora, located within the south-central region of Alentejo. The city is located 100 kilometers east of the Portuguese capital, Lisbon. Figure 3-1 shows the location of the city as well as the location of a number of landmark structures within the city's historic centre, including the subject of this case study, the roman temple (marked as item 1 on the map).

Most historians and archeologists believe that the foundation of the city could date more than two millennia [30]. However, despite numerous archeological excavations in the area, no evidence to support this theory has been found to date. The most compelling evidence for this hypothesis comes from the name of the city. During the Roman settlement in the area, from approximately first century BC until fifth century AD, the city was known as Eborā Liberalitas Iulia. Furthermore, the Roman author Pliny, writing in the first century, reports that a fortified settlement had existed at this location before the Roman Empire [31]. The name Eborā does not have a Latin root and is believed to be Celtic in origin, coming from the word “eburos” meaning the yew tree.

According to a legend popularized by humanist and writer André de Resende of Évora (1500-1573), Évora had been the headquarters of the troops of the Roman general Sertorius, who along with

Lusitanos would have faced the power of Rome [30]. What is known with certainty is that Évora, following the four year civil war, spanning 49 – 45 BC, was elevated to municipium, a distinct state under the jurisdiction of Rome, under the name Ebora Liberalitas Lulia, an honorary title presumably granted by Julius Caesar for the city's support during the war [31]. With the accession of Emperor Augustus (63 BC – 14 AD) in 27 BC and establishment of Pax Romana, the Roman Empire enjoyed a long period of relative peace which allowed for many administrative reforms to take place. During this period, Évora which had been integrated into the province of Lusitania, underwent a series of urban transformations, rising in status and stature as evidenced by the many prominent buildings which were erected in this era [32]. However with the exception of the Roman Temple of Évora and the public baths (discovered in recent excavation underneath the Évora municipal building), few traces of the urban fabric of Roman Évora remain today.

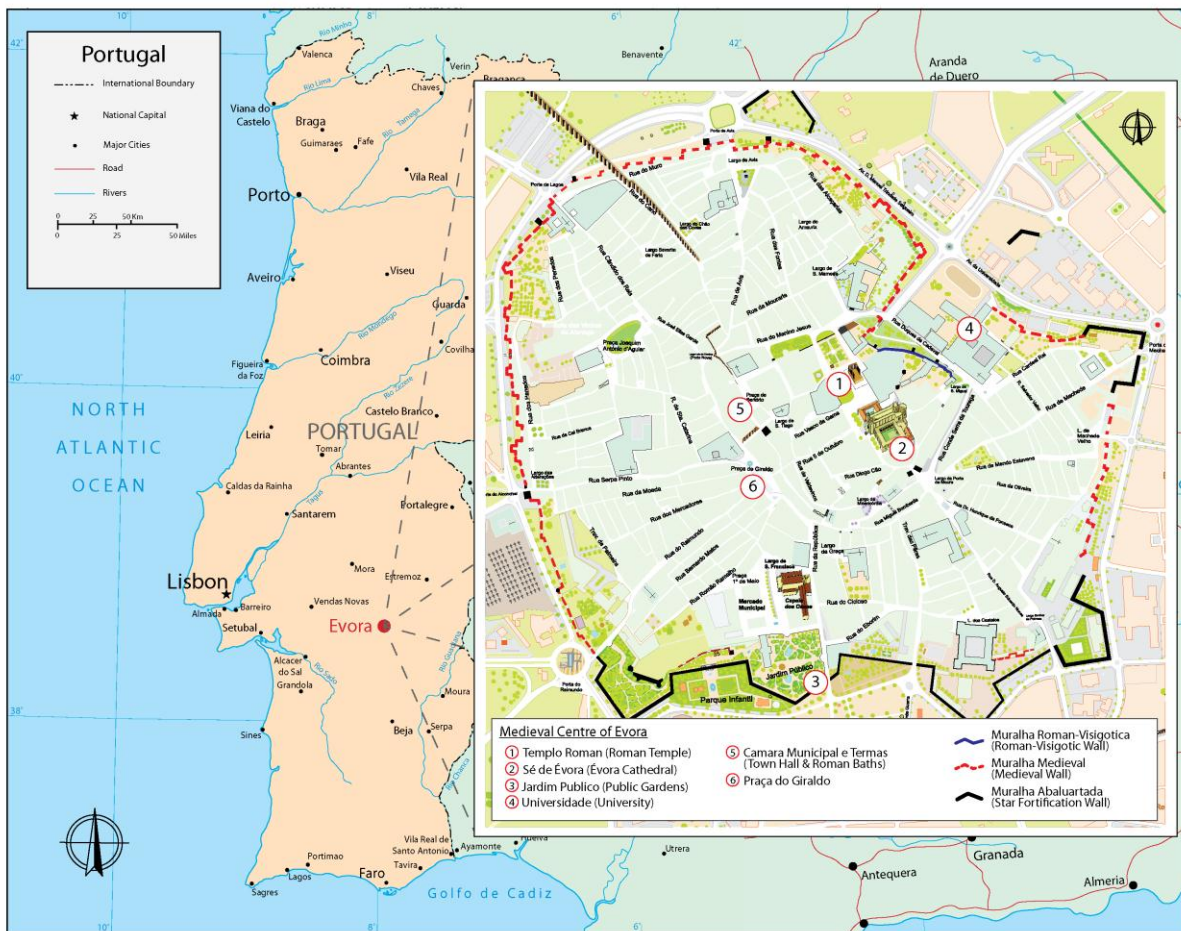


Figure 3-1: Map of Portugal and Spain, inset with plan of Medieval and Roman centre of Évora.

The Roman forum and the temple were located at the highest point within the area in accordance with the strictly codified guidelines of Roman architecture and construction, such as those reported by Vitruvius. Given the location of the temple, it is possible to establish the location of the forum as well as the principal axis of the city. Since Roman cities followed a Hippodamian grid scheme, the orientation of the remains can be used to establish the location of the two main and orthogonal

thoroughfares marking the north-south and east-west directions. While in Évora, the location of *Cardo Maximus*, the principal north-south street is known, the location of *Decumanus Maximus*, the main east-west street, is still the subject of debate [31].

The Roman Temple was most likely completed in the first century AD, given the detailing and stylistic characteristics of the capitals [33]. The temple has been traditionally associated with Diana, the Roman goddess of moon, the hunt and chastity. However, there is no archeological evidence to support this association. In fact the first references to the Temple of Diana (*Templo de Diana*) seems to be attributed to seventeenth century priest Father Manuel Fialho and appear in *Évora Gloriosa* compiled by his contemporary, Father Francisco da Fronseca [34]. Today, most experts believe that the temple was probably dedicated to the imperial cult and was associated with the worship of Emperor Augustus at its inception[32]. Archaeological excavations at the site have shown that the temple was partially surrounded by a pond and was most likely positioned at the centre of a monumental portico gallery [33]. The stone used to construct the temple has been previously analysed by Lopes et al. using a petrographic technique. The analysis revealed that the columns and architrave are made of local granite, while the marble capitals and base were extracted from the nearby quarry in Estremoz [35]. A complete description of the architectural features of the temple is provided in section 3.2.

Internal instability in the third century as well as the aftermath of the first barbarian invasions led to the fortification of many Roman outposts, including Évora. Today only fragments of the Roman walls remain, with the best preserved section currently visible at Casa de Burgos, the current home of Direcção Regional de Cultura do Alentejo. This period also witnesses the Christianisation of the peninsula, during which Évora was established as a bishopric seat. It is interesting to note Évora's importance in early Christianity since Quinciano (*Quintianus Episcopus Elborensis*) the bishop of Évora appears on the list of bishops who attended the Council of Elvira, held around the year 306.

With further disintegration of the Empire and beset by new waves of Germanic invaders, Évora was at last conquered and came under the rule of the Visigothic king Leovirgild in 584. This period is considered by some to correspond to a dark age for the city since it brought about a general decline in cultural production and importance of the city. Consequently, little information is available regarding this period of the city's history. Most experts believe that the temple was destroyed during the Visigothic invasion. However, given the lack of reliable information, it is impossible to ascertain the time and manner in which the temple suffered the major damages that left the entire southern half of the temple in ruins.

Records show that Diocese of Évora continued to exist throughout this period, as evidenced in references to the bishop of Évora in the Visigothic Councils of 597 and 633 [32]. Dias contends that these references reinforce the importance of Évora as a religious centre and can be used to support the idea that the city basilica might have been established in the now defunct temple, similar to the rededication of the *Maison Carrée* in the fourth century. This idea is further supported by the discovery

of Visigothic ornament near the temple site which could indicate later additions and modifications to the temple [32].



Figure 3-2: Evolution of the city of Évora from (a) the first century AD until (d) the medieval era (after Gustavo Silva Val-Flores, 2006).

In 714, at the height of Muslim invasion, the Visigothic Évora (known then as Elbora or Erbora) was taken by Abd al-Aziz ibn Musa, first ruler of Al-Andalus. This established a period of Moorish rule from 715 until 1165, during which the town thanks to its geographical location, slowly began to prosper again and developed into an agricultural center [31]. The Moors, who called themselves Yaburah, greatly influenced the fabric of the city, building a fortress and a mosque on top of the remains of the Roman Acropolis [36]. This period also witnessed urban densification which obscured the ancient Roman orthogonal matrix, creating a more convergent, radial and organic form of urbanism

characterized by narrow passages and winding roads, features that are still preserved in the historic center of the city.

Although the Moorish rule brought about a period of stability, the city was not immune from attacks by warring Muslim factions as well as neighboring kingdoms. In 913, Ordoño II laid siege to the city and thanks to the crumbling ancient Roman walls, the city fell and many of its inhabitants were killed. However, the city was again repopulated and new defensive walls erected on the ruins of the Roman walls. These walls continued to be the city's only defences until the fourteenth century when the wider medieval fortification was completed and the expanded quarters outside the city proper were once again reintegrated into the city. Figure 3-2 illustrates the growth and evolution of the city through the different eras as well as likely locations of some of the important monuments.

Similar to the Visigothic era, little information has been discovered about the state of the city's monuments during the Moorish rule of the city. It is possible that the Moors, who had built their fortress in the area of the ancient Roman forum, had used the temple or stones from the ruins for their construction.

In 1165, the Moorish rule of the city of Évora came to an end when the city was captured by Gerald the Fearless (Geraldo Sem Pavor) as a part of the wider Reconquista and brought under the control of the first Portuguese king, Afonso Henriques [36]. This heralded a new phase of growth for the city, which by the end of the sixteenth century had become the second most important city in the kingdom [36].

Only a limited amount of information survives about the state of the city's Roman monuments during this period. It is widely accepted that the cathedral and the old town hall were built on top of the Islamic fortress in the area of the ancient Roman forum. According to the writings of Portuguese chronicler Fernão Lopes (1385-1459), during the fourteenth century, the temple was almost in ruins and was incorporated into the town's castle and used as a vault [37]. The remains of the temple's podium, columns and architraves were embedded inside the medieval walls and a tower was constructed above the structure. Lopes indicates that by the end of fourteenth century, the structure had been transformed into a public slaughterhouse. This is further confirmed when in 1467, King Afonso V of Portugal authorized Sueiro Mendes, the town's butcher, to remove stones from the structure for building purposes and defense [37].

While the various uses of the temple have caused irreparable damage to many of its components, the continued use of the building by local population over centuries is most likely the reason why this building has been preserved until present day. Most buildings of this type, built at the outpost of the Empire quickly began to suffer from neglect, abuse and ultimately complete destruction due to cultural and religious clashes between the conquerors and the indigenous heritage as well as loss of association between the everyday life of the city and its ancient past. An example of this can be found in Évora itself, when in 1570, the remains of a Roman triumphal arch, adorned with statues and left largely intact from the Roman times, was destroyed in order to the Church of St. Anthony to Giraldo

Square. However, in the case of the Roman Temple of Évora, this fate was largely avoided since the building served a multitude of purposes along its history and remained a relevant part of the everyday life. It is also important to note that the continued importance of city as a cultural and religious centre also insured that the temple and many other buildings of architectural and cultural value were preserved to this day. Figure 3-3 shows two woodcuts produced in the eighteenth and nineteenth century showing the state of the medieval additions to the temple structure.

The sixteenth century corresponds to the peak of Évora's importance on the national scene, serving as one of the most prominent cultural and artistic centers of the kingdom. This period coincides with the height of the Portuguese Age of Discovery which lasted between 1415 and 1543. During this period, the city served as a royal residence for Portuguese kings including D. João II, D. Manuel I and D. João III, leading to the construction of many palaces, monuments and religious buildings. D. Manuel I built his royal palace at Évora, in a mixture of the Mudejar, Manueline and Renaissance styles. D. João III's reign brought about the construction of the beautiful Renaissance Igreja da Graça as well as a new Aqueduto da Água de Prata, designed by Francisco de Arruda between 1531 and 1537 [31]. Recent research has shown that the aqueduct was constructed on the ruins of the original Roman aqueduct in the same area [38].

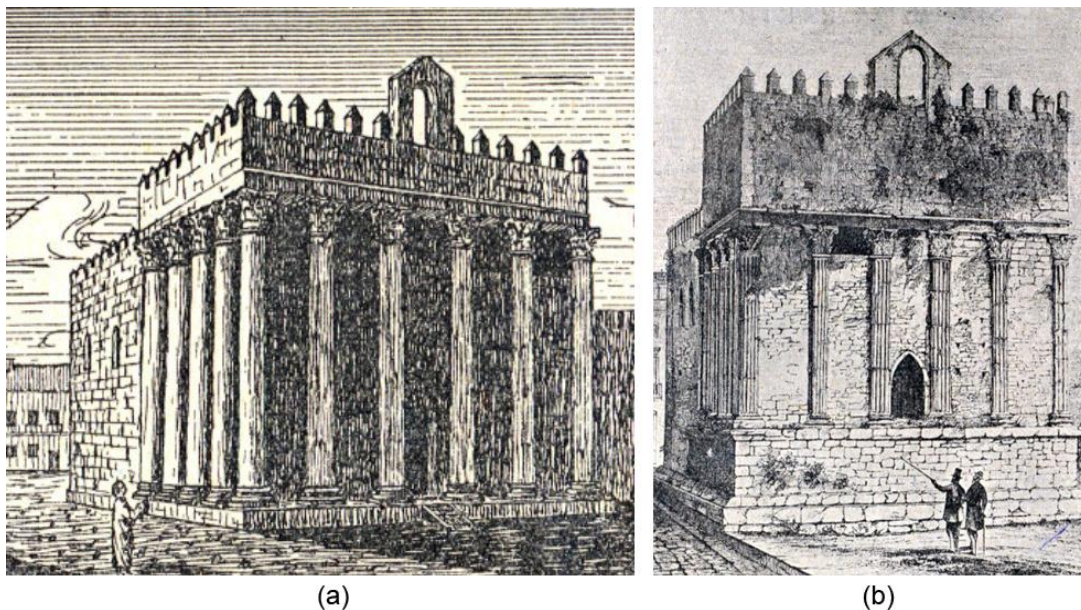


Figure 3-3: Woodcuts showing (a) the state of the structure in 1795, as drawn by Murphy and (b) the structure in 1865 with the base exposed and prior to the removal of the medieval walls and tower (after Pereira [39]).

1559 marked the founding of the University of Évora by Cardinal Infante D. Henrique (the future king of Portugal) and Pope Paul IV, to be administered by the Society of Jesus. The Jesuit college in Évora (Colégio do Espírito Santo) continued to operate until it was closed in 1759 following the expulsion of the Jesuit order by the Minister of the Kingdom, the First Marquis of Pombal [40]. During the Portuguese Inquisition, between 1536 and 1781, Évora was one of three cities, others being Lisbon and Coimbra, to host the Courts of the Inquisition.

The seventeenth and eighteenth centuries saw a continuation of building and renovation of many monuments in the Mannerist style. However, the major event of the eighteenth century was the 1755 Lisbon earthquake, which devastated Lisbon and surrounding areas and killed many thousands of people. Seismologists today estimate the Lisbon earthquake had a magnitude in the range 8.5–9.0 on the moment magnitude scale. The earthquake, as well as the tsunami and fires which followed, caused massive destruction in Lisbon, where almost eighty-five percent of building stock were destroyed. The destroyed buildings included the Royal Ribeira Palace, Carmo Convent and the new Opera House, opened just six months before. On the ruins of Lisbon emerged a new city with a new style of seismically protected buildings, known as Pombaline after the Minister of the Kingdom, the First Marquis of Pombal who oversaw the rebuilding effort. This effort is unique since it also included the first dynamic testing of models using marching troops. In addition to the earthquakes transformation of the urban fabric of Lisbon, the earthquake had a profound effect on politics and philosophy of the era.

Apart from the reconstruction effort, the 1755 earthquake is considered by many as the beginnings of the science of seismology. Following the earthquake, the Marquis of Pombal commenced an extensive campaign of documenting the effects of the earthquake throughout the kingdom. Records from these investigations seem to indicate widespread devastation in areas beyond the coastal areas. However, it appears that the city of Évora and its surrounding area remained largely unharmed by the earthquake thus allowing many of the monuments to survive the catastrophe.

The nineteenth century brought about a complete transformation of the historic centre of Évora, some of which caused the destruction of many heritage structures. The Manueline town hall and fair ground at Praça do Giraldo were demolished and in its place, the building for the Bank of Portugal was erected. The Convent of St. Francisco was also demolished to make way for new housing quarters. The medieval walls were largely preserved. However, the old gates, with the exception of the Avis gate, were all torn down.

This period also saw a renewed interest in the Roman Temple of Évora. The slaughterhouse which had continued to operate at the temple site since the fourteenth century was finally closed in 1836. In 1840, Cunha Rivara, the acting director of the Public Library of Évora was given permission to demolish the buildings annexed to the north side of the monument during the Inquisition and to commence the first archeological excavation undertaken in Portugal [37]. The excavations revealed tanks at the base of the building which were likely connected to an ancient aqueduct. During this period, under the overburden stress caused by the additions throughout centuries as well as contemporary efforts to revitalize the surrounding square, some portions of the ancient tanks as well as the roof began to cave in and threatened the stability of the entire structure. Thus in 1869, Augusto Filipe Simões proposed that the medieval additions be destroyed in order to relieve the stresses and restore the structure to its original form [37]. This proposal was preceded by a graphical restoration of the building which was completed in 1789 by architect James Murphy.

However, it would take three more years until the vestiges of the medieval structures were finally removed under the direction of Italian architect Giuseppe Cinatti. While it seems that the original plans intended to restore the structure to its “original” form, as advocated by Simões, this process did not materialise. While the reasons for this change are not clear, it is possible to speculate that Cinatti may have been influenced by a change in attitude with respect to historic monuments. The nineteenth century was marked by an awareness of architectural heritage and a need for development of theoretical framework to support application of restoration to historic buildings [41]. The prevailing restoration theories at this time included *restauro archeologico* which was favoured in Italy and influenced the work of architects Stern and Valadier, *restauro stylistico* which was spearheaded by French architect and theorist Viollet-le-Duc, and the anti-restoration movement in England as advocated by Ruskin and Morris. Figure 3-4 shows the evolution of the temple structure from the first century AD until the nineteenth century restoration by Cinatti.

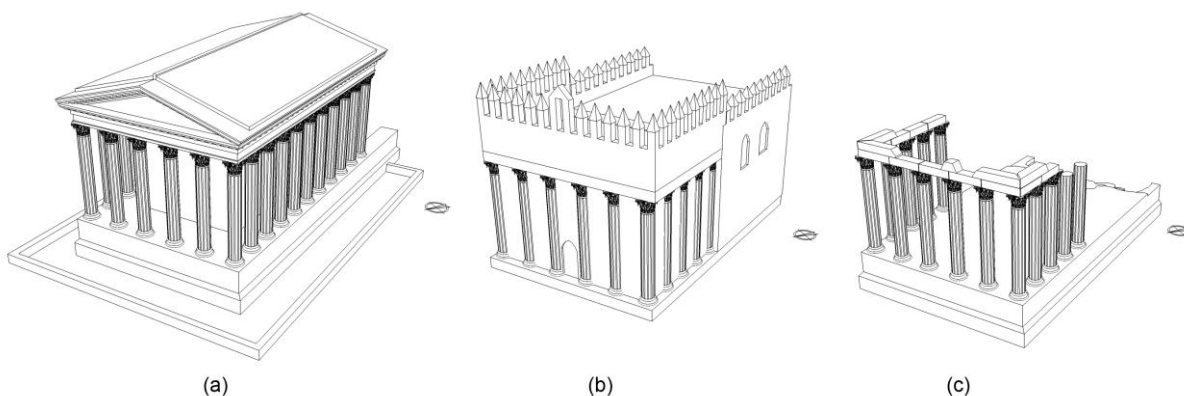


Figure 3-4: Evolution of the temple structure: (a) reconstruction of the “original” structure from first century AD; (b) remains of the medieval structure from mid eighteenth century (after Pereira [39]); (c) current condition.

While Cinatti seems to have been initially influenced by ideas of stylistic restoration, over time his attitudes seem to have shifted towards a more pragmatic and romantic approach to restoration coming from Italy and England. This is evidenced not only by his decision to remove the medieval additions to the temple (which showed a period bias typical of the era) and leave the structure in its current, ruined form, but also by his other major work in the city at the Jardim Público (public garden). Influenced by the British idea of the picturesque, the landscaping at the garden stands in stark contrast to the organised structure of the French garden. No doubt influenced by British landscape architect Lancelot 'Capability' Brown, Cinatti's design features irregular sight lines, breathtaking and sublime landscapes, and prefabricated ruins of a 'classical' structure. Examining the design of Jardim Público, it is easy to understand that when faced with the sublime beauty of the ruins of the temple, Cinatti's romantic sensibility could not allow for complete restoration of the structure.

3.2 Description of the Temple

The Roman Temple of Évora is a hexastyle building, having a back portico composed of six columns. This style of temple architecture was a standard in Greek architecture and was adapted by the Etruscans through the Greek colonization of Southern Italy and later used extensively by the Romans. Given the composition of the remaining blocks, it is most probable that the temple followed a peripteral layout, where the columns of the front portico continued along the sides and the back, usually separated from the walls of the cella, or inner walled chamber, by one or two column spaces [42].

It is speculated that the structure was composed of 32 columns in total. However, given the state of damage in the structure, it is not possible to verify this. The columns are crowned with Corinthian capitals and have twelve flutes, forming a dodecagonal section. The drums are on average 0.9 meters in diameter. However, there is slight variation in the column diameter along the columns due to entasis. Like many Roman temples, the columns were at some point covered with a stucco finish in order to hide the great variation in the height of the drum blocks and to preserve the regularity of the structure. However, during one of the previous investigations of the structure, the stucco was misunderstood as an intervention measure and removed to restore the structure.

Since the entrance and the staircase on the south end of the structure have not survived (see Figure 3-5), in the absence of records or archeological evidence, the overall layout of the structure remains a subject of much debate. Using the remains of two other Roman temples on the Iberian Peninsula, located in present day Barcelona (Temple of Augustus) and Merida (Temple of Diana), Hauschild [33] and Garcia y Bellido [43] have proposed a unique style of temple construction, called *períptica*, which combined the classical peripteral form with an elevated podium.



Figure 3-5: View of the south façade and the entrance to the temple showing the exposed interior stone fill structure of the podium.

Hauschild also theorized that then entrance to the temple was most likely through a monumental staircase flanked on either side by walls (Figure 3-6-a). However, this conclusion has been rejected by others, such as Dias [32], who maintain that the staircase was most likely located on the sides and perpendicular to the longitudinal axis of the building (Figure 3-6-b).

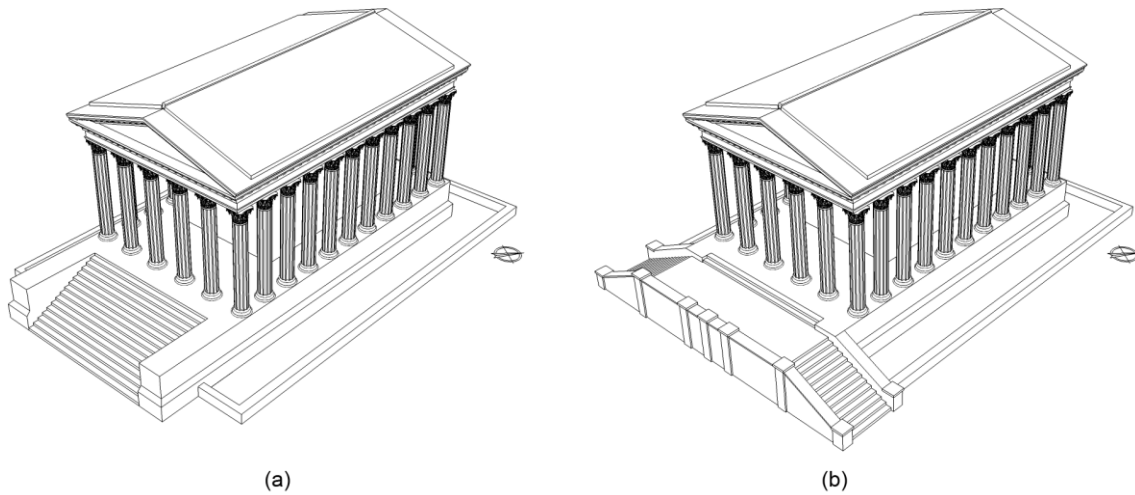


Figure 3-6: Alternative proposals regarding the entrance on the south façade.

The structure of the temple today is composed of fourteen columns, twelve of which support the remaining architrave blocks and two are freestanding (see Figure 1-3). The colonnade columns are 7.77 meters high and are composed of marble base blocks, granite drums and marble capitals. The freestanding columns are 6.77 meters high and are missing the capitals. Figure 3-7 shows the east elevation of the temple and the typical measurements of the main structural elements.

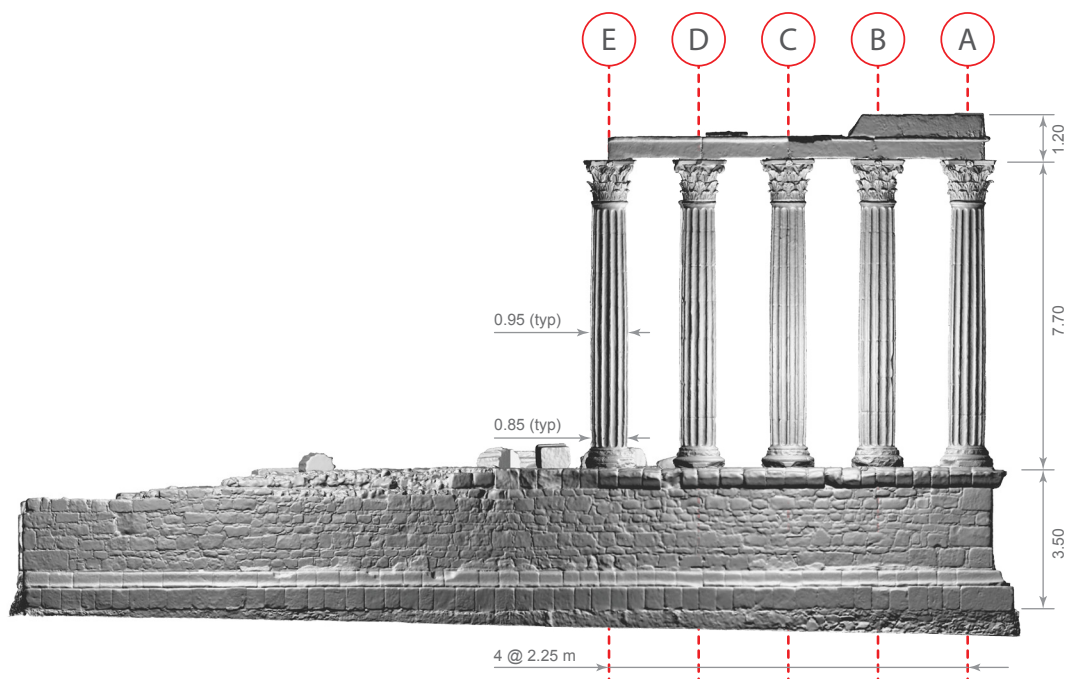


Figure 3-7: East elevation of the temple (after Direção Regional de Cultura do Alentejo [44]).

The entire structure rests atop a podium, 3.5 to 4.3 meters high, 15 meters wide and 25 meters long. The external walls of the podium are clad with regular granite block masonry. The internal composition of the podium is unknown, yet archeological evidence from other temple sites indicate that there are often intermediary walls which tie the external walls together. Figure 3-8 shows the plan view and orientation of the structure as well as the adapted grid system for the case study.

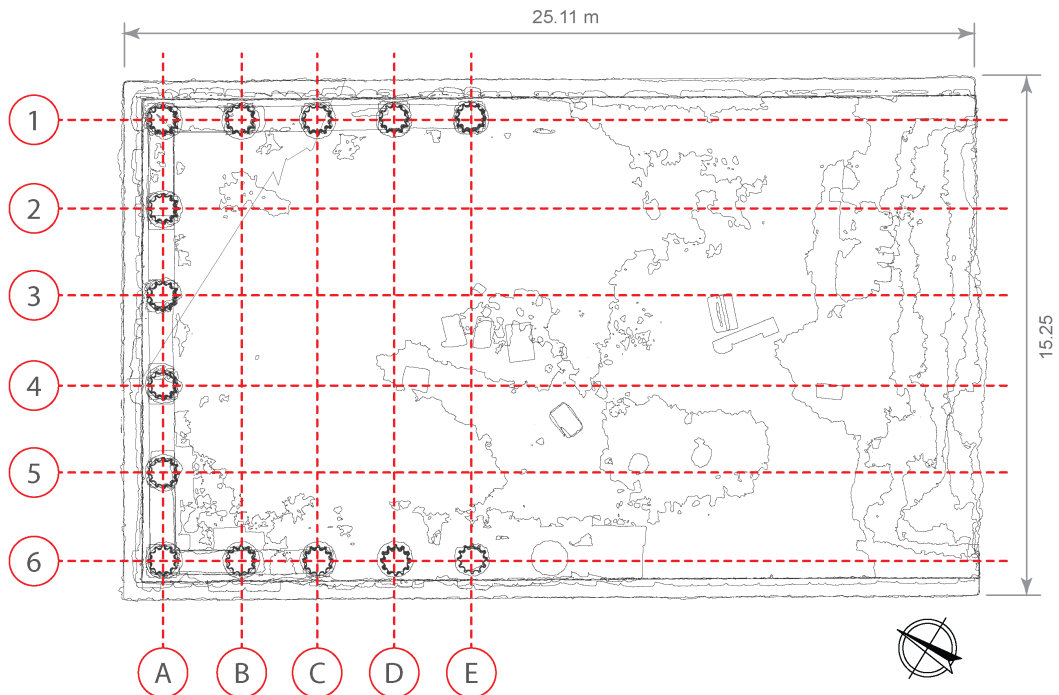


Figure 3-8: Plan view of the temple structure and the structural grid (after DRC do Alentejo [44]).

Although the temple is positioned on a northwest-southeast axis, for the purpose of the case study the façades will be referred to using the principal directions (i.e. the back façade will be known as north façade).

As mentioned earlier, through the last two millennia, the structure has undergone numerous changes and alterations, some of which have permanently damaged the blocks. During the preliminary visit to the site, a visual inspection of the structure was carried out. The visual inspection was done in conjunction with a photographic survey of the structure and the state of damage. An assortment of observed damages, representing the different classes of deterioration, is presented in Figure 3-9.

The most severely damaged components of the temple are the two middle columns, A3 and A4, on the north façade (see Figure 3-8 for description of structural grid). At this location, the column bases and drums were cut in order to accommodate the installation of a doorway, which most likely occurred during the conversion of the temple into a public slaughterhouse in the fourteenth century. The cut outs at these locations can have a significant impact on the behaviour of the structure through a change in the contact geometry and reduction of block contact area. Thus these changes in geometry will be taken into consideration in the preparation of the numerical models.

Most of the remaining marble base blocks in the structure have suffered some sort of damage and deterioration. The damage in this case ranges from erosion and chipping of small section to complete separation and splitting of blocks into two pieces (at the base of columns A1 and A2). The marble capitals have also been damaged through time, with loss of material due to impact being the most likely cause of the damage.

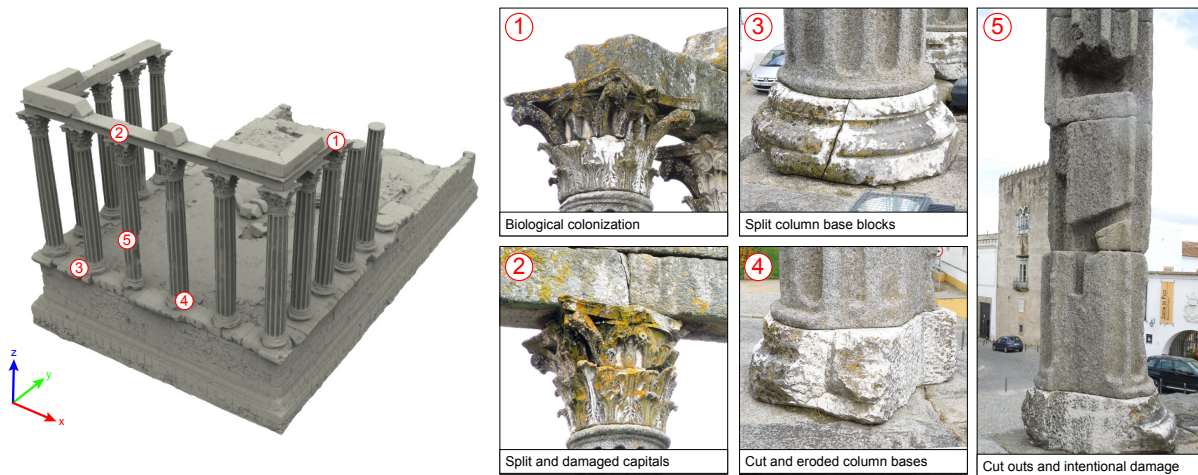


Figure 3-9: Typical damages recorded during preliminary visit.

The structure also suffers from biological colonization of lichen, algae, and moss. The column bases, capitals and the architraves are the most affected areas. No information regarding the type of biological growth is available at this time. It is reported that one of the column bases has been treated using micro-powder blasting in order to mechanically remove the accumulated growth and debris [45]. However, the effectiveness of the treatment and its long-term impact on the material is still unknown.

The visual inspection of the architraves, carried out by Grecchi, et al. [45] revealed that some of the architrave blocks are connected to each other using iron ties. The ties appear to be formed of rectangular plates which are embedded inside the blocks and covered using mortar. Given the state of the ties, they were most likely added during Cinatti's restoration of the temple as a means of stabilising the structure. Figure 3-10 shows the location of the architrave ties as well as sample pictures of how they are applied. The location of the ties was identified during the visual inspection and confirmed in two cases using ground penetrating radar. Please refer to Grecchi et al. [45] for complete details on the GPR investigation and its findings.

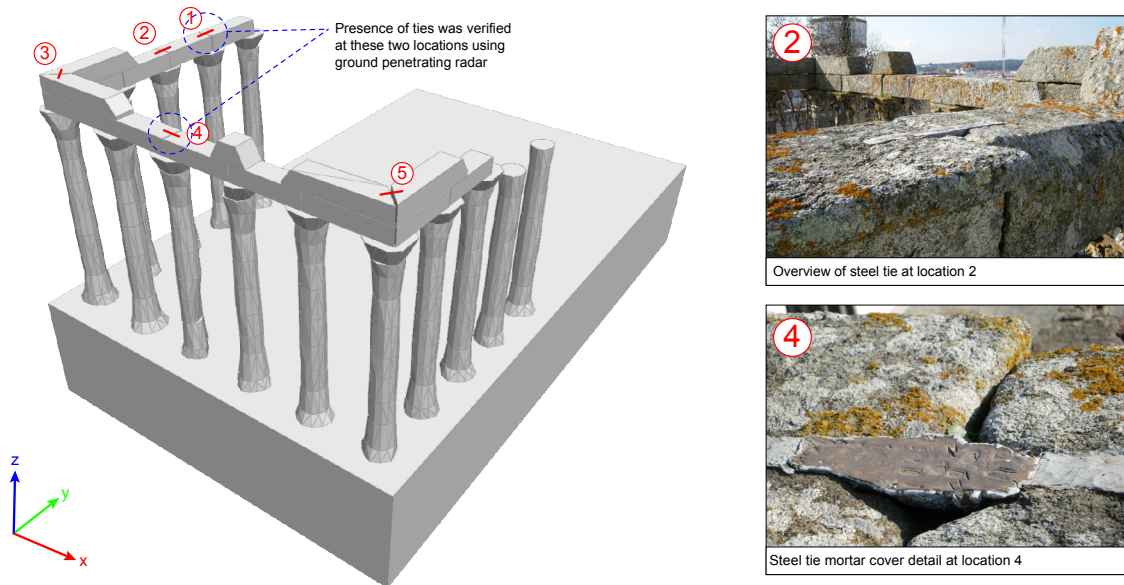


Figure 3-10: Location and detail of architrave steel tie reinforcement.

3.3 Previous Studies

In recent decades, the temple has been the subject of several archeological studies and excavations (most notably by Hauschild [33], Garcia y Bellido [43] and Ribeiro [40]). These studies have provided a large body of historical information about the structure as outlined in the previous sections. However, the studies remain largely inconclusive on several aspects of the structure's layout and history. The temple remains an important historical monument in the region and subject of regular investigation and analysis.

In 2007 and 2011, the Direção Regional de Cultura do Alentejo undertook an extensive program to document the current state of the structure using 3D scanning technology [44]. The results of this investigation are used in the present study to construct a more accurate geometric model of the structure.

The most recent, and only, structural and seismic assessment of the structure was conducted in 2012 by Grecchi et al. [45]. This study provides a comprehensive overview of the current state of the structure as well as the results of a set of in-situ tests which may be used for the characterization of the structure and the materials. The in-situ tests included visual inspection and damage survey, ground-penetrating radar (GPR), sonic velocity tests as well as two sets of dynamic identification tests. The study also provides some preliminary analysis of the structure's response and safety.

3.4 Remaining Issues

As mentioned in the introductory chapter, the current project is a continuation of the work of the previous research group and aims to extend the numerical studies performed previously to better understand the behaviour of the structure under seismic loads. While the previous study revealed that

the structure seems to exhibit a remarkable resilience to seismic action through dissipation of energy by rocking and sliding of the blocks, the study was limited to the effects of a single accelerogram for a single type of probable earthquake in the region. The present study will consider a wider range of actions and evaluate the sensitivity of the structure to the input ground motion.

Chapter 4

QUASI-STATIC ANALYSIS USING LIMIT AND PUSHOVER ANALYSIS

This section provides an overview of the application of quasi-static analysis methods to the seismic analysis and assessment of multi-drum structures like the Roman Temple of Évora. Two methods of analysis, namely limit analysis and non-linear static (pushover) analysis are applied and the results of the analysis enumerated.

4.1 Overview

Quasi-static methods of seismic analysis provide computationally efficient methods of analysis which have been successfully applied to many problems in the seismic assessment of masonry structures. However, a review of literature dealing with the seismic assessment of classical monuments reveals that quasi-static methods, especially limit analysis, are not widely applied to these problems.

The aim of this chapter is to investigate the viability of using limit analysis and non-linear pushover analysis for the seismic assessment of the Roman Temple of Évora. The results of these analyses are then compared to the results of the more robust but computationally demanding non-linear time history analysis presented in Chapter 5.

4.2 Limit analysis

4.2.1 Overview of methodology

As it was discussed in section 2.1.1.1, limit analysis is one of the oldest structural analysis methods still in use today. When applied properly, it provides an intuitive and quick method of evaluating the

stability of structures. Thus, it is particularly well suited for the study of masonry structures under seismic loads [7].

As stated previously, the classical formulation of limit analysis for masonry structures includes three assumptions as formalised by Heyman [5]: masonry blocks have infinite compressive strength; the blocks will not slide; and the joints possess no tensile strength. The limit analysis approach applied in the current study is based on the formulation provided by Orduña in 2003 [7]. This formulation overcomes the first two assumptions of classical limit analysis. First, the assumption of infinite compressive strength is overcome by the means of a yield function which is capable of accounting for limited masonry compressive strength. Next, the no-slip constraint is removed by applying a method of limit analysis for materials with non-associated flow rules which aids in the representation of the non-dilatant friction failure mode in masonry.

The approach proposed by Orduña is implemented in the software application *Block*, which was developed at the University of Minho. *Block* was designed specifically for the seismic assessment of historical masonry and has been successfully applied to a number of case studies [7], [4]. Given its strengths and demonstrated abilities, *Block* is used in the current study for the limit analysis of the Temple.

4.2.2 Description of Numerical Models

4.2.2.1 Geometric definition

The geometric model for limit analysis is built using information obtained from the 3D scan of the structure. The original drawings of the structure, prepared by Direção Regional de Cultura do Alentejo did not take into account leaning, rotation, loss of section, and cracking, thus not reflecting the actual state of individual column drum elements.

Five planar models of the structure are used for the analysis, representing each of the three facades as well as the two free standing columns. Each model is used for analysis of instability due to horizontal seismic loads in both positive and negative directions. The models incorporate as many features of the actual as is possible to represent in the two-dimensional model. These features include leanings of columns, cut outs and loss of contact areas.

The study makes use of two different model types as shown in Figure 4-1. The first model type (denoted here as m01) represents each of the stone pieces in the structure as a singular block element in the macro-element model. However, for the 2D analysis of the structure, the blocks are assumed to have a uniform thickness, thus forming a prismatic block. As a result, the column blocks cannot represent the true geometry of the cylindrical drums (see Figure 4-2 (b)). The second model provides a method of approximating the cylindrical shape of the drums through discretization of each drum element into smaller elements with varying thicknesses (see Figure 4-2 (c)). The block thicknesses are computed per column based on the average diameter of the drums in each column.

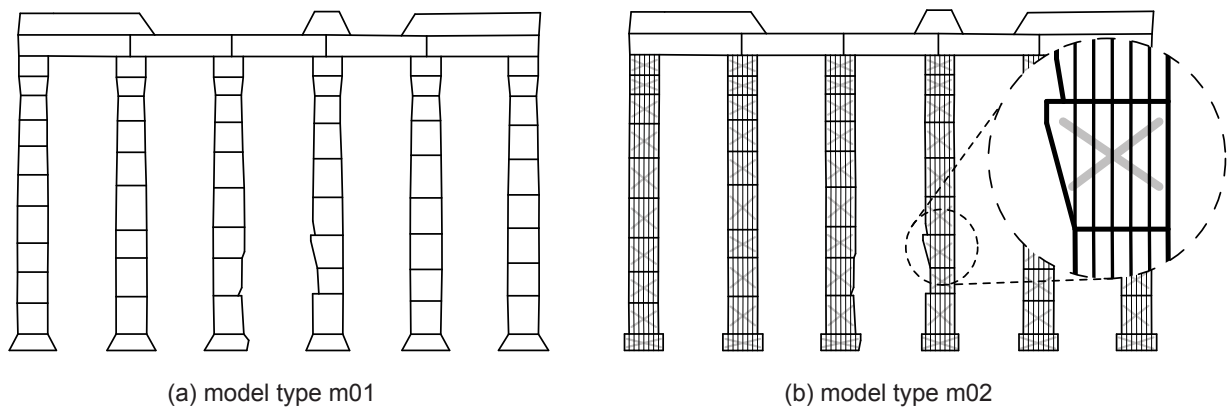


Figure 4-1: Limit analysis model types (a) m01 using single blocks and (b) m02 using discretized blocks.

A set of Visual Basic macros developed for AutoCAD are used to construct the discretized model (see Figure 4-2). The macros allow the results of models with different level of discretization to be compared. In the brief parametric study of the discretization, it was found that refinement beyond six elements does not change the model results. Thus, the final model geometry uses six blocks to approximate each of the drums. Once the drums have been discretized, rigid body motion amongst blocks representing a single drum is constrained using tie elements (shown as x's in each block in Figure 4-1) which hold the entire assemblage of blocks together, thus allowing it to behave as a solid rigid block.

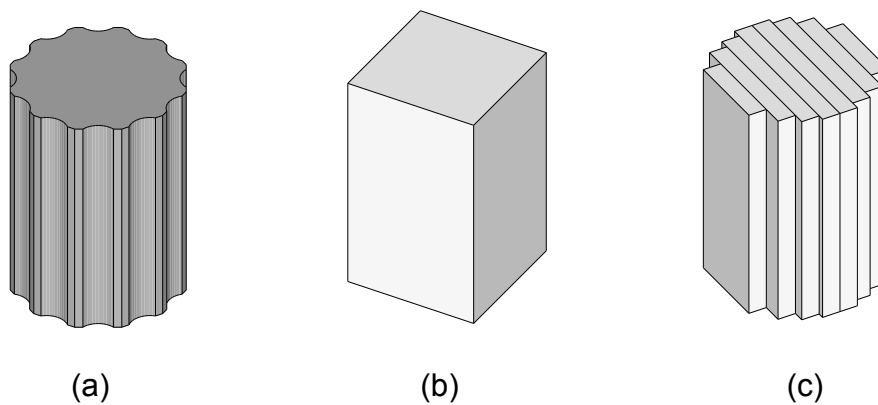


Figure 4-2: Macro-block representation of (a) actual column drums (b) with a single block and (c) with discretized block sections.

The two model types which are investigated in the study aim to illustrate the influence of out-of-plane geometry of the blocks on the overall performance of the model. Furthermore, given that the formulation implemented in *Block* assumes finite compressive strength, the use of smaller corner blocks allows for a better approximation of stress concentration at the perimeter of the drums while rocking.

4.2.2.2 Material properties

The material properties used in the limit analysis for the blocks and block interfaces are presented in Table 4-1. These material properties are based on general available information about granite. Although a number of field tests were conducted on both some of the structure's granite components during the investigation by Grecchi et al. [45], the results of these test were inconclusive.

Table 4-1: Material parameters used for limit analysis.

Compressive strength (Pa)	10×10^6
Tensile strength (Pa)	0
Friction coefficient	0.7
Block specific density (N/m ³)	26000

4.2.2.3 Representation of reinforcing elements

As discussed in section 3.2, architrave blocks are reinforced and tied together using a number of steel ties (see Figure 3-10). The numerical models prepared for limit analysis, however, do not include the reinforcing elements since there is still considerable uncertainty about the location of other ties not visible from the outside, as well as the dimension, material and form of the connections.

4.2.3 Results and Discussion

A total of twenty models are analysed, representing all planes of the structure, with horizontal forces applied in both positive and negative directions, in the plane of the model. The results of the analysis are summarised in Table 4-2. The results obtained from the analysis are presented as a seismic coefficient, α , for each model. The seismic coefficient is the ratio of applied horizontal forces causing destabilisation to the vertical forces due to gravity. Thus in this case, the seismic coefficient can be treated as an equivalent measure of block accelerations (in units of g) needed to cause destabilisation of the entire system.

Table 4-2: Comparison of the results of limit analysis for model types m01 and m02.

Model	Seismic coefficient, α					
	Positive horizontal forces			Negative horizontal forces		
	m01	m02	% diff	m01	m02	% diff
E6	0.117	0.120	2.8%	0.119	0.123	2.8%
D6	0.116	0.120	3.3%	0.126	0.130	3.1%
West	0.100	0.103	2.4%	0.103	0.106	2.6%
North	0.098	0.102	3.1%	0.098	0.101	3.5%
East	0.105	0.108	2.5%	0.094	0.097	3.0%
Average % difference:			2.8%	3.0%		

It is important to note that while there is some difference between the results of the solid (m01) and discretized (m02) models, the differences are minor (on average 3% difference). The differences in the

seismic coefficient calculated in each model could be the consequence of the improved geometrical model and the slightly different distribution of weights and contact geometries. However, the results provide confidence that the simplifications assumed in singular block models does not have a significant impact on the results.

It can be seen from the results that the free-standing columns have higher seismic coefficients (between 1.2 and 1.3 for m01 model) and are thus more stable. This is due in part to the fact that they are shorter than the columns connected by architraves. Furthermore, since the architraves are not continuous across the columns, they do not provide any additional stability through framing action. In fact, it seems that the additional weight of the architraves, when mobilized by rotation of blocks at the base, contributes to the rotations and thus destabilises the entire system.

Looking at the failure mechanisms for both colonnades and free-standing columns (Figure 4-3), it can be seen that the failure is initiated through rotation of upper portions of the columns about the first or second block at the bottom. The response shows that blocks will most likely rock and fail as a large group rather than as individual blocks or smaller isolated groups.

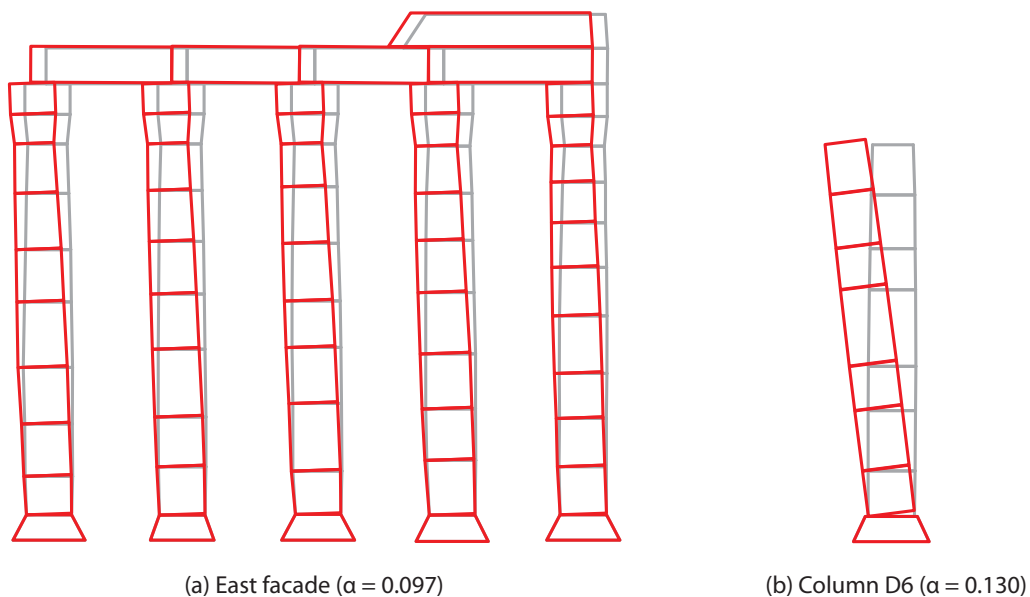


Figure 4-3: Failure mechanisms for (a) east façade ($\alpha=0.097$) and (b) column D6 ($\alpha=0.130$) due to negative horizontal forces.

The minimum seismic coefficient for the sections with architraves is 0.101, which corresponds to almost to a horizontal acceleration of 0.1 g at the block level. It is important to note that the peak ground acceleration for the design earthquake in Évora is also 0.1 g (see section 5.4 for more information about the seismicity in the area). Thus, it seems from the results of the limit analysis that in the event of a design earthquake (which has a return period of 475 years), the structure will most certainly collapse. However, these results must be verified using other analysis methods.

A comparison of the results of limit analysis with non-linear static (pushover) analysis (section 4.3) as well as incremental dynamic analysis (Chapter 5) is presented in Chapter 6.

4.3 Non-linear static (pushover) analysis

4.3.1 Overview of methodology

Non-linear static or pushover analysis is a numerical technique whereby a non-linear model is analysed under monotonically (i.e. static) increasing horizontal loads. As the applied horizontal load increases, the structure begins to exhibit non-linear behaviour through degradation of stiffness and redistribution of the internal forces. The non-linear behaviour of the structure is captured by monitoring the displacements of a control point and comparing it with the applied horizontal force (often normalized with respect to vertical loads).

The choice of the applied horizontal load pattern is an important consideration in the analysis process. Section 4.3.3.4.2.2 of Eurocode 8 [10] specifies that “at least two distributions of the lateral loads should be applied:”

- a “uniform” pattern, based on lateral forces that are proportional to mass regardless of elevation (uniform response acceleration);
- a “modal” pattern, proportional to lateral forces consistent with the lateral force distribution in the direction under consideration determined in elastic analysis (in accordance with lateral force method or modal response spectrum analysis).

While Eurocode 8 requires the use of both force patterns when applying pushover analysis, the present study considers only the mass-proportional loading due to time constraints. Future studies could use the models developed for this study to evaluate the response under other load patterns.

4.3.2 Description of numerical model

In order to perform a pushover analysis, any of the modelling techniques described in section 2.2 may be used to represent the structure. For the present study, the discrete element model prepared for the incremental dynamic analysis (presented in Chapter 5) is also used to perform the non-linear static analysis. Since the model is specifically designed for the incremental dynamic analysis, the details about the model geometry and material parameters are presented and discussed in section 5.2. In this section, the important features and major difference between the models used for pushover analysis will be presented.

The models used for the analysis are composed of 3D rigid block elements, modeled for use in the discrete element software 3DEC, made by Itasca Consulting [46]. Further detail about 3DEC and the discrete element model are provided in Chapter 5. Although a full 3D model of the entire structure is available, five other models, representing the three facades and the two free-standing columns independently, are also tested to determine the response of the structure in plane without interaction with adjacent out-of-plane segments.

The analysis is carried out as a series of static analysis within 3DEC. For each run the magnitude of horizontal forces is set by the program’s internal gravity vector. Thus in addition to the full vertical

gravitational acceleration, each run applies an increment of horizontal gravitational forces to the blocks. All the planar models are analyzed using forces in both positive and negative direction. The global 3D model is tested using horizontal forces applied in transverse (x) and longitudinal (y) directions, with both positive and negative scenarios considered in each case. 3DEC uses an explicit solution process even for cases with static analysis. The solution of the static analysis is calculated through dynamic relaxation [47].

4.3.3 Results and discussion

Table 4-3 provides a summary of the results of all the pushover analyses. The results present the highest horizontal accelerations for which the structure is still stable, along with the components of horizontal displacement at that stage. It is important to note that the acceleration computed using pushover analysis provides the same measure as the seismic coefficient, α , provided by limit analysis.

Table 4-3: Summary of pushover response of models, including the horizontal acceleration and components of the horizontal displacements.

Model	Force Plane	Pushover Response					
		Positive Horizontal Forces			Negative Horizontal Forces		
		<i>accl</i> [g]	<i>dist x</i> [m]	<i>dist y</i> [m]	<i>accl</i> [g]	<i>dist x</i> [m]	<i>dist y</i> [m]
E6	x	0.120	0.027	0.001	-0.124	-0.029	-0.003
	y	0.137	0.002	0.025	-0.133	0.002	-0.022
D6	x	0.122	0.024	0.002	-0.146	-0.017	0.000
	y	0.128	0.008	0.052	-0.139	0.002	-0.021
West	y	0.115	0.005	0.040	-0.117	0.005	-0.030
North	x	0.109	0.033	-0.002	-0.109	-0.037	-0.004
East	y	0.115	-0.005	0.037	-0.107	-0.003	-0.033
3D	x	0.094	0.036	0.002	-0.088	-0.030	-0.003
	y	0.097	0.001	0.033	-0.087	-0.001	-0.056
Min response:		0.094	-0.005	-0.002	-0.146	-0.037	-0.056
Max response:		0.137	0.036	0.052	-0.087	0.005	0.000

A number of observations can be made regarding the response. First, the results indicate that the free-standing columns D6 and E6 are able to withstand higher horizontal forces than the rest of the structure. The 3D model which includes all of the columns and architraves, on the other hand, has the poorest performance of all the models, regardless of direction. The planar response of the east and west colonnades is identical, having an acceleration of 0.115 g in the positive direction and 0.117 g in the negative direction.

Another method of analysing the results of pushover analysis is through plots called capacity or pushover curves. The demand curve relates the displacements at a point at the tip of the structure to

the ratio of the applied horizontal forces to the vertical forces (i.e. the seismic coefficient). Figure 4-4 provides a series of selected pushover curves for the structure based on the results of the analysis.

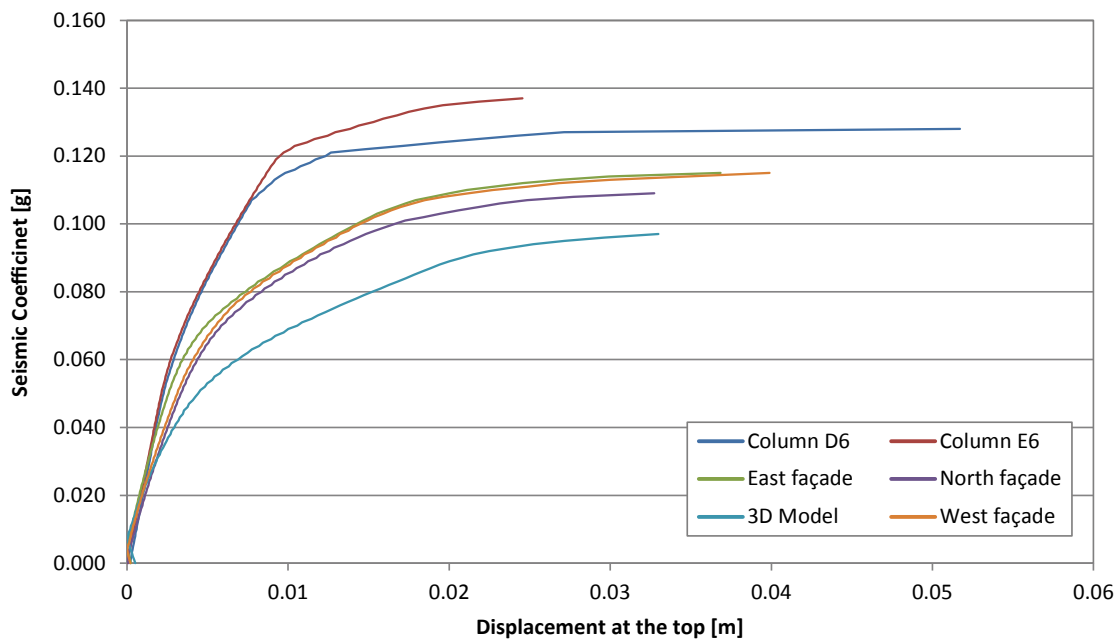


Figure 4-4: Pushover capacity curves for selected models.

The failure mechanisms for the east colonnade and free-standing column D6 are shown in Figure 4-5. The plots reveal that the failure is initiated through rotation of upper portions of the columns about the second block at the bottom. The response shows that blocks will most likely rock and fail as a large group rather than as individual blocks or smaller isolated groups.



Figure 4-5: Failure mechanisms for (a) east façade ($\alpha=0.107$) and (b) column D6 ($\alpha=0.146$) due to negative horizontal forces.

It is important to briefly note that the response presented above is very similar to the results obtained from limit analysis in the previous section. As it will be shown in Chapter 5, the failure mechanism found through either static method is consistent with the results of the dynamic analysis. A comparison of the results of pushover analysis with limit analysis (section 4.2) as well as incremental dynamic analysis (Chapter 5) is presented in Chapter 6.

This page is left blank on purpose

INCREMENTAL DYNAMIC ANALYSIS USING DISCRETE ELEMENT MODEL

This chapter presents the methodology and the results of incremental dynamic analysis performed using a discrete element model of the Temple. Starting with an overview of the applied methods, the following sections will highlight the powerful features which make the discrete element method especially suitable for representation of multi-drum structures. A complete description of the numerical model used for the dynamic analysis of the temple structure is presented along with a proposed algorithm for extraction of a simplified geometric model from 3D scan data. The chapter also includes the results of the experimental dynamic identification test performed at the site and explores the challenges faced in calibration of numerical models to the experimental data.

5.1 Incremental dynamic analysis approach

During a strong earthquake, classical monuments like the Roman Temple of Évora exhibit a complex behaviour, composed of sliding and rocking motions of stones either independently or in groups. As reported by Psycharis et al. [27], previous numerical and experimental investigations have shown that such structures *“do not possess natural modes of vibration in the classical sense and the periods of free vibration are amplitude dependant.”* Numerical models have revealed that during a seismic event, the response continuously changes between different modes of vibration governed by different sets of equations of motion. Thus the structural response during seismic events is highly non-linear, whereby a structure may collapse under a certain input excitation yet be stable under same excitation scaled by a factor greater than one. This behaviour is clearly demonstrated in the numerical response of a free-standing column reported by Psycharis et al. [27] and reproduced here as Figure 5-1. Looking at the

response of the column to the Kalamata earthquake record (a), it can be observed that for PGAs between 0.5 and 0.8 g, the response shifts between failure and relatively small displacements, demonstrating a clear non-linear relationship between response and the excitation intensity.

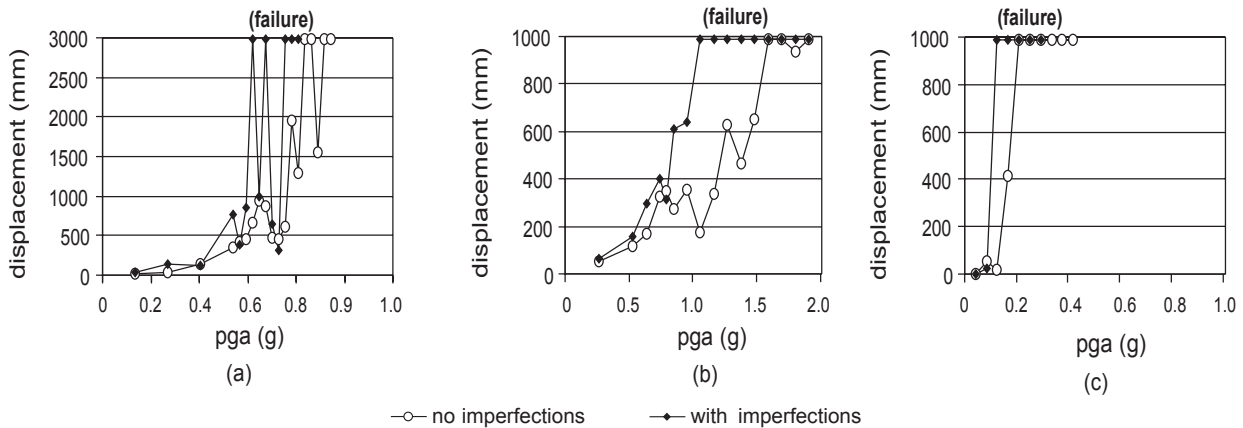


Figure 5-1: Maximum permanent displacement of a free-standing column, with or without imperfections, subject to earthquake records: (a) Kalamata (PGA = 0.27 g), (b) Aigion (PGA = 0.50 g) and (c) Bucharest (PGA = 0.20 g) (after Psycharis et al. [27]).

In order to account for the non-linear response of the structure, the present work will use the incremental dynamic analysis technique introduced in section 2.1.2.3 to study the response of the structure over a range of input excitation intensities. The input velocity records are successively scaled until a factor of seven, and the response for each simulation is recorded and used to produce a curve of response parameterized using a desired measure (e.g. maximum displacement or number of failed blocks) versus intensity level. More information about the response curves is presented in section 6.2.

Another general characteristic of the response of classical multi-drum structures is the sensitivity of the response to minute and trivial changes in system parameters or input excitations [27]. Both experimental and numerical tests have shown that even in cases of virtually identical models, small changes can significantly alter the observed response. Looking at the response of the free-standing column presented in Figure 5-1, it can be seen that changes to the model geometry (i.e. addition of imperfections) as well as the ground motion record can significantly alter the response even for the same PGAs.

It is important to note that the predominant period of the ground motion has been identified as one of the most important parameters which determines the vulnerability of the structure to seismic events [27]. It has been noted that multi-drum classical column and colonnades are especially sensitive to low-frequency earthquakes. It has also been observed in both numerical and experimental simulations that low-frequency excitations cause intensive rocking, while high-frequency ground motions produce significant sliding of the drums instead. For the case of the free-standing column investigated by Psycharis et al., it is possible to see that the Bucharest record causes severe damage to the structure even at very low ground motion intensities. This is due to the fact that the Bucharest earthquake has a

very low dominant frequency. Thus, it is the rocking of blocks, usually caused by low-frequency base excitations, which causes the most severe damage for these types of structures.

For the present study, two types of earthquakes are considered. The earthquake types correspond to the Eurocode 8 classification of earthquake as far field (type 1) and near field (type 2). Furthermore, in order to observe the sensitivity of the response to variations in input ground accelerations, three independent artificial ground acceleration records are generated and used for each type of earthquake. Further details regarding the input seismic excitations are presented in section 5.4.

5.2 Description of the numerical model

5.2.1 Geometric definition

The accurate geometric representation of the structure is an important step within the modelling process. As reported by Psycharis et al., imperfections and trivial changes in system parameters can significantly alter the structural behaviour [27]. Furthermore, as section 5.3 later illustrates, the model geometry has a significant impact on the dynamic properties of the structure. Thus, imperfections and anomalies such as cut-off of drum corners, displaced drums, inclined columns and split blocks should be considered carefully when creating the geometric model of the structure in order to balance the need for model simplification while still representing the important features that affect the structural response.

The numerical model used for the time history analyses, shown in Figure 5-2, is composed of 156 blocks (including the block representing the podium). It includes all fourteen existing columns, twelve of which are connected together with the architrave blocks, forming the colonnade, while the remaining two are free-standing. The colonnade columns are 7.77 meters high and are composed of a base block, drums and two blocks representing the capitals. The freestanding columns are 6.77 meters high and are missing the capitals.

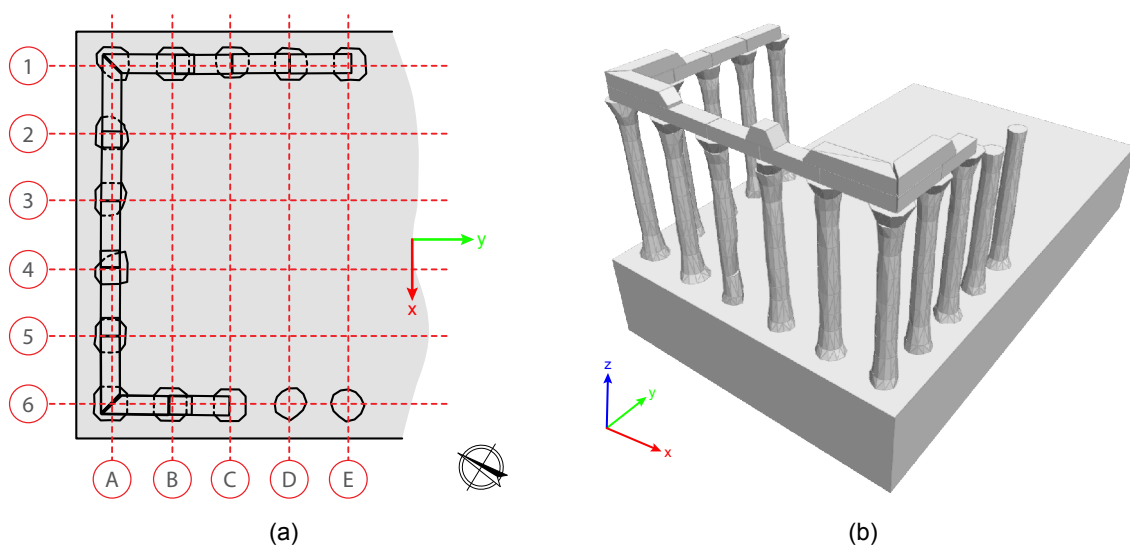


Figure 5-2: Discrete element model (a) plan and (b) perspective view.

The columns, including the base, drums and capitals are modeled as convex polyhedral 12-sided prisms. The architrave blocks are also modeled as convex polyhedral prisms and placed on top of the columns. Care is taken to appropriately represent the gap between architrave blocks. The podium is represented as a single fixed block, 4.4 meters high, 15.5 meters wide and 25.6 meters long. The podium block is used as the model base and the ground excitation velocity is applied at its centroid.

Figure 5-2 shows a plan view of the 3DEC discrete element block model and the adapted coordinate system for the analysis. A right-handed coordinate system is used for the model, with the x-axis representing the transverse direction and the y-axis representing the longitudinal.

In order to construct the geometric model of the existing structure, information from a recent 3D scan of the Temple is used [44]. The 3D scan data is imported and processed using Rhinoceros 3D, a general purpose 3D NURB modelling tool [48]. Depending on the quality of the 3D scan data, the resulting 3D model may require manual processing and repair using various mesh editing tools [49]. Once the global model mesh is repaired, each of the block elements is cut and separated into distinct, closed meshes (see Figure 5-3). While Rhinoceros 3D is not the best tool for manipulation of triangular meshes, it provides a parametric, generative modelling plug-in called Grasshopper, which allows users to perform complex geometric manipulations and calculations using simple visual programming components. This feature is used to generate the simplified block model for 3DEC based on the 3D scanned model of the structure. This approach allows for reusing of existing geometry data to produce the simplified block models while also providing a means for direct checking of the model geometry against the real structure.

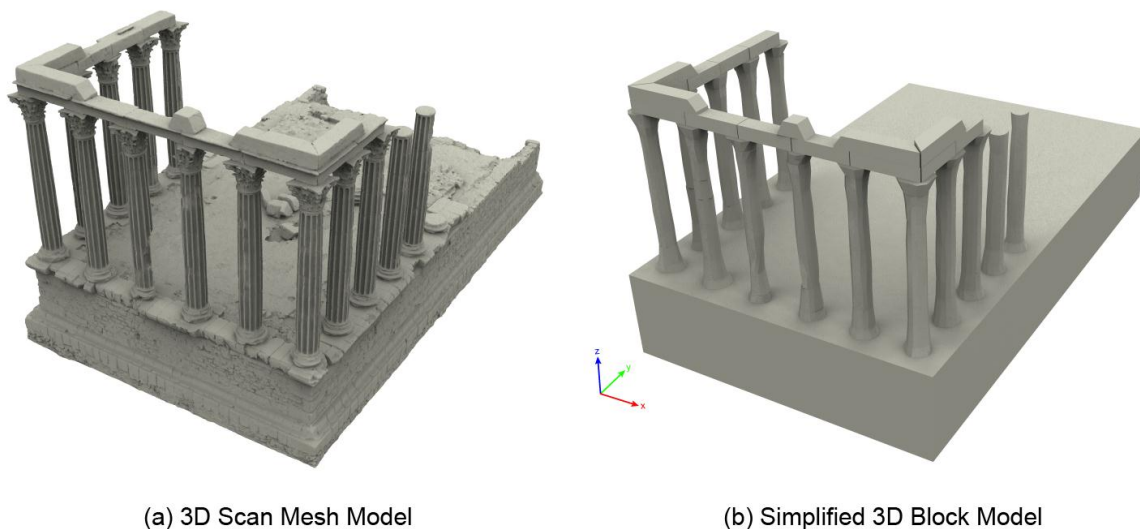


Figure 5-3: Perspective view of (a) the refined 3D scan mesh and (b) the simplified block model for discrete element analysis with 3DEC.

The algorithm developed in this work for generating the simplified block geometry is designed to fulfill three general criteria with respect to the actual block geometry recorded in the 3D scan, namely:

- 1) to match the contact area between adjacent blocks;
- 2) to match, as closely as possible, the contact surface geometry, taking into account imperfections and loss of section;
- 3) to match the block volume in order to insure an accurate distribution of block weights.

The general approach of the geometry algorithm is based on analysis of the contact surfaces at the interface between blocks. An illustrative example of the application of the procedure to a sample block is presented in Figure 5-4.

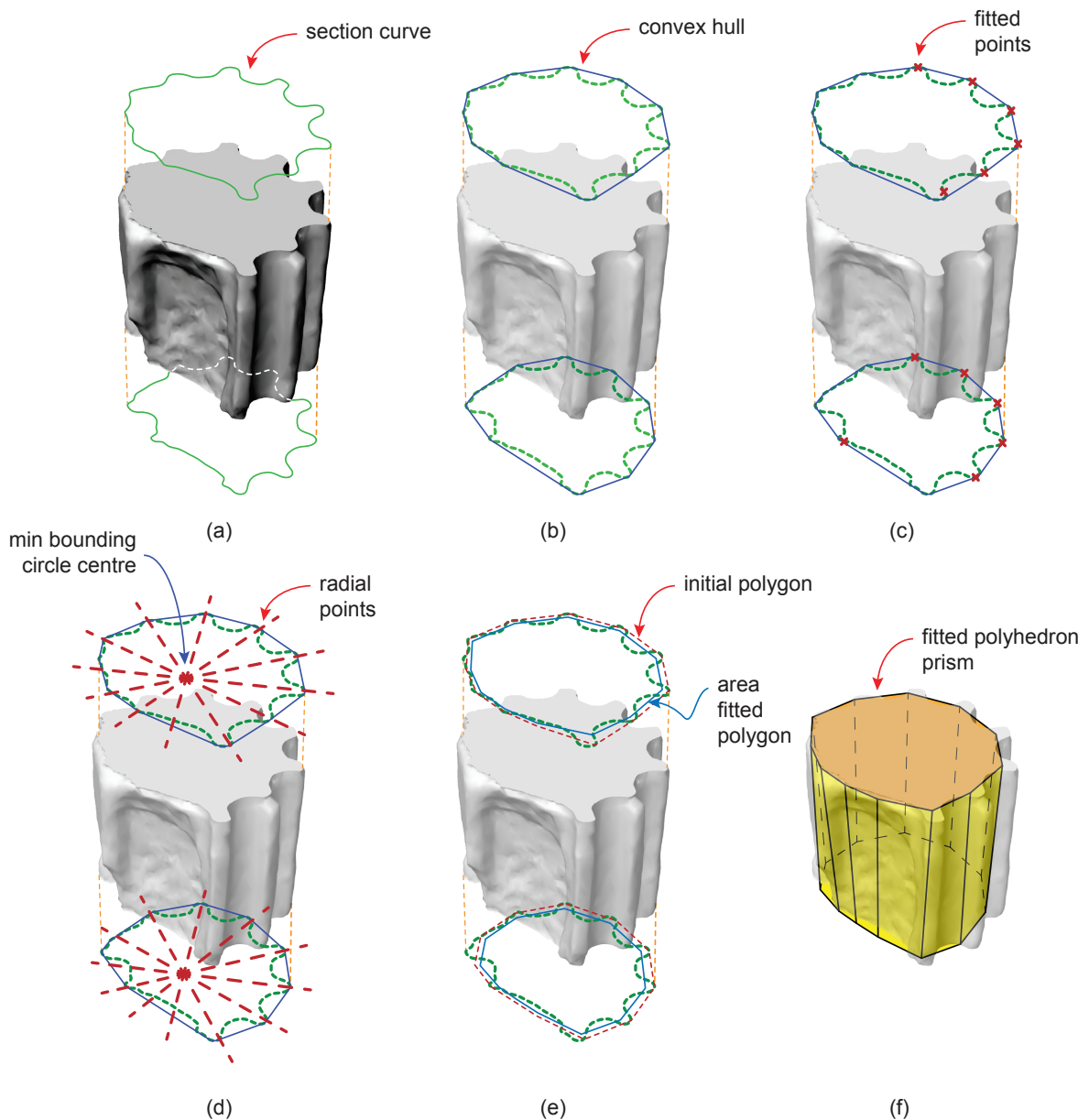


Figure 5-4: Illustrative example of the application of the general algorithm for generating the simplified block model based on real geometry data using Rhinoceros 3D and Grasshopper.

At the beginning, the contact area at each end of the block mesh is identified and converted into a closed curve (Figure 5-4-a). Then the convex hull of the contact curves is calculated (Figure 5-4-b). This step is required since 3DEC only permits convex blocks in order to simplify the contact detection procedures. A custom algorithm, written in VB.Net, is used to detect the location of the flutes along the section. This component uses the proximity of the convex hull curve to the section curve to detect locations where the two curves are tangent to each other. This is followed by a filtering procedure in which only segments within a range of tangent lengths are maintained (Figure 5-4-c). In addition to the flute points detected in the previous step, twelve other points are selected based on a radial distribution around the centre point of a minimum bounding circle around the section curve (Figure 5-4-d). In the final step of the process the twelve-sided polygons on both ends are scaled iteratively until the bound areas match the area of the actual section.

Using the above procedure, the final geometric model meets the general criteria discussed earlier, having an average contact area ratio of 1.00 and an average block volume ratio of 0.99. This means that the geometric model provides as close an approximation to the real geometry of the structure under the constraints of the simplifying assumptions made during the construction of the model. It is important to note that although this procedure produces a consistent approximation of the blocks, it will not be able to capture cut out and missing sections within the blocks, as seen in columns A3 and A4 (see Figure 1-3 and Figure 3-9). However, given that the blocks are modeled as rigid elements, the internal imperfections do not play a role in the overall behaviour of the structure and can be ignored.

5.2.2 Block and contact representation

The block elements composing the columns and architraves are assumed to behave as rigid blocks. Although 3DEC provides access to deformable blocks through internal discretization of the blocks as finite elements, previous studies by Papantonopoulos et al., [2] and [27], have shown that for structures made of massive stiff blocks, the majority of deformations occur at the system level due to sliding or rotation at the joints. These studies have also shown that the rigid block models appropriately represent the dynamic behaviour of multi-drum structures and the failure mechanisms associated with seismic forces.

The entire structure rests on top of the podium. As mentioned earlier, the outside walls of the podium are made of large solid granite blocks on which the columns are erected. It is believed that the interior is composed of stone rubble fill. It is very common in these types of structures to have interior walls that connect the exterior walls together. Given the non-homogeneous structure of the podium it may be more appropriate to model the podium as a deformable structure. However, due to the uncertainty regarding the actual composition of the block and lack of experimental data to characterize the behaviour of this part of the structure, for the purposes of this study, the podium is assumed to be a single rigid block.

For the purpose of contact calculations, faces of the rigid blocks are triangulated into sub-contacts. 3DEC provides a number of triangulation patterns for use in the models. The model used for the

present study uses a radial triangulation technique with a central node and radial edges. This scheme has been used by previous authors [27] and has been found to produce reliable results.

5.2.3 Material properties and joint parameters

Since rigid block elements are used for the analysis, the only material parameter of interest for the blocks is the granite and marble density. As part of the investigation program of the previous study of the Temple by Grecchi et al. [45], direct and indirect ultrasonic tests were conducted on both the granite and marble components within the structure. However, due to the rough and inconsistent nature of the surfaces on these elements, no conclusive data could be obtained. Consequently, results from previous laboratory experiments by Vasconcelos [50], [51] conducted on similar granite samples from Portalegre, Portugal (100 km north of Évora) are used to set the densities for the blocks in the numerical model. The granite blocks are assumed to have a density of 2625 kg/m^3 while the marble components are assumed to have a density of 2563 kg/m^3 .

3DEC utilizes a soft contact (or deformable contact) model for the joints, where the contact stiffness is defined by two springs in the normal and shear directions, whose stiffness relates contact stresses with relative block displacements [3]. By default 3DEC uses a Mohr-Coulomb constitutive model for the mechanical behaviour of the joints [47]. In the normal direction (i.e. perpendicular to the contact surface), the joint behaviour is governed by the normal stiffness parameter. For dry joints, this stiffness parameter can be used to represent the localized deformations at the periphery and irregular surfaces between two blocks [3]. Laboratory tests could be used to compute this value. However, typical values as reported by Vasconcelos [50] are used which are then calibrated based on the results of the dynamic identification tests (see section 5.3 for more details). No tensile strength is considered thus resulting in a compression-only spring in the normal direction.

In the shear direction, an elasto-plastic stress-displacement law is assumed, where the shear stiffness represents the elastic range and the Coulomb friction coefficient (without cohesion) represents the shear strength [47]. Due to time constraints, no further investigation of the material properties of the joints has been conducted. Thus, reported relations from literature by Sinrain [52] and Lemos [3] is used whereby the shear stiffness is assumed to be half of the joint normal stress. In the absence of reliable data about all the joints, this assumption allows the model to be calibrated using a single parameter, namely the joint normal stress. Table 5-1 provides a summary of joint properties following calibration of the model (see section 5.3 for details regarding calibration).

Table 5-1: Mechanical properties of joints for discrete element model.

Normal stiffness (Pa/m)	2.95×10^9
Shear stiffness (Pa/m)	1.47×10^9
Friction angle	35°
Tensile strength	0
Cohesion	0

5.2.4 Representation of reinforcements

As discussed in section 3.2, it is believed that during the 1872 restoration of the Temple by Cinatti, architrave blocks were reinforced and tied together using a number of steel ties (see Figure 3-10). The visual inspection of the architraves as well as GPR investigation by Grecchi, et al. [45] confirmed the presence of steel elements at five locations along the top of the structure.

The numerical model prepared for analysis using 3DEC, however, does not include the reinforcing elements. This is due to a number of factors. First, there is still considerable uncertainty about the location of other ties not visible from the outside, as well as the dimension, material and form of the connections. Second, while 3DEC offers an axial reinforcing element for use in block models, this element has been designed primarily to represent rock anchors and can only connect blocks which are in contact with each other. Given that the architrave blocks are clearly separated from each other, the axial reinforcing elements cannot be used in the model. Finally, modal analysis, conducted using small blocks to represent the ties, has shown that ties have a minor effect on the dynamic properties of the global model and their exclusion should not alter the structural response adversely. For more detail on the results of the modal analysis, please refer to section 5.3.

5.2.5 Damping

Experimental results [53] have shown that classical multi-drum structures have very low attenuation. Thus, it has been recommended that numerical simulations are performed with stiffness-proportional component of Rayleigh damping, using very low damping values, so that with the addition of damping effects of friction, the results would still be conservative [27]. The present analysis uses stiffness-proportional Rayleigh damping with a 2.2% damping ratio at 2.8 Hz.

5.3 Dynamic identification and calibration of numerical model

5.3.1 Overview

Among the experimental non-destructive methods commonly used to define the behaviour of a full scale system, dynamic modal identification has gained widespread acceptance and use in recent decades as one of the most complete and efficient procedures. Dynamic modal identification is a procedure that combines vibration test data and analytical signal processing methods to determine modal (natural) parameters including frequencies, mode shapes, and damping of a structural system. Given the broad range of structural parameters measured using this method, the results of the assessment can be used both to verify and calibrate theoretical and numerical models and to monitor the performance of the structural system during its operational use.

For the present study, the dynamic identification technique has been applied in order to obtain information about the modes of vibration of the structure so that the numerical discrete element model could be calibrated to better represent the dynamic properties and thus the dynamic response of the structure. The work is carried out in two parts. First a numerical model representing the structure is

prepared and analyzed in order to obtain the structure's modal frequencies and mode shapes. Then, the results of field dynamic testing is analyzed and compared to the numerical results. Finally, the numerical model is calibrated by successively changing one or more model parameter(s) until the numerical modal properties are close to those found during the experiments.

To date no research has been released regarding the application of dynamic identification to multi-drum structures. This is due in part to the complexity of the structural response and the difficulties faced by analysts in order to extract meaningful results from the recorded data. It is hoped that the results of the work presented here will provide a starting point for further research in this area.

5.3.2 Numerical modal analysis

As stated earlier in this chapter, multi-drum structures such as the Roman Temple of Évora are sometimes sensitive to trivial changes in system parameters. Thus, in order to compute the numerical modal parameters, four discrete element models are used. Each model provides a variation to the simplifying assumptions made during the modeling process and is used to find the model which best represents the real structural response measured by the experimental test. The unique features of each model are listed in Table 5-2.

Table 5-2: Features of four discrete element models used for modal analysis.

Model	Description	Model	Description
m01	- perfect dodecagonal cross sections - incorporates leaning and cut outs - no separation between architrave blocks	m03	- new geometry algorithm to approximate cross section outline - architrave blocks are separated by gaps
m02	same as model m01, except: - architrave blocks are separated by gaps	m04	same as model m03, except: - five blocks representing reinforcing elements are added

The above models share many features and are used to investigate variations in modal properties by changes in model geometry. Models m01 and m03 demonstrate the impact of geometry imperfections on the dynamic response of the structure. Models m01 and m02 show the effect of contact between architrave blocks on the overall stiffness of the structure. Finally, models m03 and m04 provide a way to compare the effect of reinforcing elements on the overall behaviour.

Given the above differences and keeping all other parameters constant, the modal properties of each model are evaluated. Table 5-3 presents the modal frequencies for all four models along with the experimental frequencies obtained through dynamic identification.

Table 5-3: Modal frequencies for the first ten modes of numerical models.

Mode	Modal Frequency [Hz]				
	m01	m02	m03	m04	exp
1	1.61	1.60	1.89	1.92	1.56
2	1.62	1.60	2.02	2.03	2.34
3	1.97	1.91	2.39	2.42	
4	2.15	2.04	2.51	2.59	
5	2.72	2.72	2.88	2.92	
6	2.72	2.72	3.04	3.10	
7	2.80	2.75	3.08	3.15	
8	2.80	2.80	3.16	3.19	
9	2.83	2.80	3.74	3.82	
10	5.02	2.91	5.10	5.18	

Based on the results of this analysis, it is decided that the model m03, which incorporates the most accurate geometry (including gaps between architrave elements), provides the best performance and should be used for the incremental dynamic analysis.

5.3.3 Experimental dynamic identification

In order to conduct dynamic identification of a structure, the following procedure is typically used: i) an array of accelerometers are placed at various locations on a structure and connected to amplifiers and data recorder, ii) an excitation is applied, and iii) the analog acceleration time histories and input forces are recorded for each accelerometer and each force input. Using the data collected on site the frequency response functions of the structure's response is calculated and analyzed in order to obtain the dynamic structural parameters.

For the Roman Temple of Évora, the dynamic identification tests were carried out over a period of two days. The tests involved the placement of twelve independent accelerometers throughout the structure in five different configurations. Two tests were carried out for each configuration: the first test consisted of creating data from just the ambient condition of the structure, so as to be a baseline for analysis; the second test consisted of using an excitation hammer to introduce external excitation throughout the structure to compare to the results from the ambient data. Each test lasted fifteen minutes, with the goal of generating data that would, after synthesis, provide dynamic behavior information about the freestanding columns and the entire structure. Figure 5-5 shows a sample Fourier spectrum for column E6, with the first four modal frequencies highlighted.

The experimental results obtained at the site have proved to be very difficult to interpret. The results capture a large number of local modes which make identification of global structural modes difficult and in some cases impossible. This fact is exacerbated by the very limited number of accelerometers used for the study which reduce the available input data, while increasing the likelihood of identification of incorrect parameters. Thus, in order to assist the interpretation of the dynamic results,

the results of numerical analysis from the previous section are used to filter and identify similar global modes within the experimental results obtained from the modal analysis software, ARTeMIS Extractor. The results of the experimental tests are presented in the next section along with the calibrated structural model.

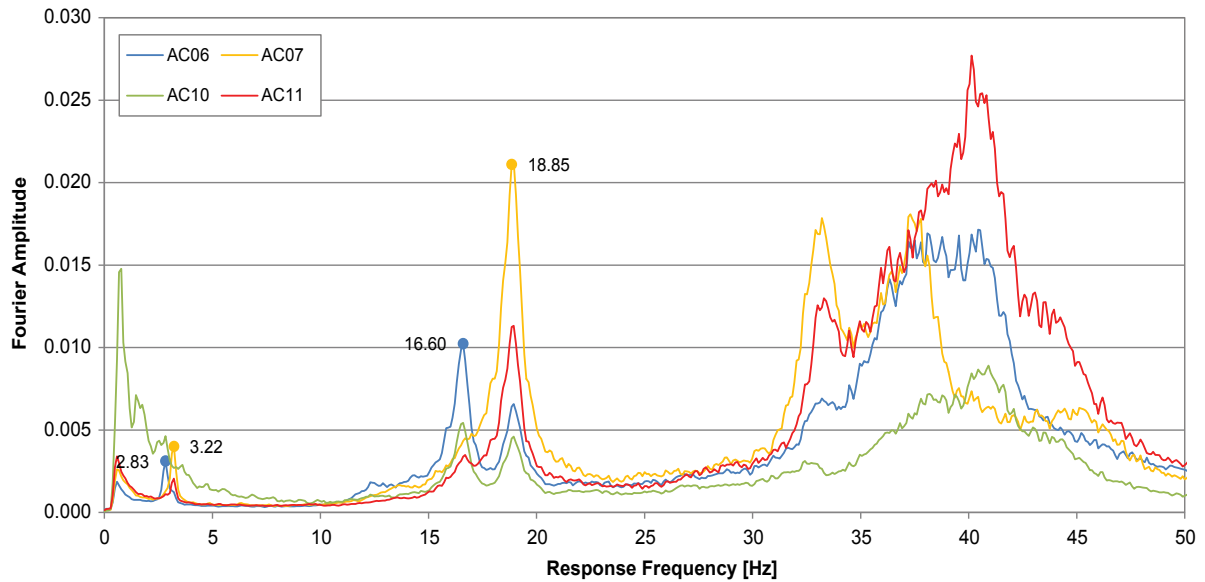


Figure 5-5: Fourier amplitude spectrum of the experimental results for Column E6 (setup 5) using four accelerometers.

The formation of each setup as well as the location of the accelerometers are available in the report by Grecchi et al. [45].

5.3.4 Calibration of numerical model

Having found the mode shapes and frequencies for both the experimental and numerical models, it is then possible to calibrate the numerical model in order to approximate the dynamic properties of the actual structure.

Due to limited time resources, a manual calibration method is used for the current study. In order to calibrate the model, the joint normal stiffness is changed iteratively until the best agreement between the numerical results and the experimental data is achieved. For the present case study, the calibration process is carried out on the free-standing columns, in particular column E6. This is due to the simplicity of the structural model and the availability of the first four modes for comparison. The modal shapes and frequencies for columns D6 and E6 are presented in Figure 5-6 and Figure 5-7 respectively.

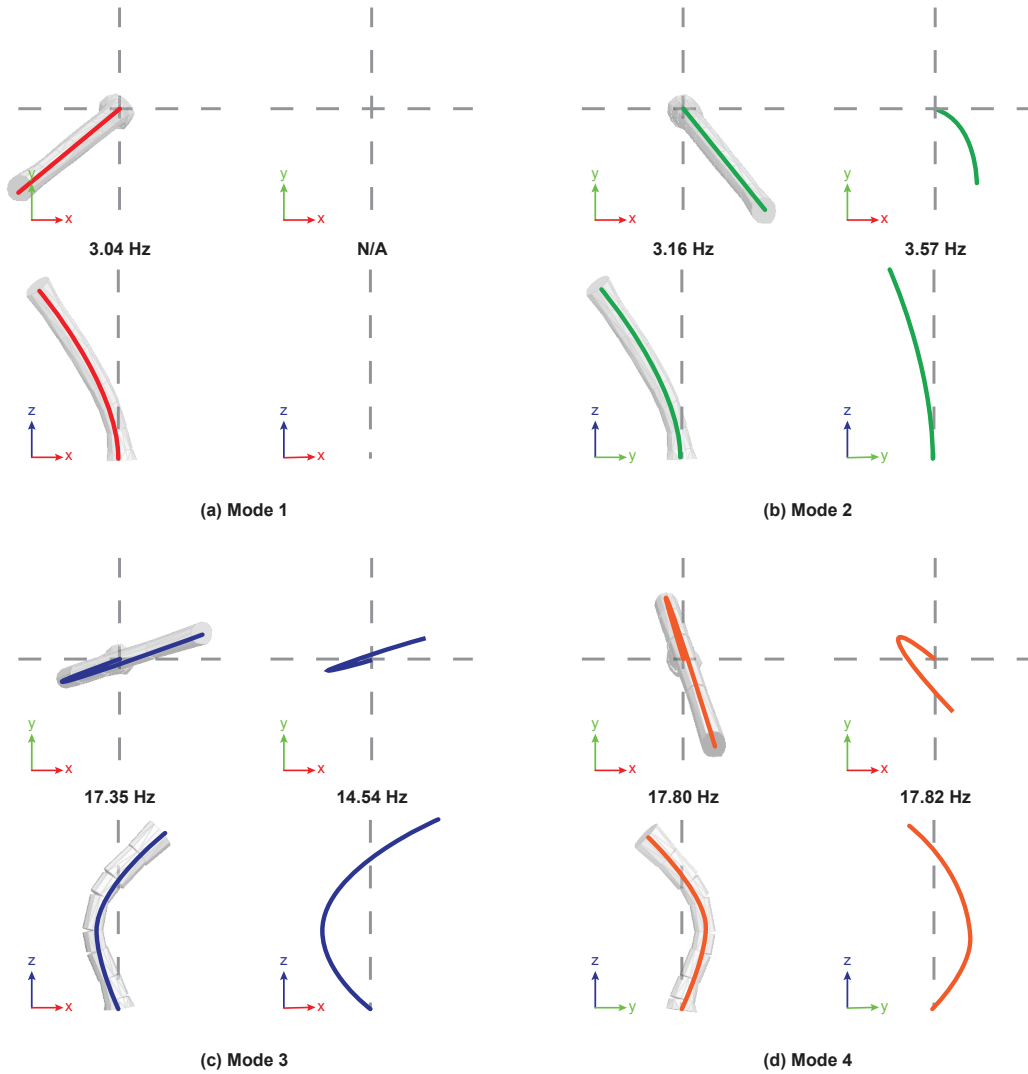


Figure 5-6: Numerical and experimental mode shapes and frequencies for column D6.

Once the free-standing columns have been calibrated, the results are applied to the global model. The modal shapes and frequencies for the global model are presented in Figure 5-8. Table 5-4 provides a direct comparison of the modal frequencies of the calibrated model and the experimental results.

Table 5-4: Comparison of modal frequencies of the calibrated model and the experimental results.

Mode	Modal Frequency [Hz]								
	Global Model			Column D6			Column E6		
	model	exp	% diff	model	exp	% diff	model	exp	% diff
1	1.89	1.56	21%	3.04	-	-	2.88	2.81	2%
2	2.02	2.34	14%	3.16	3.57	11%	3.08	3.21	4%
3	2.39			17.35	14.54	19%	15.76	16.52	5%
4	2.51			17.80	17.82	0%	17.14	18.90	9%
Average % difference:			17%	10%			5%		

Note: Analysis of results did not yield any conclusive results about the first mode of column D6.

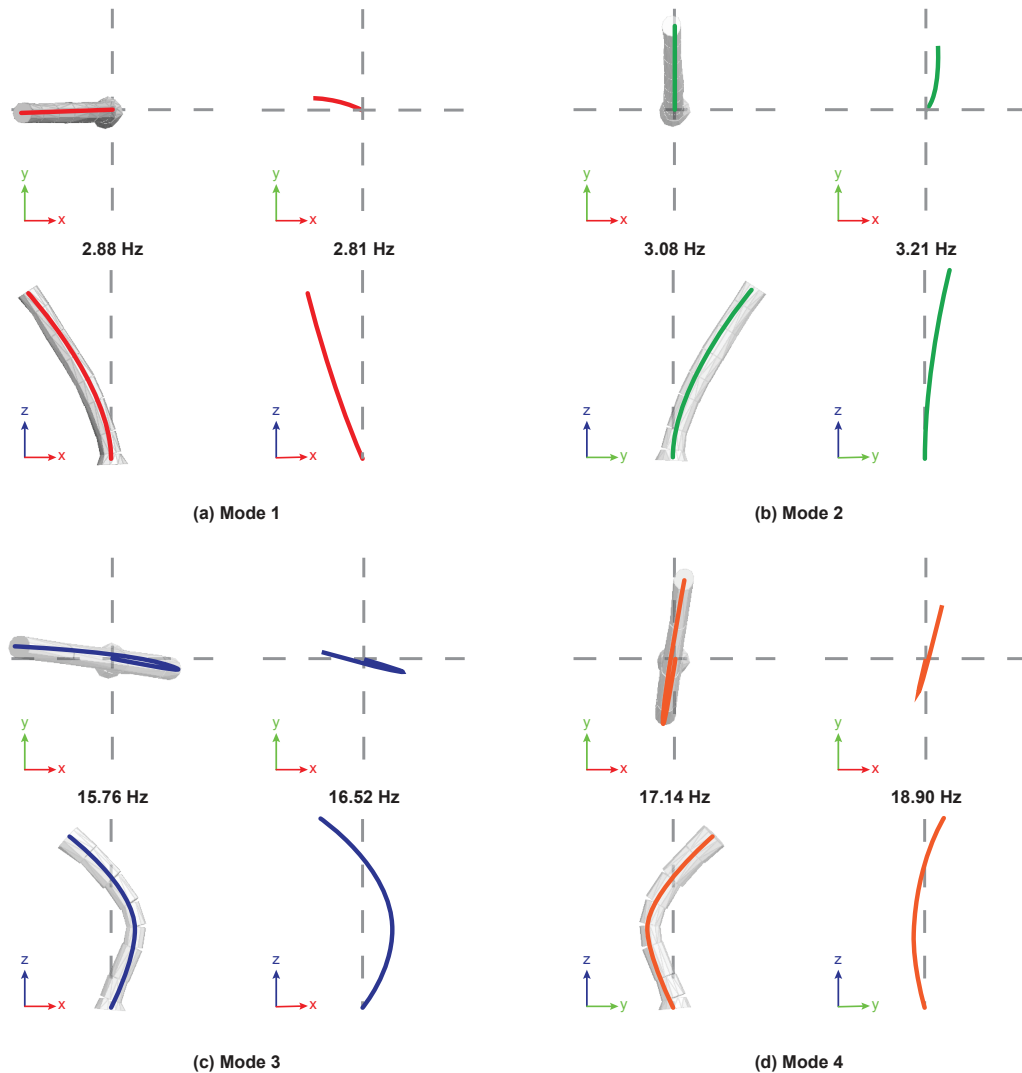


Figure 5-7: Numerical and experimental mode shapes and frequencies for column E6.

Although it is possible to use a variation of joint properties to achieve a closer agreement with the experimental results, this approach will be arbitrary and without a sound methodological basis. Consequently, more reliable information, provided by other in-situ and non-destructive tests are required to achieve a better agreement between the experimental and numerical results. This information can also be used as constraints for a systematic method of calibration where many structural parameters are varied at the same time in order to find the best set of parameters.

For a linear dynamic system, there are a number of effective calibration methods. For nonlinear systems such as blocky structures like classical temples, however, few effective methods are available. Some existing methods which require prior knowledge or rely on assumptions, may only work for specific types of nonlinearities. A main difficulty in dealing with a nonlinear system lies in finding a reliable mathematical model for it. Without a reliable model, it is usually impossible to proceed with system identification or obtain good calibration of the numerical models.

One of the most interesting and promising advances in system identification research in recent times has been the application of neural networks to the problems of dynamic analysis, especially in highly non-linear systems. Neural networks have been successfully implemented for identification of dynamic properties of structures [54] [55], structural optimization and structural health monitoring [56]. An artificial neural network is a network made of a large quantity of simple, yet highly interconnected processing elements analogous to neurons in the human brain. This architecture creates a highly intricate nonlinear dynamic system which is capable of storing, processing and learning about its environment. Such a system lends itself well to applications where dynamic non-linear signal processing is required.

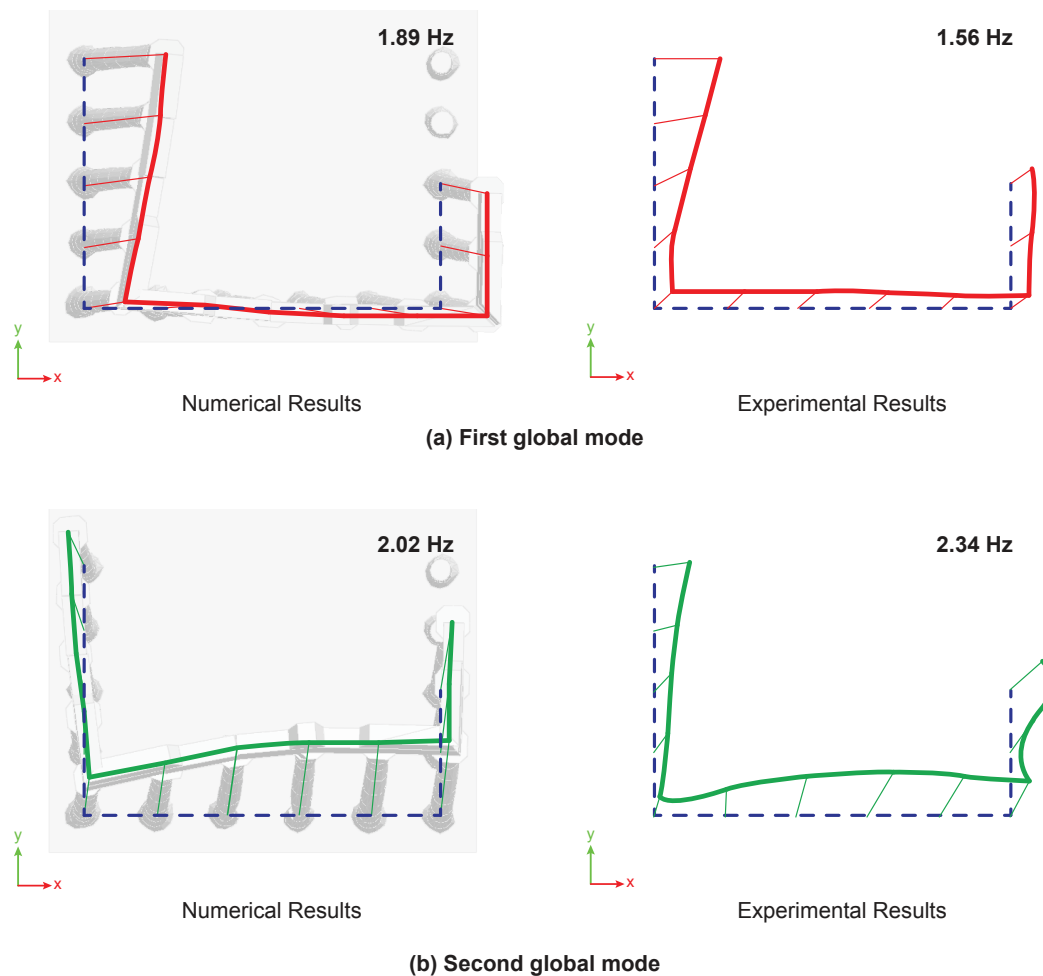


Figure 5-8: Numerical and experimental mode shapes and frequencies for the global model.

In comparison to other optimization and processing algorithms, neural networks do not rely on preconceived mathematical models or number of parameters. Given its nonlinear nature and ability to learn and adapt to the system environment, artificial neural networks are well suited for nonlinear system identification. By cycling through the output data at each step of the tests, the network 'trains itself' by adjusting the weight values as each processing neuron. Thus, the trained network reflects the input-output characteristics of the system it intends to represent.

Although this type of analysis is beyond the scope of the present study, its application to dynamic identification of multi-drum block structures could prove useful. Coupled with a more comprehensive testing campaign, the neural network approach could provide more useful information about the dynamic characteristics of the temple and allow for better calibration of numerical models. However, based on a comparison of mode shapes and frequencies, the agreement between the model and experimental data is considered satisfactory.

5.4 Seismic input

In order to perform a dynamic time history analysis, a ground acceleration time history, or accelerogram, is required as an input. The accelerogram may represent a real earthquake record, taken from the growing database of seismic records stored around the world, or it may be artificially generated to have specific characteristics. Eurocode 8 provides specific guidelines regarding the use of strong motion records. The first condition requires that at least three independent accelerograms are used for analysis. Furthermore, the chosen set of accelerogram, must have an average elastic spectrum that does not underestimate the code spectrum, within a 10% tolerance, in a broad range of periods depending on the structure's dynamic properties [10].

Recent research has shown that artificially generated accelerograms sometimes do not reflect the real phasing of seismic waves and cycles of motion, and by extension, of seismic energy. As a result, there is a growing body of research dealing with the use of real scaled records for dynamic analysis [57]. While there are records which match the required response spectra for the region around Évora, the records currently available in the seismic databases are not related to this region and may not represent the real seismogenic conditions of the area. Thus, for the present study, only artificially generated accelerograms are used.

As described earlier, Eurocode specifies that at least three accelerograms should be used for each type of elastic response spectrum under consideration. The code specifies that unless other data is available, two types of elastic response spectrum, corresponding to far field and near field earthquake events, must be considered. Therefore, the incremental dynamic analysis will feature six curves along a range of scaled intensities, resulting in a multi-record incremental dynamic analysis [19].

As Figure 5-9 indicates, Évora lies within a region of moderate seismicity with a far field PGA of 1.0 m/s^2 (seismic zone 1.4) and a near field PGA of 1.1 m/s^2 (seismic zone 2.4). For the present study, the soil factor is take equal to 1 (rock). Table 5-5 shows the input parameters used for generating the artificial earthquakes.

Table 5-5: Seismic parameters for the Roman Temple of Évora (return period 475 years).

Type	a_g [m/s^2]	Elastic Resp. Spec. Parameters				Duration [s]			
		S_{max}	T_B	T_C	T_D	Rise	Steady	Fall	Total
1	1.0	1.0	0.1	0.6	2.0	3	30	3	36
2	1.1	1.0	0.1	0.3	2.0	2	10	2	14

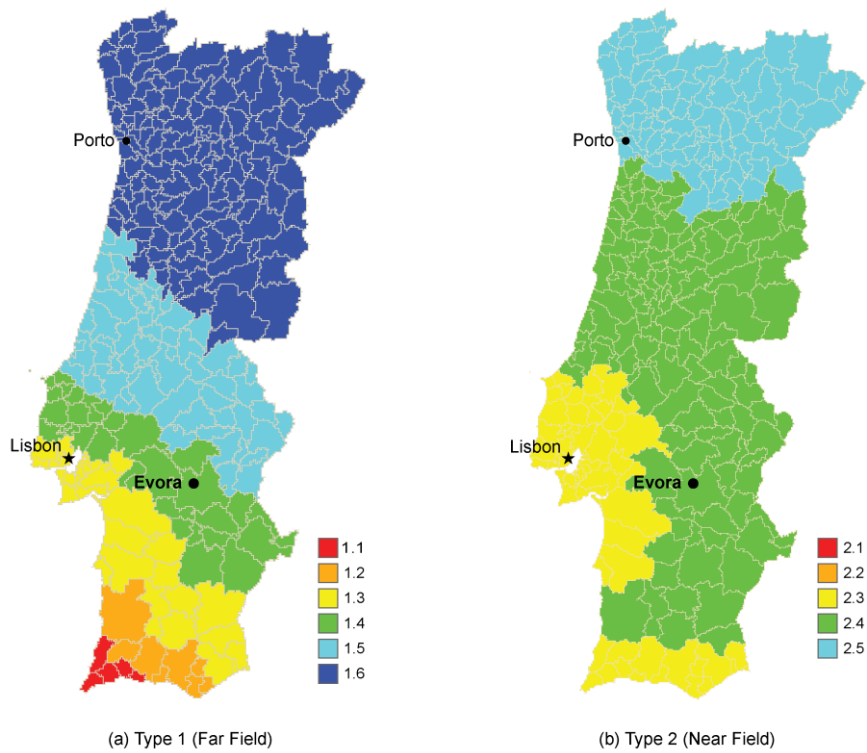


Figure 5-9: Seismic hazard map for continental Portugal (after Norma Portuguesa [58]).

Given the ground motion parameters described above, the program *Simqke_gr* [59], developed by Prof. Piero Gelfi at the Università degli Studi di Brescia, is used to generate three accelerograms for each type of earthquake to be considered. Baseline correction and bandpass filtering of the generated records is then performed using the program *SeismoSignal* [60] from Seismosoft. Figure 5-10 presents two examples of each type of accelerogram following post-processing.

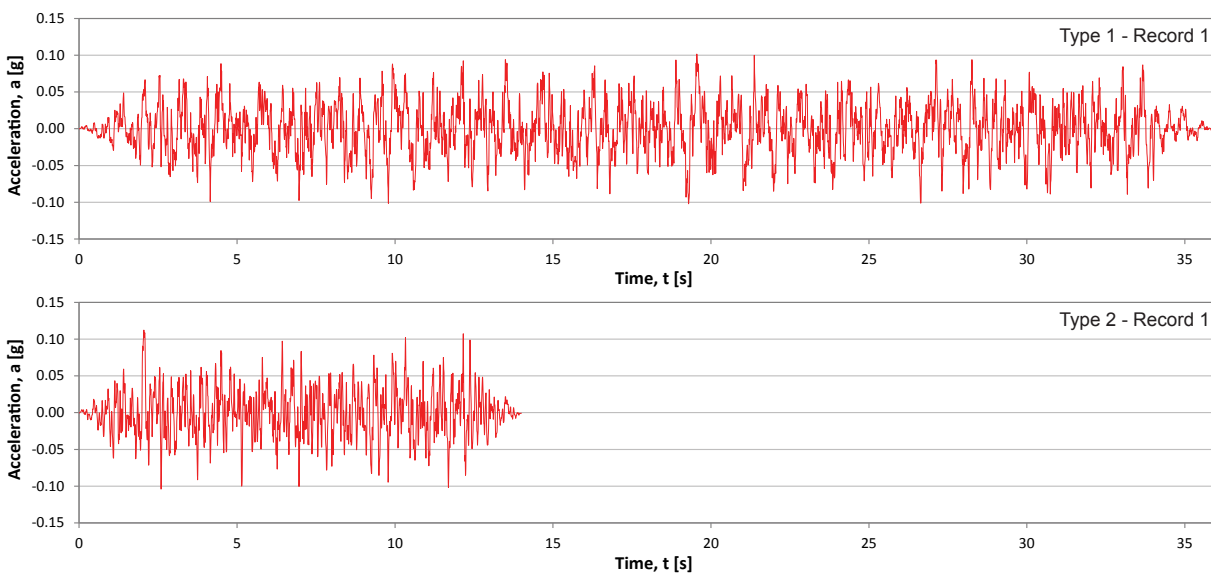


Figure 5-10: Examples of artificially generated accelerograms for Eurocode type 1 and 2 earthquakes.

Figure 5-11 presents the acceleration and displacement response spectra for all the records for both earthquake types. It is important to note that all the spectra for both acceleration and displacement are within 10% of the code specified spectra (indicated by the dashed line) and thus satisfy the requirements in section 3.2.3.1.2 of Eurocode 8 [10].

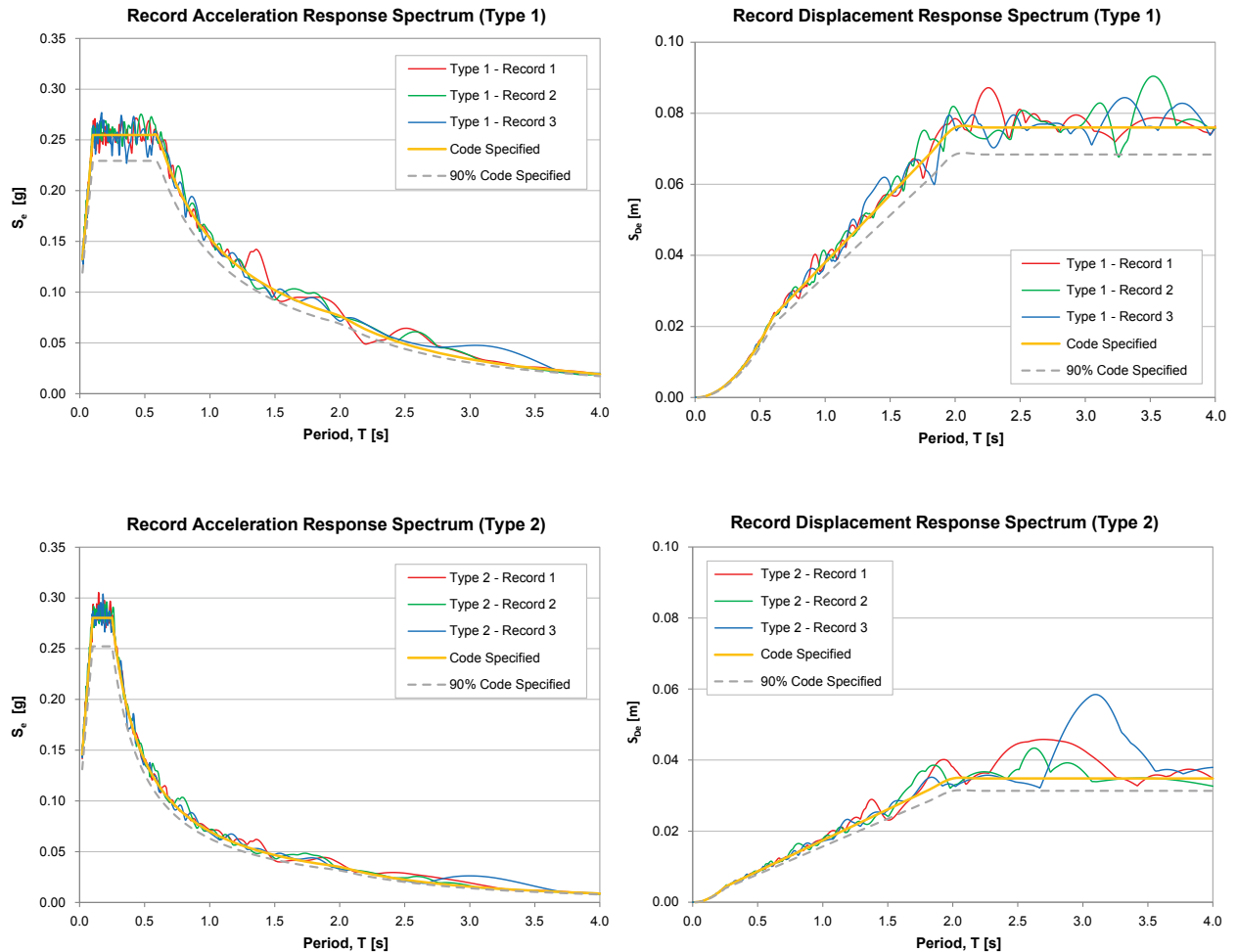


Figure 5-11: Comparison of the acceleration and displacement response spectrum of artificial records and the Eurocode specified spectra for type 1 and 2 earthquakes.

It is important to note that 3DEC requires direct input of ground velocities for calculation of seismic behaviour. Thus, using SeismoSignal, the velocity time history for each record is computed which is then applied at the centroid of the block representing the podium.

5.5 Discussion of results

This section will provide an overview of the results of the incremental dynamic analysis with a strong focus on illustrating the behaviour of the structure under seismic loads. A discussion of structural performance and damage indicators developed based on the results of this analysis will be presented in section 6.2.

In order to understand the global dynamic behaviour of the structure, in each analysis, the displacement of nine control points are monitored and the output stored. The location of the control points is presented in Figure 5-12.

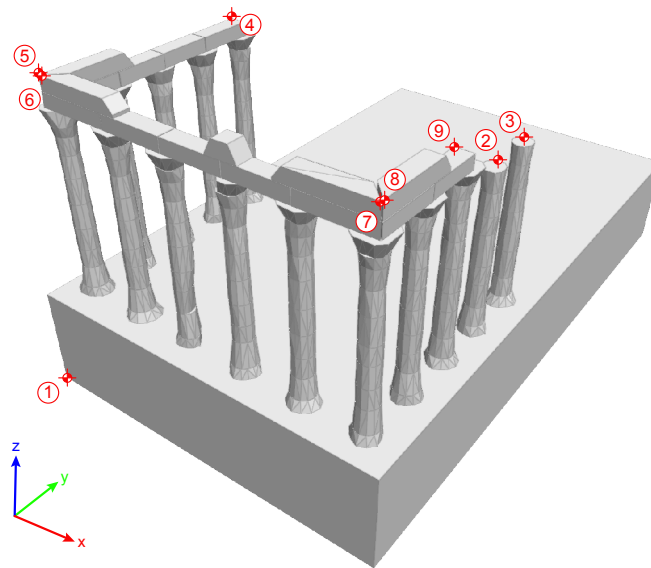


Figure 5-12: Location of the nine control points monitored during the time history analysis.

Using the output generated by the control points, it is then possible to generate time history plots of the node displacements and to evaluate the magnitude of block movements during the entire simulations. It has been observed that in most cases, the magnitude of the displacements during the earthquake far exceeds the residual displacement at the end of the analysis. Therefore, examining the displacement history of various points on the structure will shed some light on the manner in which dynamic stability due to block rocking motion acts to prevent destabilisation of the entire structure.

5.5.1 Response of a free-standing column

The results of the analysis for the free-standing columns provide some interesting information since the response is largely unaffected by adjacent columns and not restrained by the architraves. In this section, the time history response of control point 2, located at the tip of column D6 will be examined in detail. Figure 5-13 shows a plot of the horizontal components of displacement at control point 2.

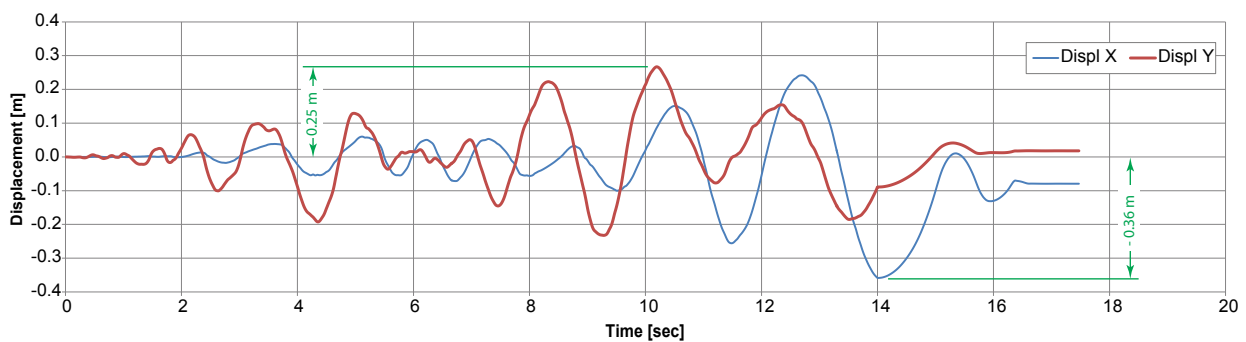


Figure 5-13: Displacement time history response of control point 2 (top of column D6) in the transverse (x) and longitudinal (y) directions, due to type 2 earthquake in the y-direction (PGA 0.66g).

As the plot demonstrates, even though the applied excitations are in the longitudinal (y) direction, the maximum response of the structure is in fact in the transverse (x) direction. This behaviour can be observed more clearly by looking at a top view of the column, presented in Figure 5-14.

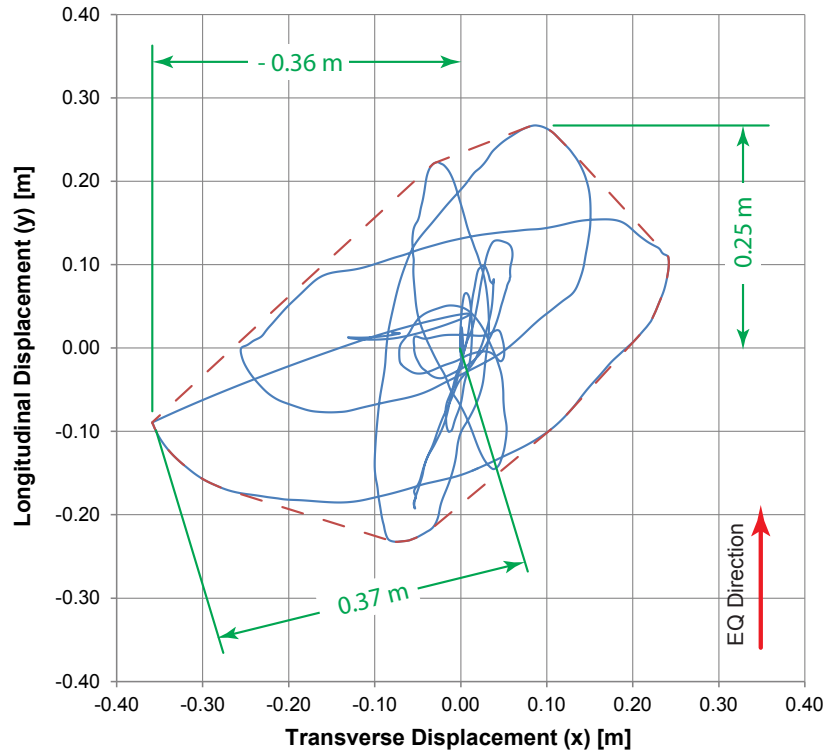


Figure 5-14: Horizontal time history response of control point 2 (top of column D6) as viewed from the top, due to type 2 earthquake in the longitudinal (y) direction with scale factor of 6.0 (PGA 0.66g).

As the figure shows, the predominant direction of the horizontal motion of column D6 is orthogonal to the direction of the applied excitations. This behaviour is consistent with the general response observed in experimental and numerical investigations performed by others [27]. This behaviour also makes it clear that even for free-standing structures such as columns, the use of planar models will provide an incomplete picture of the structural behaviour and that a full 3D analysis is recommended in most cases.

It is also important to note that the direction of maximum horizontal displacement, in this case 0.37 m, is in fact the direction of the first mode for the column (see Figure 5-6 for the mode shapes). Looking at the results from simulations with excitations in the transverse (x) direction, it shows that the horizontal motion at the control point will follow the second (orthogonal) mode of the column.

As Figure 5-14 shows, while the magnitude of each component of horizontal displacement is quite large in comparison to the values computed using limit analysis and pushover analysis, the magnitude of total horizontal displacement is even larger. Figure 5-15 shows the magnitude of the total displacements during the entire analysis. As the figure shows, the maximum horizontal displacement is 0.37 m. It is also interesting to observe the upward trend in the magnitude of displacements as time progresses.

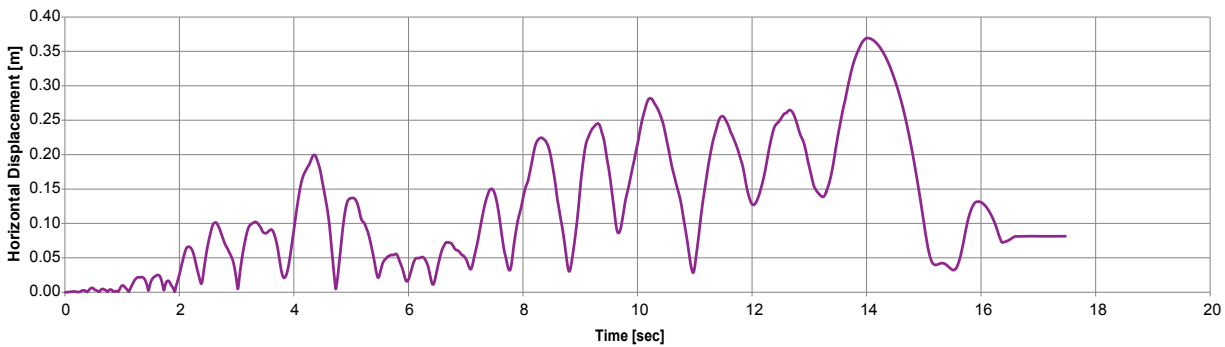


Figure 5-15: Horizontal displacement time history response of control point 2 (top of column D6), showing the magnitude of the total displacements, due to type 2 earthquake in the longitudinal (y) direction with scale factor of 6.0 (PGA 0.66g).

The vertical displacement time history of control point 2 is presented in Figure 5-16. It is clear that since only horizontal ground motion is applied to the model, the vertical response is insignificant. Although this analysis does not include analysis of response to vertical ground motion, further study in this area may prove interesting.

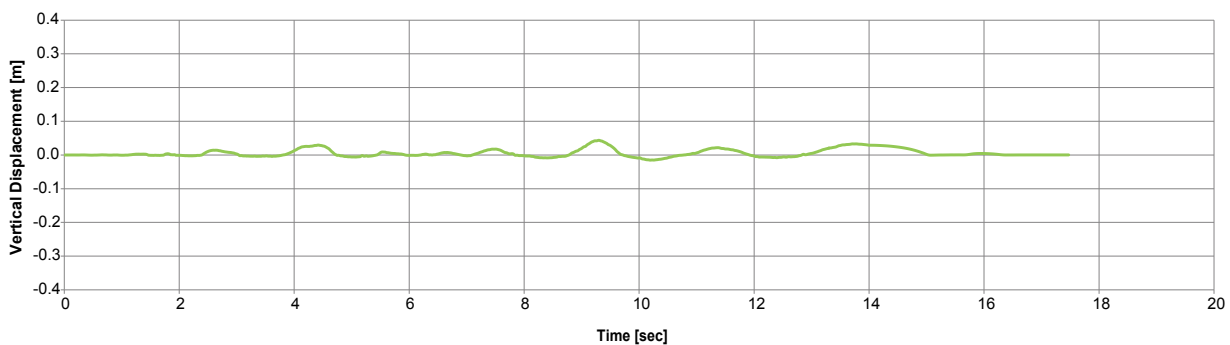


Figure 5-16: Vertical displacement time history response of control point 2 (top of column D6) due to type 2 earthquake in the longitudinal (y) direction with scale factor of 6.0 (PGA 0.66g).

In order to view the motion of the blocks and compare results of different model configurations and parameters, a custom visualization post-processor is created using Processing Java environment. This software, along with associated subroutines developed using the FISH language for 3DEC, allows users to extract rigid block displacements during the analysis and reconstruct and animate the motion of the blocks in a 3D environment. The user can view the animation and rotate the model in real-time, thus gaining insight into the behaviour of the numerical model without the need to generate multiple sets of static plots during the analysis process. The program along with the required data files for all the simulations created for this study (eighty-four simulations in total) are included in the DVD found at the back of this document.

The visualisation program is used to produce graphical time history plots like the one shown in Figure 5-17. As the picture illustrates, the motion of the blocks is very complex, at times involving groups of blocks while in others being limited to individual blocks. Furthermore, the sequence shows a complicated combination of rocking, rotation and sliding.

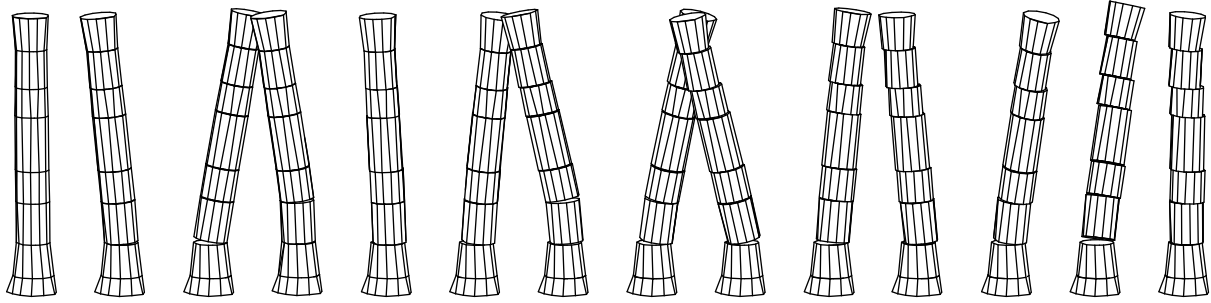


Figure 5-17: Time history response of column D6 (in the y-plane) due to type 2 earthquake in the longitudinal (y) direction with scale factor of 6.0 (PGA 0.66g). Note that the response has been magnified by a factor of five in order to emphasize the behaviour.

By looking at the global displacements at various nodes in the structure, an understanding of the overall behaviour can be obtained. However, it is sometimes instructive to look at local behaviour at the joint level. The joint between the second and the third block is used for this purpose as the joint seems to be active throughout the analysis, as seen in Figure 5-17.

Three joint parameters, namely joint normal (opening) displacement and normal stress as well joint shear (sliding) displacement, provide useful insight into the behaviour of the model at the local level. A plot of the time history evolution is presented in Figure 5-18, Figure 5-19 and Figure 5-20, respectively.

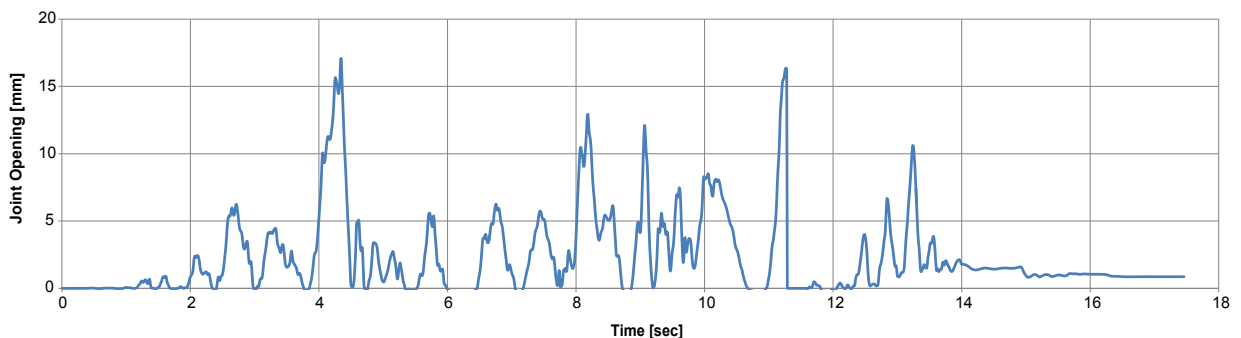


Figure 5-18: Joint opening time history response at the joint between the second and third block in column D6, due to type 2 earthquake in the longitudinal (y) direction with scale factor of 6.0 (PGA 0.66g).

It is important to point out that the periods corresponding to zero normal stress represent instances in which the blocks are completely separated and show the sequence of rocking motion experienced at this particular joint location. Looking at the normal stress plot (Figure 5-19), it is possible to also observe that the rocking at the beginning of the simulation usually consists of high frequency and low amplitude sequence of opening and closing, which over time and with continued excitation developed into lower frequency movements with larger joint separation. The larger amplitude of normal displacements, in turn produced higher stresses upon joint closure and impact between the blocks.

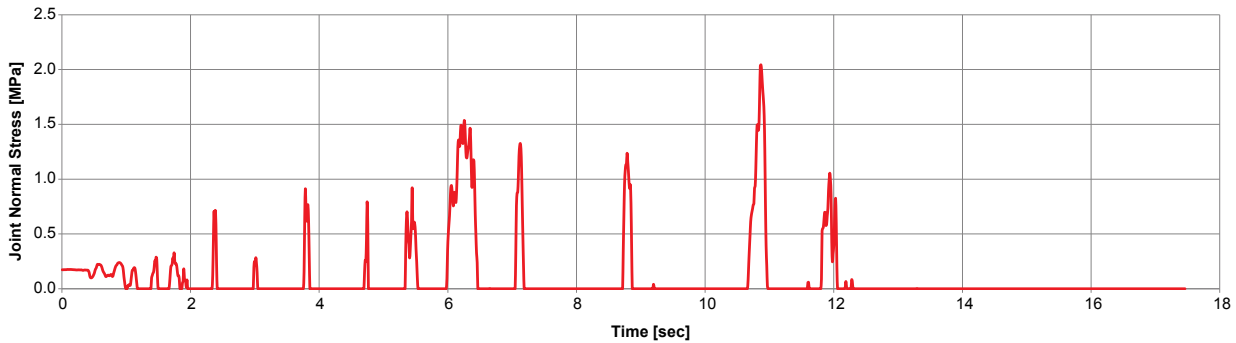


Figure 5-19: Joint normal stress time history at the joint between the second and third block in column D6, due to type 2 earthquake in the longitudinal (y) direction with scale factor of 6.0 (PGA 0.66g).

The time history record of the joint sliding provides an interesting view of the nature of the block motions as well as the magnitude of relative displacements experienced by the blocks during a strong earthquake. The spike in shear displacement at around eleven seconds is particularly interesting. Looking at the sequence of movements (Figure 5-17) and other joint parameters, this sudden jump and decline in sliding is due to the radial rocking motion of the upper group of blocks about the perimeter of the second block in column D6. Please consult the accompanying DVD for an interactive view of the model response.

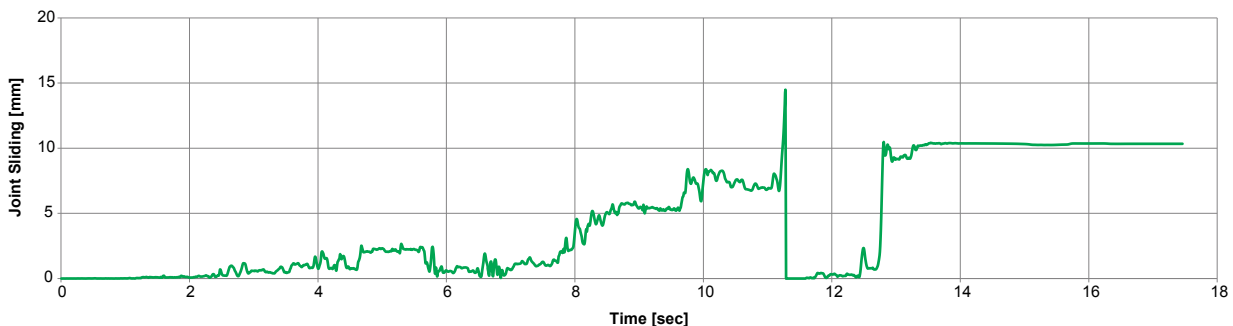


Figure 5-20: Joint sliding time history at the joint between the second and third block in column D6, due to type 2 earthquake in the longitudinal (y) direction with scale factor of 6.0 (PGA 0.66g).

5.5.2 Response of the overall structure

An evaluation and analysis of the overall response of the structure is very challenging and time-consuming. This is due to the fact that almost all of the runs exhibit some unique characteristics which make it difficult to determine general patterns. Given the time constraint for the present study, a thorough analysis of the overall response with the aim of finding patterns will not be presented. Instead, this section will provide some qualitative description of the patterns of failure and the overall response of the structure to the two types of earthquakes considered for the analysis.

The global pattern of failure varies between the different simulations. However, it is observed that several components tend to fail more consistently than others. In most cases of failure, either the free-standing columns (columns D6 and E6) or the columns at the extreme of the east façade (columns

C1, D1 and E1) are the first components of the structure to fail. This is often followed by the entire west corner of the structure, after which the structure may continue to fail in a more or less random manner.

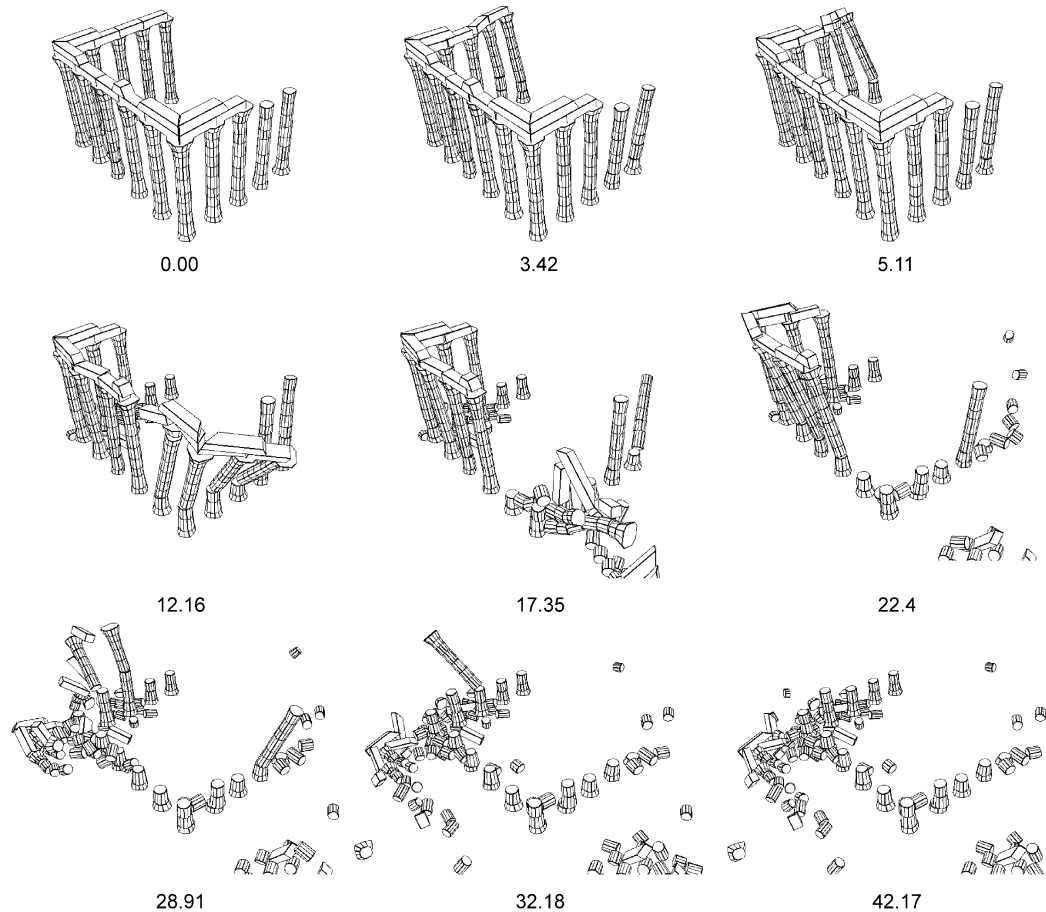


Figure 5-21: Time history response of the of the entire structure due to type 1 earthquake in the transverse (x) direction with a scale factor of 6.0 (PGA 0.6g). Note that the response has not been magnified.

It is important to note that in almost all cases, the columns fail as a result of rotation about the second or third block from the bottom. Although independent motion of blocks may be observed during the simulation, failure is almost exclusively due to rotation of a group of blocks. This is an interesting outcome since the failure modes are in most part consistent with those evaluated using 2D limit analysis. There is of course a large element of out-of-plane motion and displacement which also contributes to the failure of columns which cannot be captured using a planar analysis. A comparison of the results of incremental dynamic analysis with the quasi-static methods of limit analysis (section 4.2) and non-linear static (pushover) analysis (section 4.3) is presented in Chapter 6. Other patterns of failure may also be observed and a detailed analysis of these patterns may reveal more information about the response of other similar structures. More examples of failure sequence are provided in Appendix B.

Another important consideration in the evaluation of global results is the impact of the two types of earthquakes on the structure. As Figure 5-22 clearly illustrates, type 1 earthquakes have a more devastating impact on the structure. Even at very high scale factors, the level of failure due to type 2 earthquakes remains very limited. There exists some variation in the magnitude of the failure experienced by the structure due to the non-linear behaviour of these types of structures. However, there is a general pattern which seems to indicate that with increasing intensity levels, type 1 earthquakes can cause considerable damage, while type 2 earthquakes require very high amplitudes of ground acceleration to cause even minor damage.

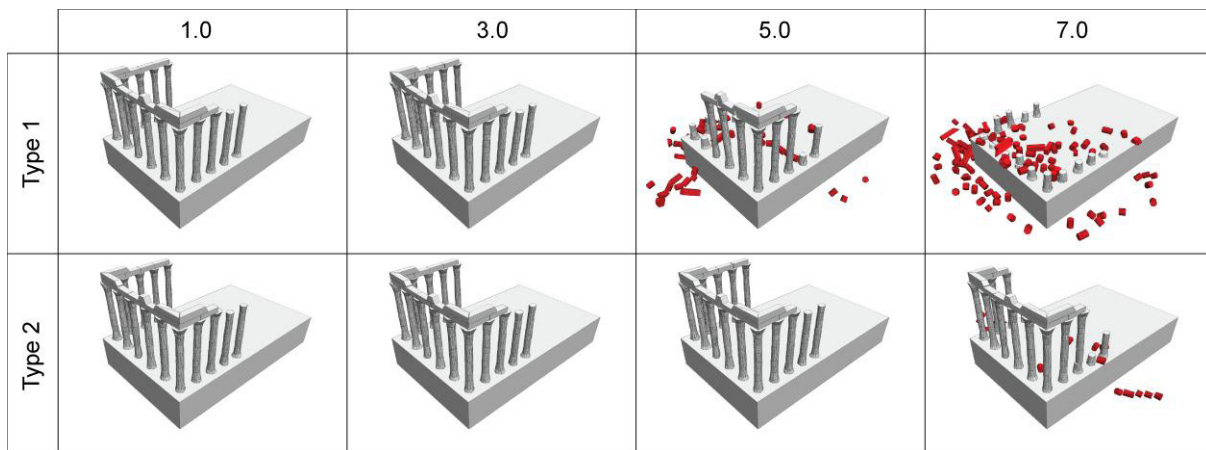


Figure 5-22: Examples of structure response due to type 1 and type 2 earthquake applied in the transverse (x) direction at various PGA scale factors.

As it was discussed earlier, there are three main differences between the two types of earthquakes considered by the analysis. First, the frequency content of the ground accelerations is very different between the two types of earthquake. This can be seen by comparing the response spectrum for both types (see Figure 5-23).

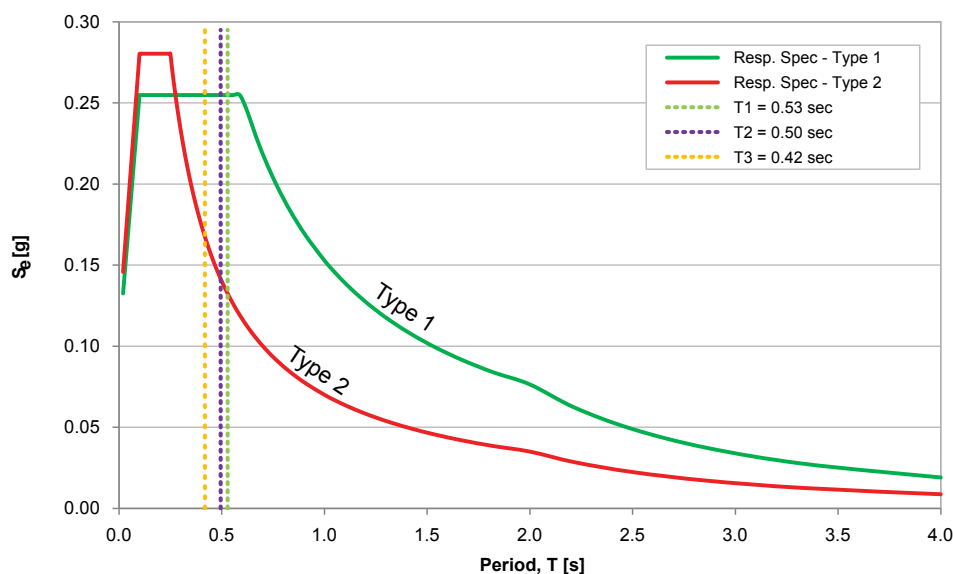


Figure 5-23: Type 1 and type 2 elastic response spectrum for Évora according to the Eurocode 8.

It was mentioned before that multi-drum structures are highly susceptible to failure due to low frequency excitations [27], [53]. Type 1 earthquakes are richer in higher periods (thus lower frequencies) which can explain the more devastating impact of these types of earthquakes.

Second, the duration of type 1 earthquake is more than 2.5 times that of type 2 (see accelerograms in Figure 5-10). This can have a significant impact since the longer the duration of the seismic event, the more opportunity exists for displacements and damage to develop and accumulate, causing ultimate failure.

Third, the magnitude of the peak ground acceleration prescribed for each type is also different. Type 1 earthquakes in the region of Évora have a PGA of 1.0 m/s^2 while type 2 earthquakes have a PGA of 1.1 m/s^2 . However, it can be seen that the slight variation in the PGA does not have as significant an impact as the previous two cases.

Finally, it is worth noting that while there exists some scatter in the response of the structure with respect to the direction of applied earthquake, the differences are very minor which seem to indicate that for this structure and under these ground motions, the direction of the excitation does not have a significant impact. A more thorough discussion of earthquake direction is presented in section 6.2.

Appendix A presents a complete table of the model states at the end of the simulation for both types of earthquakes under consideration.

This page is left blank on purpose

Chapter 6

PERFORMANCE ASSESSMENT

This chapter provides a brief review of the results of the numerical analysis performed for this study. First, the results of the three analysis methods explored in the study are compared in order to demonstrate the advantages and shortcoming of each method and to provide recommendations on the most appropriate tools to be used for analysis of similar structures. This discussion is followed by a presentation of three damage indicators which could be used to characterise the degree of damage based on the results of the incremental dynamic analysis.

6.1 Comparison of numerical methods

Examining the results of both pushover and limit analysis, it is clear that both methods provide very similar results. Table 6-1 provides a comparison of the results of these two methods.

Table 6-1: Comparison of the seismic coefficient calculated using limit and pushover analysis

Model	Seismic coefficient, α					
	EQ Positive Direction			EQ Negative Direction		
	LA	PO	% diff	LA	PO	% diff
E6	0.120	0.120	0.2%	0.123	0.124	1.2%
D6	0.120	0.122	1.9%	0.130	0.146	11.0%
West	0.103	0.115	10.6%	0.106	0.117	9.7%
North	0.102	0.109	6.8%	0.101	0.109	7.1%
East	0.108	0.115	6.4%	0.097	0.107	9.3%

*LA stands for results of limit analysis while PO stands for results of pushover analysis

This is not surprising since both methods essentially apply the same technique in order to establish the equivalent static horizontal force for which the structure would be destabilized. Given that no

material non-linearity has been specified for the blocks, the models for both analyses are almost identical.

Both limit analysis and non-linear pushover analysis indicate that by having higher seismic coefficients, the free-standing columns are less vulnerable to the action of horizontal forces (e.g. seismic coefficients for column D6 are 0.120 using limit analysis and 0.122 using pushover analysis). However, examining the results of the time history analysis, it is clear that in some cases the free-standing columns are the first parts of the structure to fail during the earthquake and suffer significant damage. Looking at the behaviour of columns with architraves, it is possible to see that while these columns experience high out of plane displacements due to torsional rocking about the base, they maintain their stability because of the presence of the architraves.

There is no direct correlation between the seismic coefficient, calculated using limit analysis and pushover analysis, and peak ground acceleration since the seismic coefficient is a measure of acceleration at the structure level rather than at the ground. In fact for most structures, the peak ground accelerations are typically smaller than the acceleration at the structure due to amplification effects. Thus it is difficult to compare the results of static analysis with those of the incremental dynamic analysis. It is however possible to conclude that the ground accelerations estimated by the static methods would have to be less than 0.1 g. The results of dynamic analysis, on the other hand, indicate that for ground accelerations below 0.2 g, the structure suffers no failure. Thus it appears that the static methods underestimate the capacity of the structure. The static methods, however, provide failure mechanisms which are consistent with the general failure pattern observed in the time history analysis.

6.2 Definition and application of damage indicators

This section provides a brief overview of possible damage indicators which may be employed in order to quantify the level of damage experienced by the structure during a simulation. Given that the results of pushover and limit analysis do not provide any reliable information about damage beyond the point of destabilization, this discussion will be limited to the results of the incremental dynamic analysis using the discrete element model.

Identifying damage indicators and defining the criteria for damage for this type of structure is very challenging. Damage indicators must take into account all the modes of damage and failure for the structure and provide consistent results across all probable situations. Ease of use and an intuitive connection to easily identifiable characteristics of the structure or its behaviour are also important considerations.

It is also important to make a distinction here between two words which are often used interchangeably, namely damage and failure. For the purposes of this study, damage represents any inelastic deviation (mostly in terms of displacements) from the initial state of the structure caused by

the seismic action. Failure, on the hand is defined as complete loss of stability, be it for a single block or the entire structure.

For the current study, three measures are proposed and presented. Each measure provides a different view of the response and the resulting damage level in the structure. For each measure, the results of each of the incremental dynamic analysis, corresponding to each of the six accelerograms, is presented as a single curve. Thus all indicators will have six curves representing the response of the structure over range of peak ground accelerations.

6.2.1 Maximum permanent displacement

As it was discussed in section 5.1, maximum permanent displacement has been reported in some literature as a reliable criteria for quantifying damage for a single column [27], [52]. The maximum permanent displacement is a measure of residual displacement at the end of the time history simulation. Figure 6-1 presents three plots: the first two plots provide the results from the six earthquake records applied in the x and y direction respectively; the third plot provides an average of the displacements for each earthquake type (type 1 and type 2) and each direction. This format of plots will be used for the other two indicators presented in the following chapters in order to demonstrate a consistent structural behaviour.

It is important to notice that all three plots feature two clusters of three curves, clearly separated from each other. The upper cluster represents the result of the type 1 earthquakes while the lower cluster represents the results of the type 2 earthquakes.

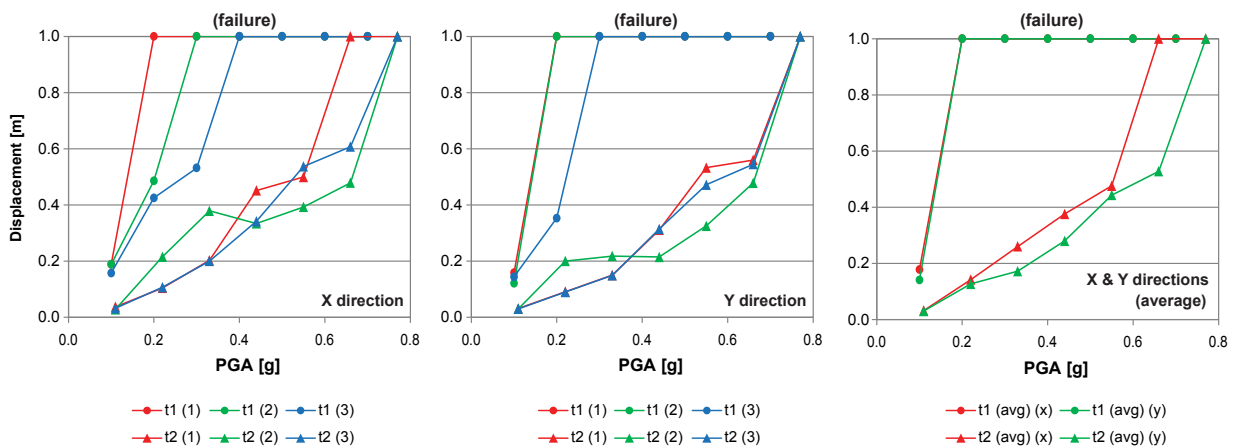


Figure 6-1: Maximum permanent displacement at various PGA intensities for earthquake runs in both x and y directions.

As it was outlined in section 5.5.2, type 1 earthquake produces the most extreme response, regardless of direction, where intensities beyond the code prescribed 1.0 m/s^2 will cause at least one block in the structure to fail. Looking at the plots above, it is easy to see that the maximum permanent displacement indicator successfully identifies all instances of failure, indicated by maximum displacements higher than 1.0 meters.

It is also important to observe that although there is some scatter in the results between the runs of the same earthquake type, the results are very consistent. Furthermore, within each type of earthquake (i.e. type 1 or type 2), the average displacements for earthquakes in either direction is almost identical. This indicates that for both earthquake types, the direction of the application of the earthquake does not alter the response significantly.

Looking at the plots, it is interesting to notice that while maximum permanent displacements can provide a reliable indicator of whether or not there has been any failure, they cannot be used to quantify the magnitude of the failure. This is especially true in the case of multi-column monuments where a failure of a single block will be interpreted and represented as a total failure by the indicator. Thus, a different measure is required in order to quantify the magnitude of failure suffered by the structure following the initial failure.

As a measure of damage, maximum permanent displacement may be a useful indicator as it provides a measure of drift in the structure in cases where no failure is observed. It is possible to modify and combine this indicator with other measures in order to exclude failed blocks so as to capture the state of damage for the remaining structure.

6.2.2 Failed blocks

Given that the structure under consideration is composed of a finite number of block elements, each of which represent actual blocks within the structure, it is natural to use the number of failed blocks as an indicator for the level of damage in the structure.

The criteria for failure of blocks will not always be the same and require careful consideration of the structure's composition and behaviour. For the present case study, the failure criterion is defined as follows. First, the initial position of the blocks within the undamaged structure is stored as two sets of coordinates representing the bounding box for each block. Following the completion of the analysis, the location of each block's centroid is compared to the position of the initial bounding box. Each block whose centroid has moved outside the initial bounding box is marked as failed. Figure 6-2 demonstrates the failure criterion schematically.

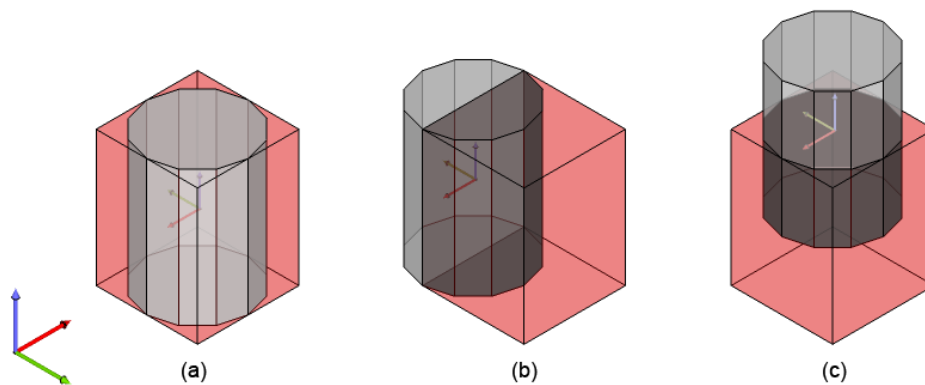


Figure 6-2: Failed blocks are identified when the block centroid moves outside (b and c) of the initial position bounding box (a).

Using this definition, it is then possible to calculate the number of blocks which have failed during the analysis and express this value as a percentage of the initial block count. Figure 6-3 shows a plot (similar to the plot developed in the previous section) for the percentage of failed blocks. As before, the figure presents three plots: the first two plots provide the results from the six earthquake records applied in the x and y direction respectively; the third plot provides an average of the percentage of failed blocks for each earthquake type (type 1 and type 2) and each direction.

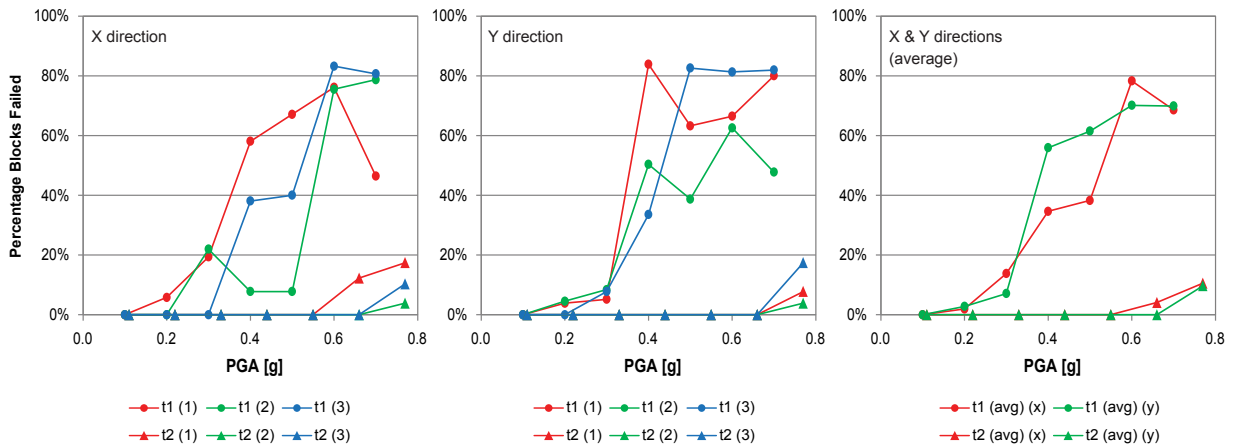


Figure 6-3: Percentage of failed blocks at various PGA intensities for earthquake runs in both x and y directions.

It is important to notice that these plots share a number of similarities with the plots presented in the previous section. First, the plots again show a clear separation between near and far field earthquakes. Furthermore, the average results for each type of earthquake indicate that the direction of the applied ground acceleration does not alter the results in a significant way. Finally, type 1 (far field) earthquakes produce the most extreme response whereas type 2 (near field) earthquakes do not cause any failure for the range of PGAs under 0.55 g.

However, in comparison to maximum permanent displacements, the percentage of failed blocks provides more information about the state of the model following the end of the simulation. As with maximum permanent displacements, it is easy to distinguish cases of failure simply by finding cases where the percentage of failed blocks is higher than zero. The plots can also be used to quantify the level of failure from cases where a limited number of blocks have failed (such as type 1 earthquake at 0.2 g) up to cases where almost the entire structure has collapsed (such as type 1 earthquake at 0.7 g intensity).

It is interesting to observe that this indicator provides a better picture of the non-linear behaviour of the structure. As the plots indicated, there exists a range of intensities within which the level of failure can vary unpredictably. This information is very useful in characterising the response of the structure and the reliability of the analysis being performed.

While the percentage of failed blocks provides a reliable measure of failure, it does not provide any useful information in regards to degree of damage to the remaining blocks. This is due to the inherent definition of the indicator and what it measures.

6.2.3 Contact area loss

Looking at the response of the structure, it is clear that the principal form of damage to multi-drum structures, apart from material loss and cracking, is characterized by sliding and movement of the blocks. Thus a measure of the change in the relative position of blocks is needed which can account for rocking, twisting and sliding of blocks relative to one another.

The percentage of block contact area loss is a good indirect measure of block displacement relative to one another. This indicator measures the changed state of block contacts at the end of the simulation and it can account for both damage (i.e. sliding and displacement) as well as failure (i.e. complete loss of contact by separation). Figure 6-4 shows a plot, similar to the plot developed in the previous sections, for the percentage of block contact area loss. As before, the figure presents three plots: the first two plots provide the results from the six earthquake records applied in the x and y direction respectively; the third plot provides an average of the percentage of contact area loss for each earthquake type (i.e. type 1 and type 2) and each direction.

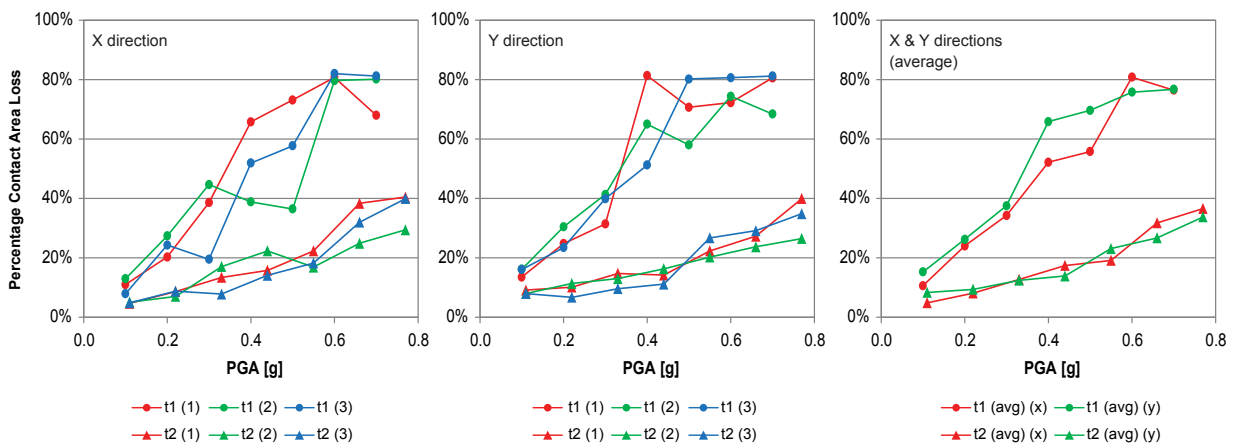


Figure 6-4: Percentage of contact area loss at various PGA intensities for earthquake runs in both x and y directions.

As with the plots for the previous two indicators, three general observations can also be made for these plots. First, the distinct separation between near and far field earthquake results is clearly visible in these plots. Furthermore, the average results for each type of earthquake indicate that the direction of the applied ground acceleration does not alter the results in a significant way. Finally, type 1 (far field) earthquakes produce the more extreme response.

One of the most interesting features of these plots is that the response seems to be almost linear. This may seem contrary to the general understanding of the structure's behaviour. However, upon closer examination, it can be understood that the change in contact area provides a measure of the progression and accumulation of damage through the relative sliding of blocks against each other and thus in a way fills the gap between the parameters measured by the other two indicators.

Loss of block contact area provides a measure of both damage and failure. However, this parameter does not provide a distinction between the two or a direct method of determining whether the losses constitute sliding of blocks relative to one another or complete detachment of blocks.

One way to mitigate this shortcoming may be to compute the frequency distribution of contact area loss based on individual contacts. This measure allows for a qualitative assessment of how the contact area loss is distributed in the structure and it helps in the understanding of the current state of the structure. An example of such a distribution is presented in Figure 6-5 for type 1 earthquake.

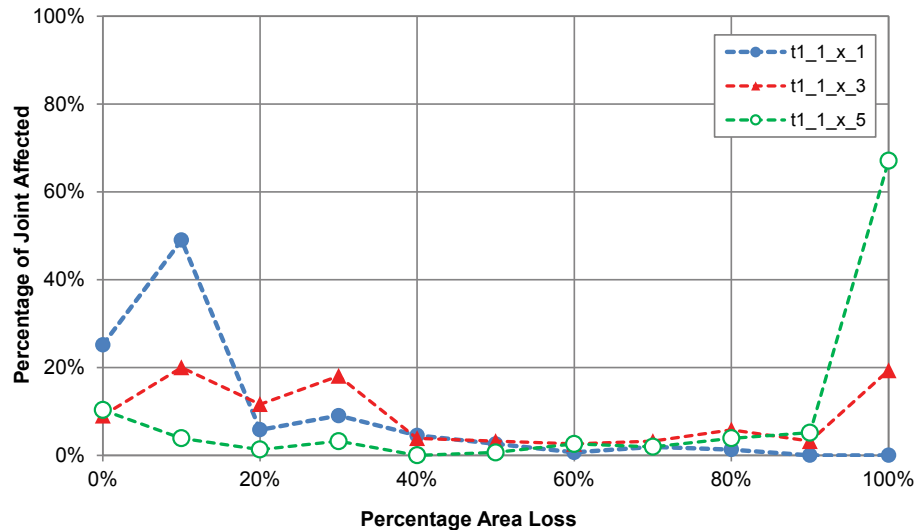


Figure 6-5: Distribution of block contact area loss for type 1 earthquake in the x-direction (scaled by 1, 3, and 5).

It is important to note that the extremes on the x-axis correspond to number of intact blocks on the left and the number of detached/failed blocks on the right. It is important to note the distribution is presented as a percentage of joints affected with respect to the total number of joints in the model (155 joints). Figure 6-6 provide a similar plot for type 2 earthquake

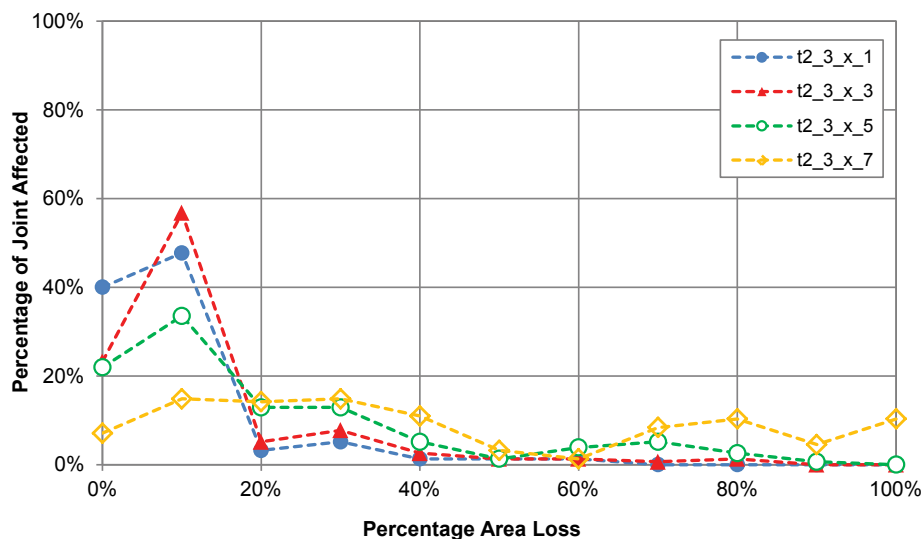


Figure 6-6: Distribution of block contact area loss for type 2 earthquake in the x-direction (scaled by 1, 3, 5 and 7).

It can be seen from the plots that with increasing earthquake intensity the number of failed blocks increases and the distribution shifts from the left to the right, with the middle representing area loss due to sliding.

6.2.4 Summary of results

Figure 6-7 provides a comparison of the average results for each of the damage indicators discussed in this section. As it was previously presented, the indicators share a number of characteristics which show that each indicator can provide a sound and consistent measure of the state of the structure. However, each indicator has its own disadvantages, meaning that for most cases involving complicated structures, multiple indicators must be used.

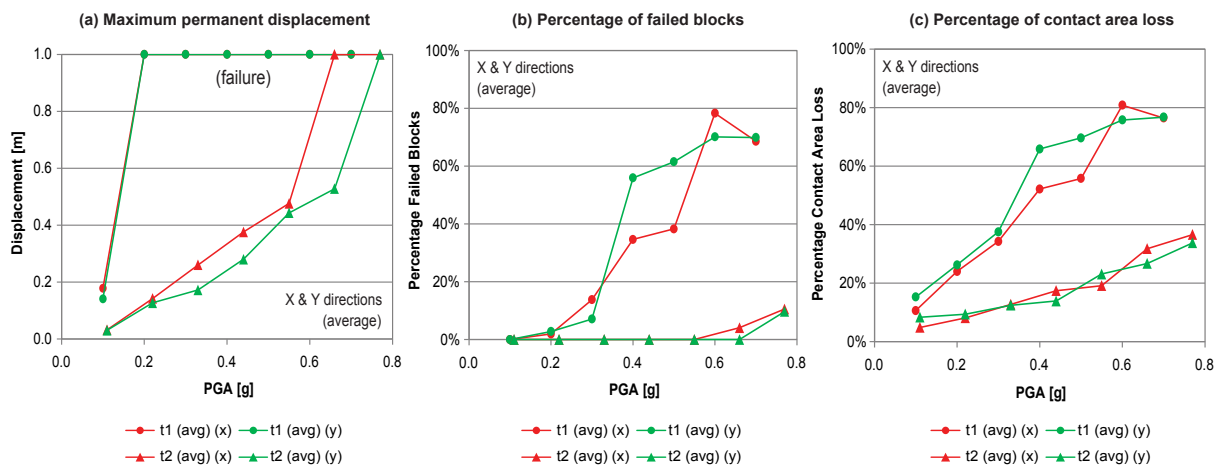


Figure 6-7: Comparison of damage indicators at various PGA intensities for earthquake runs in both x and y directions.

It is also important and useful to establish correlation relations which allow information from one indicator to be converted into an equivalent measure in another. This is especially useful in the case of losses in block contact area since unlike maximum permanent displacements or number of failed blocks, losses in block contact area is a difficult parameter to measure in physical. Furthermore, although it measures a real quantity, it does not provide an intuitive feel about the state of the structure as other indicators do.

Chapter 7

CONCLUSIONS

7.1 Main conclusions

Although non-linear incremental dynamic analysis is the most computationally intensive method available for evaluation of seismic response of structures, the results of the analysis performed for this study indicate that it is the only method which can provide reliable results for the assessment of slender multi-drum classical structures. While limit and pushover analysis are able to predict the principal failure mechanism for the structure, their failure to take into account the dynamic stability of the structure during shaking, ultimately underestimates the capacity of the structure. Therefore, the static methods are not recommended for seismic evaluation of structures of this type.

The analysis revealed that type 1 earthquakes cause the most severe response in the structure. This is due to two important differences between the two earthquake types. First, the frequency content of the ground accelerations is very different between the two types of earthquakes. This was demonstrated by comparing the response spectrum for both types. Previous research has indicated that multi-drum structures are highly susceptible to failure due to low frequency excitations. Type 1 earthquakes are richer in higher periods (lower frequencies) and thus cause considerably more damage even at low ground acceleration intensities. Second, the duration of type 1 earthquake is more than 2.5 times that of type 2. This can have a significant impact since the longer the duration of the seismic event, the more opportunity exists for displacements and damage to develop and accumulate, causing ultimate failure.

It is difficult to assess the safety of the structure given that very few guidelines are available regarding the assessment criteria which must be employed. However, using the design and assessment

framework provided by Eurocode 8, the results of the analysis indicate that at the code prescribed ground acceleration levels, the structure will experience some damage (mainly due to relative sliding of blocks) but will not fail. Given these results, it seems that interventions to improve the seismic response of the structure may not be necessary. However, it is important to note that the incremental dynamic analysis shows that a limited number of blocks (on average about 2.5%) begin to fail when the ground acceleration levels of type 1 earthquakes are doubled (0.2 g). Thus, further investigation of this interval may be necessary to establish the range over which the structure continues to perform without any failures.

The time history analyses reveal that the response of the structure is non-linear. This result is consistent with those reported in the literature. However, the degree of non-linearity for the actions considered in the case study is not as severe as those reported in some literature. It has been demonstrated that changes in structural parameters at the joints as well as in the geometry of the contact surface geometry can alter the response of the dynamic time history simulations. The use of the results of the experimental dynamic identification for the calibration of the model as well as a more methodical approach to generating the simplified model geometry helped to mitigate the sensitivity of the structure.

The three damage indicators presented in this study provide useful information about the state of the model following the earthquake. While the first two indicators, namely maximum permanent displacements and percentage of failed blocks, provide a good measure of failure in the structural model, they do not present any information about the state of damage in the model. The third indicator, on the other hand, measuring the loss of contact area over time provides a means of monitoring accumulation of damage. Each of the measures has inherent strengths which should be utilised in conjunction with other indicators in order to obtain a reliable picture of the analysis results.

7.2 Opportunities for further research

As part of the present study, a number of areas for further research have been identified. These areas can be classified into two groups, one focusing on the Roman Temple of Évora as a case study to further our understanding of the structure's behaviour, and the other focusing on results of other case studies in more general terms to develop general knowledge about the seismic behaviour of masonry and in particular classical multi-drum structures.

While some previous studies [29], [61] have shown that the response of multi-drum structures to vertical excitations is not as critical as the response to horizontal seismic forces, further research in this area is needed. The Temple structure could serve as a case study structure for this purpose since the results of the response due to horizontal excitations are available for comparison. Furthermore, as discussed in section 5.4, better characterisation of ground motion based on real earthquake records should also be explored.

Further GPR analysis using appropriate antenna as well as more in depth material characterization should be used in order to properly characterise the internal structure of the podium and evaluate the effect of the improved model on the response of the column-architrave system.

As previously reported, the response of classical multi-drum structures is very sensitive even to trivial changes of the parameters of the system or the input excitation. The present study investigated the sensitivity of the structure to input excitation by examining the response under near and far field earthquakes. The sensitivity of the structure to the direction of the applied excitation was also investigated and reported. Thus further research on this structure should aim to characterise the sensitivity of the various system parameters (such as material properties) and develop a methodology in order to manage the model sensitivity in order to insure reliable and consistent results.

An important area of research is the development of tools to investigate the condition of dry joints so that future models can better represent the conditions of the structure. Further work on development of methods of dynamic identification better suited for use with multi-block structures should also be a top priority.

As it was reported by previous studies, the out of plane behaviour of the structure, even in cases where the loads are applied in a planar direction, is of great significance and in most cases drives the response and failure mechanism of the structure. Thus, future developments in this area should incorporate complete three dimensional formulation of the response in order to capture the true response of the structure.

Further development of tools specifically designed for evaluation of these types of structures may accelerate the assessment of structures and allow for a more consistent methodology to be applied in the analysis. As a part of the current study, a collection of FISH function libraries for 3DEC were created which can help streamline and accelerate analysis of similar structures in the future. These tools, coupled with the geometric pre-processing algorithm (see section 5.2.1) and the visual post-processor (see section 5.5) also developed for this project, will accelerate evaluation of multi-drum structures and allow for more extensive study of structural behaviour in the future. It is hoped that future generation of analysis software will incorporate some of these features into their workflow in order to assist analysts to focus on understanding structural behaviour.

Finally, the global expert community should prepare more detailed criteria for the evaluation of these types of structures so that architects, engineers and planners can quantify risks and properly assess the need for intervention in a more consistent manner.

This page is left blank on purpose

REFERENCES

- [1] G. Croci, *The conservation and structural restoration of architectural heritage*. Southampton, United Kingdom: Computational Mechanics Publications, 1998.
- [2] C. Papantonopoulos, I. N. Psycharis, D. Y. Papastamatiou, J. V. Lemos, and H. P. Mouzakis, "Numerical prediction of the earthquake response of classical columns using the distinct element method," *Earthquake Engineering & Structural Dynamics*, vol. 31, no. 9, pp. 1699-1717, Sep. 2002.
- [3] J. V. Lemos, "Discrete element modeling of masonry structures," *International Journal of Architectural Heritage*, vol. 1, no. 2, pp. 190-213, May 2007.
- [4] A. Orduña and P. B. Lourenço, "Three-dimensional limit analysis of rigid blocks assemblages. Part II: Load-path following solution procedure and validation," *International Journal of Solids and Structures*, vol. 42, no. 18–19, pp. 5161-5180, Sep. 2005.
- [5] J. Heyman, "The stone skeleton," *International Journal of Solids and Structures*, vol. 2, pp. 249-279, 1966.
- [6] P. Block and J. Ochsendorf, "Thrust network analysis: a new methodology for three dimensional equilibrium," *Journal of the International Association for Shell and Spatial Structures*, vol. 48, no. 3, pp. 167-173, 2007.
- [7] A. Orduña, "Seismic assessment of ancient masonry structures by rigid blocks limit Analysis," University of Minho, 2003.
- [8] C. Modena, "SA1 - General methodology for analysis and restoration." MSc SAHC 2011-2012, pp. 45-112, 2011.
- [9] A. Orduña, A. Preciado, F. Galván, and J. C. Araiza, "Vulnerability assessment of churches at Colima by 3D limit analysis models," in *Structural Analysis of Historical Construction*, no. Cfe 1993, D. D'Ayala and E. Fodde, Eds. London, United Kingdom: Taylor & Francis, Inc., 2008, pp. 1297-1302.
- [10] Comité Européen de Normalisation, "Eurocode 8: Design of structures for earthquake resistance - Part 1: General rules, seismic actions and rules for buildings," vol. 3. 2004.
- [11] H. Krawinkler and G. D. P. K. Seneviratna, "Pros and cons of a pushover analysis of seismic performance evaluation," *Engineering Structures*, vol. 20, no. 4–6, pp. 452-464, Apr. 1998.
- [12] P. Pan and M. Ohsaki, "Nonlinear multimodal pushover analysis for spatial structures," Kyoto, Japan.

- [13] F. Omori, "Seismic Experiments on the Fracturing and Overturning of Columns," *Publications of the Earthquake Investigation Committee in Foreign Language*, vol. 4, pp. 69-141, 1900.
- [14] F. Omori, "On the overturning and sliding of columns," *Publications of the Earthquake Investigation Committee in Foreign Language*, vol. 12, pp. 8-27, 1902.
- [15] G. W. Housner, "The Behavior of inverted pendulum structures during earthquakes," *Bulletin of the Seismological Society of America*, vol. 53, no. 2, pp. 403-417, 1963.
- [16] C.-S. Yim, A. K. Chopra, and J. Penzien, "Rocking response of rigid blocks to earthquakes," *Earthquake Engineering & Structural Dynamics*, vol. 8, no. 6, pp. 565-587, 1980.
- [17] F. Prieto, "Applications of non-linear dynamics to masonry collapse mechanisms," University of Minho, 2007.
- [18] D. Oliveira, "Experimental and numerical analysis of blocky masonry structures under cyclic loading," University of Minho, 2003.
- [19] D. Vamvatsikos and C. A. Cornell, "Incremental dynamic analysis," *Earthquake Engineering & Structural Dynamics*, vol. 31, no. 3, pp. 491-514, Mar. 2002.
- [20] K. J. Bathe, *Finite element procedures in engineering analysis*. Englewood Cliffs, New Jersey, USA: Prentice-Hall, 1982.
- [21] P. B. Lourenço, "Computational strategies for masonry structures," Delft University of Technology, 1996.
- [22] M. J. DeJong, "Seismic response of stone masonry spires: Analytical modeling," *Engineering Structures*, Apr. 2012.
- [23] L. Papaloizou and P. Komodromos, "Parameters influencing the seismic response of ancient columns and colonnades," in *Proceedings of the 12th International Conference on Civil, Structural and Environmental Engineering Computing*, 2009.
- [24] A. Orduña, "Block: User's manual," Guimarães, Portugal, 2004.
- [25] N. Bićanić, "Discrete Element Methods," in *Encyclopedia of computational mechanics*, no. Figure 1, E. Stein, R. de Borst, and T. J. R. Hughes, Eds. Chichester, UK: John Wiley & Sons, Ltd, 2004, pp. 311-337.
- [26] C. Papantonopoulos, H. P. Mouzakis, D. Y. Papastamatiou, I. Psycharis, C. Zambas, and J. V. Lemos, "Predictability of experiments on the seismic response of classical monuments," in *Proceedings of the 11th European conference on earthquake engineering*, 1998.

- [27] I. N. Psycharis, J. V. Lemos, D. Y. Papastamatiou, C. Zambas, and C. Papantonopoulos, "Numerical study of the seismic behaviour of a part of the Parthenon Pronaos," *Earthquake Engineering & Structural Dynamics*, vol. 32, no. 13, pp. 2063-2084, Nov. 2003.
- [28] P. Komodromos, L. Papaloizou, and P. Polycarpou, "Simulation of the response of ancient columns under harmonic and earthquake excitations," *Engineering Structures*, vol. 30, no. 8, pp. 2154-2164, Aug. 2008.
- [29] L. Papaloizou, P. Polycarpou, and P. Komodromos, "Numerical analysis of ancient multi-drum columns with epistyles under dynamic loadings," in *Proceedings of the 14th World Conference on Earthquake Engineering*, 2008, no. Figure 1.
- [30] Município de Évora, "Das Origens as Sec. XII," 200AD. [Online]. Available: http://www2.cm-evora.pt/itinerarios/das_origens_sec_xii.htm. [Accessed: 08-Jul-2012].
- [31] M. D. V. M. Simplício, "Évora: Origem e Evolução de uma Cidade Medieval," *Revista da Faculdade de Letras do Porto: Geografia*, vol. 19, no. 1, pp. 365-372, 2003.
- [32] R. M. V. Dias, "A cidade romana Liberalitas Iulia Eborac - fórum, e maquete de reconstituição do templo," *A Cidade de Évora: Boletim de Cultura da Câmara Municipal (2ª Série)*, no. 7, pp. 195-212, 2007.
- [33] T. Hauschild, "El templo romano de evora," *Cuadernos de Arquitectura Romana*, vol. 1, pp. 107 - 117, 1991.
- [34] F. da Fonseca, *Evora Glorios*. Rome: Na Officina Komarekiana, 1728, p. 444.
- [35] C. Lopes, "Caracterização petrográfica dos monumentos Romanos de Évora," in *Boletim Cultural A cidade de Évora, II série, n.º 4*, Câmara Municipal de Évora, Ed. Évora, Portugal: , 2000, pp. 129 - 142.
- [36] H. Vilar and H. Fernandes, "O Urbanismo de Évora no Período Medieval," *Monumentos*, vol. 26, pp. 6-15, 2007.
- [37] M. Branco and R. Gordalina, "Templo Romano de Évora," *Sistema de Informação para o Património Arquitectónico*, 1996. [Online]. Available: http://www.monumentos.pt/Site/APP_PagesUser/SIPA.aspx?id=2863. [Accessed: 11-Jul-2012].
- [38] F. Bilou, *A refundação do aqueduto da água da prata, em Évora, 1533-1537*. Colibri, 2010.
- [39] G. Pereira, "O Templo Romano," in *Estudos diversos: (arqueologia, historia, arte, etnografia)*, Coimbra, Portugal: Imprensa da Universidade de Coimbra, 1934, pp. 219-222.

- [40] O. Ribeiro, "Évora: Sítio, origem, evolução e funções de uma cidade," Lisbon, Portugal, 1986.
- [41] J. I. Jokilehto, "A history of architectural conservation. The contribution of English, French German and Italian thought towards an international approach to the conservation of cultural property," The University of York, England, 1986.
- [42] F. D. K. Ching, *A Visual Dictionary of Architecture*. New York: John Wiley & Sons, Ltd, 1995.
- [43] A. Garcia y Bellido, "El recinto mural romano de Évora Liberalitas Ivlia," *Conimbriga*, vol. 10, pp. 85-92, 1971.
- [44] 3D Total Laserscanning Services, "Templo Romano da Acropole de Évora: Relatório de Inspeção," Évora, Portugal, 2011.
- [45] G. Grecchi, A. McCall, J. Noh, E. Speer, and M. Tohidi, "The Roman Temple in Évora: A conservation proposal," Guimarães, Portugal, 2012.
- [46] Itasca Consulting Group, "3DEC: Numerical modeling code for advanced geotechnical analysis of soil, rock, and structural support in three dimensions." 2012.
- [47] Itasca Consulting Group, *3DEC: Theory and Background*. Minneapolis, Minnesota: Itasca Consulting Group, Inc., 2007.
- [48] Robert McNeel & Associate, "Rhinoceros 3D." 2011.
- [49] Robert McNeel & Associate, "Using Rhinoceros: Scan, Cleanup, and Remodel," 2006.
- [50] G. Vasconcelos, "Experimental investigations on the mechanics of stone masonry : Characterization of granites and behavior of ancient masonry shear walls," University of Minho.
- [51] G. Vasconcelos and P. B. Lourenço, "Experimental properties of granites," in *Proceedings of the 6th International Symposium on the Conservation of Monuments in the Mediterranean Basin*, 2004.
- [52] G. E. Sincaian, "Seismic behaviour of blocky masonry structures: A discrete element method approach," Universidade Tecnica de Lisboa, 2001.
- [53] I. N. Psycharis, D. Y. Papastamatiou, and A. P. Alexandris, "Parametric investigation of the stability of classical columns under harmonic and earthquake excitations," *Earthquake Engineering & Structural Dynamics*, vol. 29, no. 8, pp. 1093-1109, Aug. 2000.
- [54] J. He and Z.-F. Fu, "System identification using neural network," in *Modal Analysis*, Oxford: Butterworth-Heinemann, 2001, pp. 241-251.

- [55] H. Adeli and X. Jiang, "Dynamic Fuzzy Wavelet Neural Network Model for Structural System Identification," *Journal of Structural Engineering*, vol. 132, no. 1, pp. 102-111, Jan. 2006.
- [56] S. Saadat, G. D. Buckner, T. Furukawa, and M. N. Noori, "An intelligent parameter varying (IPV) approach for non-linear system identification of base excited structures," *International Journal of Non-Linear Mechanics*, vol. 39, no. 6, pp. 993-1004, Aug. 2004.
- [57] I. Iervolino, G. Maddaloni, and E. Cosenza, "Eurocode 8 compliant real record sets for seismic analysis of structures," *Journal of Earthquake Engineering*, vol. 12, no. 1, pp. 54-90, Jan. 2008.
- [58] Norma Portuguesa, "Eurocódigo 8: Projecto de estruturas para resistência aos sismos Parte 1: Regras gerais, acções sísmicas e regras para edifícios." 2009.
- [59] P. Gelfi, "Simqke_gr: Artificial earthquakes compatible with response spectra." Università degli Studi di Brescia, Italy, 2011.
- [60] Seismosoft, "SeismoSignal." Seismosoft, Pavia, Italy, 2011.
- [61] L. Papaloizou and P. Komodromos, "The dynamic analysis of multi-drum ancient structures under earthquake excitations," in *The Second International Workshop on Active Tectonics, Earthquake Geology, Archaeology and Engineering*, 2011.

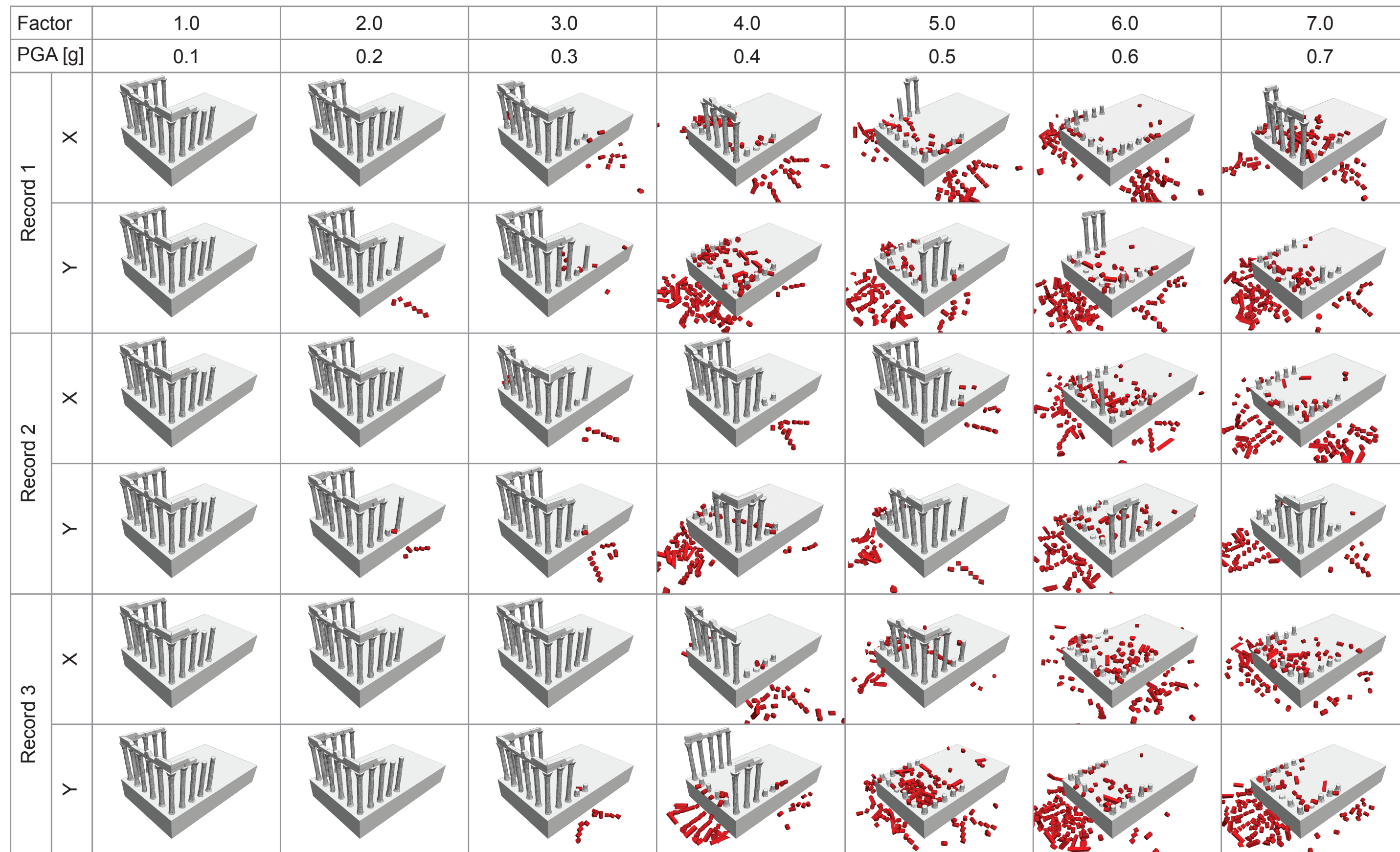
This page is left blank on purpose

APPENDIX A: FINAL STATE OF MODELS FOR DYNAMIC ANALYSIS

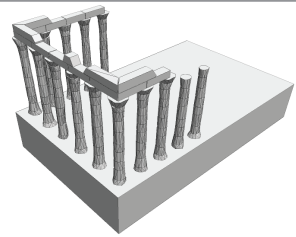
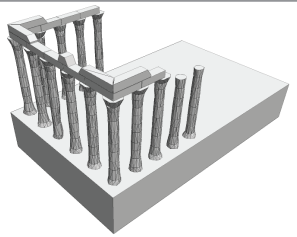
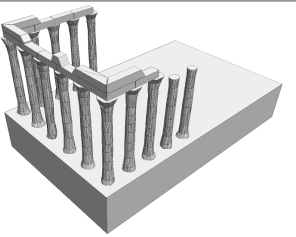
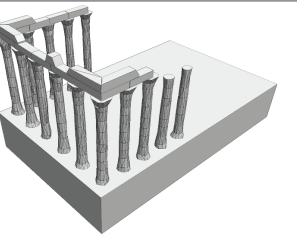
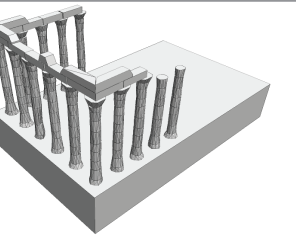
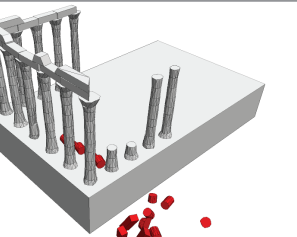
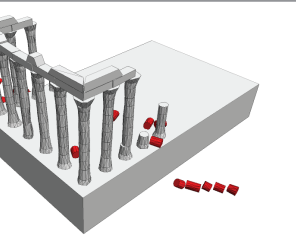
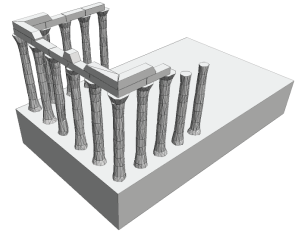
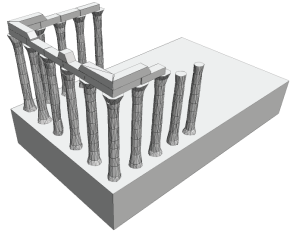
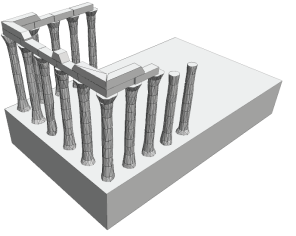
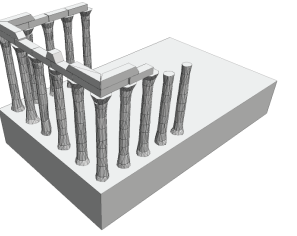
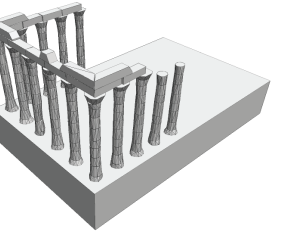
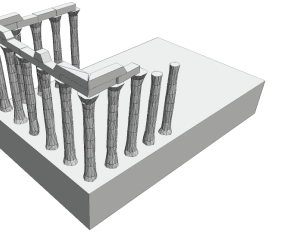
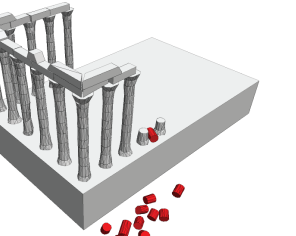
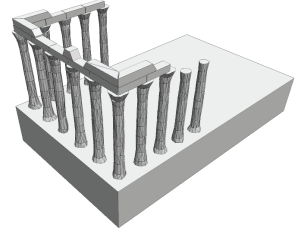
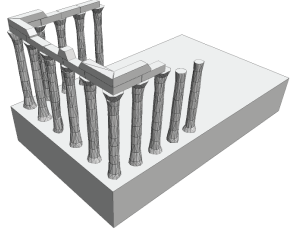
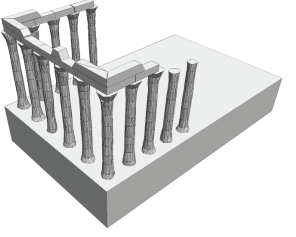
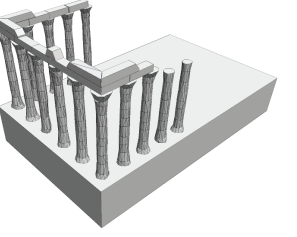
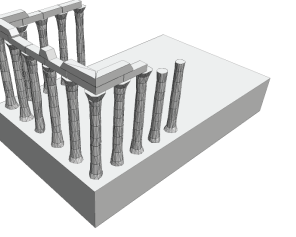
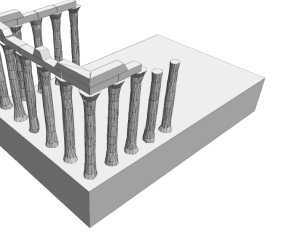
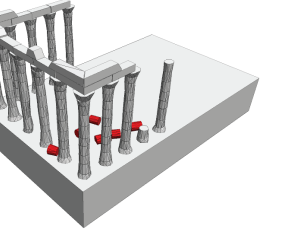
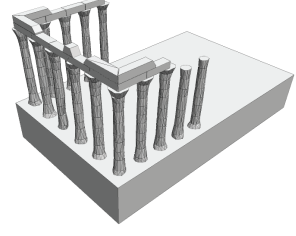
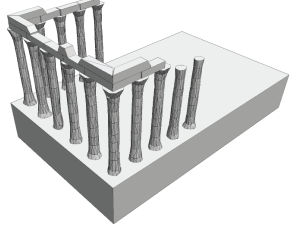
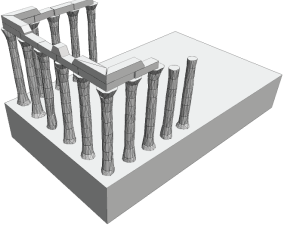
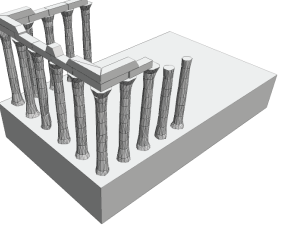
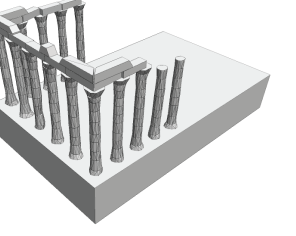
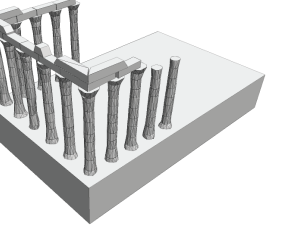
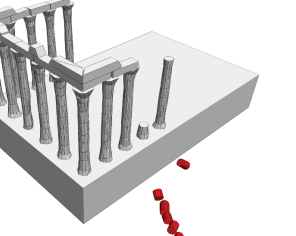
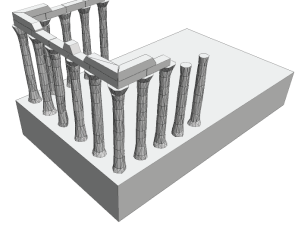
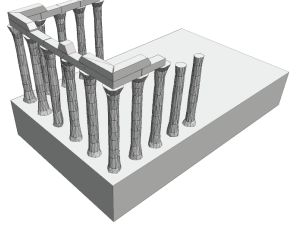
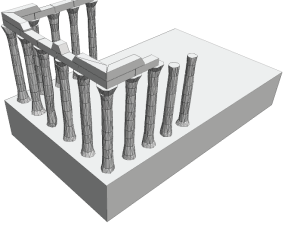
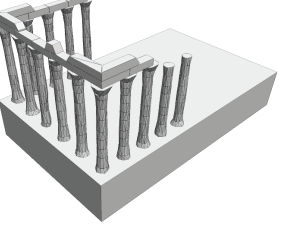
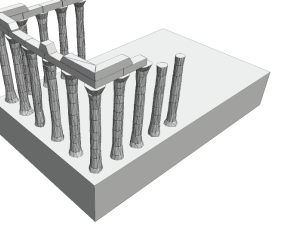
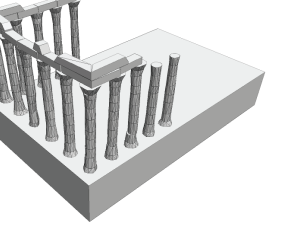
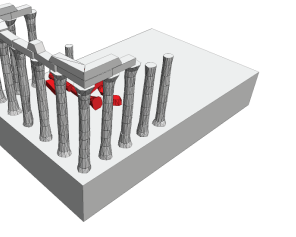
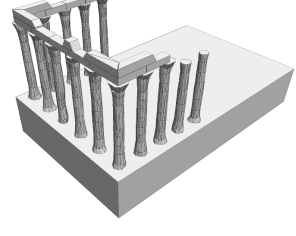
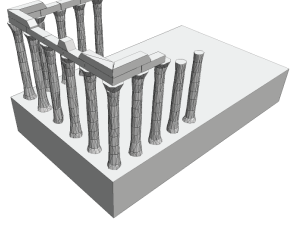
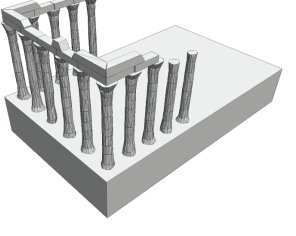
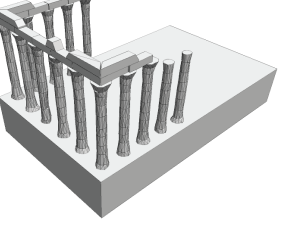
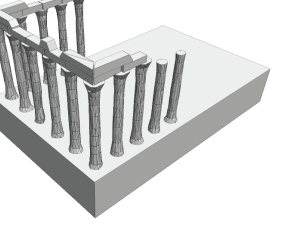
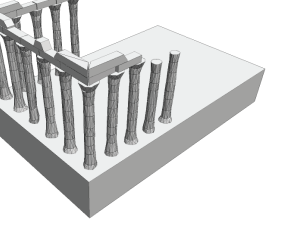
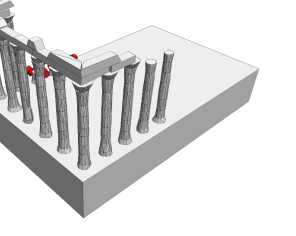
This appendix provides a visual table of analysis results from the incremental dynamic analysis which shows the final state of the models in order to observe the residual displacements and magnitude of the failures for each simulation. The table is presented on two pages, separated by the earthquake type.

This page is left blank on purpose

Final State of Models after Dynamic Analysis: Type 1 Earthquake



Final State of Models after Dynamic Analysis: Type 2 Earthquake

Factor		1.0	2.0	3.0	4.0	5.0	6.0	7.0
PGA [g]		0.11	0.22	0.33	0.44	0.55	0.66	0.77
Record 1	X							
	Y							
Record 2	X							
	Y							
Record 3	X							
	Y							

APPENDIX B: TYPICAL FAILURE PATTERNS OF DYNAMIC ANALYSIS

This appendix compiles a sample of the sequence of failure observed for eight simulations (four examples for each type of earthquake, with two sequence in each direction of applied accelerations). It is important to note that the two types have different duration.

This page is left blank on purpose

Example Failure Sequence for Type 1 and Type 2 Earthquakes

